

THE UNIVERSITY OF MANITOBA

Structural Characterization of Glycans

by Mass Spectrometry

by

Julian Ajit Saba

B. Sc. (University of Manitoba) 1998

A thesis submitted to the FACULTY OF GRADUATE STUDIES in partial

fulfillment of the requirements for the degree of

DOCTOR OF PHILOSOPHY

Department of Chemistry

2004

Winnipeg, Manitoba

THE UNIVERSITY OF MANITOBA
FACULTY OF GRADUATE STUDIES

COPYRIGHT PERMISSION

Structural Characterization of Glycans
by Mass Spectrometry

BY

Julian Ajit Saba

**A Thesis/Practicum submitted to the Faculty of Graduate Studies of The University of
Manitoba in partial fulfillment of the requirement of the degree
Of
DOCTOR OF PHILOSOPHY**

Julian Ajit Saba © 2004

Permission has been granted to the Library of the University of Manitoba to lend or sell copies of this thesis/practicum, to the National Library of Canada to microfilm this thesis and to lend or sell copies of the film, and to University Microfilms Inc. to publish an abstract of this thesis/practicum.

This reproduction or copy of this thesis has been made available by authority of the copyright owner solely for the purpose of private study and research, and may only be reproduced and copied as permitted by copyright laws or with express written authorization from the copyright owner.

Dedicated to
Miss M.P. William
Miss A. William
Mr. D.S. William
Miss R. William
Miss S. William

I do not want anyone to want for me—I want to want for myself.

Yevgeny Zamyatin

There is no final revolution. Revolutions are infinite.

Yevgeny Zamyatin

ACKNOWLEDGEMENTS

Foremost I would like to express sincere thanks to my Ph. D. supervisor Dr. Hélène Perreault who has introduced me to the fascinating field of biological mass spectrometry. Dr. Perreault has provided me absolute support, has expressed considerable interest in my research and has carefully guided me over the course of my Ph. D. I thank the other members of my Ph.D. thesis committee, Dr. James C. Jamieson, Dr. Art Chow and Dr. Mike Butler for their time, comments and suggestions regarding my research.

Sincere appreciation is expressed towards Dr. Werner Ens and Dr. Kenneth G. Standing of the Time-of-Flight Laboratory, Department of Physics, University of Manitoba for use of instrumentation and support.

I would like to thank the members of my laboratory, C.H. Lee, V.C. Chen, T.T.J. Williams, M. Ethier, X. Shen and S.I. Snovida for their assistance in the laboratory

I thank Dr. J.P. Kunkel Dr. M.E. McComb and S. Shojania from the Department of Chemistry, University of Manitoba, Dr. O. Krokhin and M.P. Bromirski from the Department of Physics, University of Manitoba, for their assistance and collaborations.

I would like to thank my collaborators external to the university: Dr. Mark A. Bernards, Department of Plant Sciences, University of Western Ontario, London, ON.

I thank J.J.N. Perry and J.D.Oman for making the entire graduate studies experience most enjoyable.

Sincere gratitude and appreciation are expressed to the staff at I.Q.'s, especially A. Au, C. E. Bourgeois, F.G. Carreiro and S. Tsuchi.

Finally, I would like to thank my family for their love, support and understanding.

Table of Contents

1 INTRODUCTION	20
1.1 GLYCANS	20
1.1.1 Nomenclature and structural rules for oligosaccharides in glycoproteins	21
1.1.2 Protein glycosylation	21
1.2 MASS SPECTROMETRY	28
1.2.1 ESI	28
1.2.2 ESI process	29
1.2.2.1 Production of charged	29
1.2.3 Matrix-assisted laser desorption ionization	34
1.2.4 The MALDI process	34
1.3 MASS ANALYZERS	37
1.3.1 Triple quadrupole mass analyzer	37
1.3.1.1 Collision-induced dissociation	40
1.3.2 Time-of-flight mass spectrometry (TOF-MS)	42
1.4 CHEMICAL DERIVATIZATION	46
1.5 SAMPLE INTRODUCTION	50
1.5.1 Delivering carbohydrates to ESI-MS	51
1.5.2 The effect of detergents on glycan analysis	51
1.5.3 General detergent properties	52
1.6 REFERENCES	54
2 EFFECT OF 1-PHENYL-3-METHYL-5-PYRAZOLONE LABELLING ON THE FRAGMENTATION BEHAVIOUR OF ASIALO AND SIALYLATED N-LINKED GLYCANS UNDER ELECTROSPRAY IONIZATION CONDITIONS	58
2.1 INTRODUCTION	58
2.2 EXPERIMENTAL	60
2.2.1 Materials	60
2.2.2 PMP-derivatization	61
2.2.3 ESI-MS	61
2.2.4 ESI-MS/MS	61
2.2.5 On-line HPLC/ESI-MS	62
2.3 RESULTS	62
2.4 DISCUSSION	71
2.5 CONCLUSIONS	74
2.6 REFERENCES	75

3 INVESTIGATION OF DIFFERENT COMBINATIONS OF DERIVATIZATION, SEPARATION METHODS AND ELECTROSPRAY IONIZATION MASS SPECTROMETRY FOR STANDARD OLIGOSACCHARIDES AND GLYCANS FROM OVALBUMIN	77
3.1 INTRODUCTION	77
3.2 EXPERIMENTAL	80
3.2.1 Materials	80
3.2.2 Preparation of PMP derivatives	80
3.2.3 Preparation of ANTS derivatives	81
3.2.4 Enzymatic release of asparagines-linked oligosaccharides from ovalbumin	81
3.2.5 FACE profiling	81
3.2.6 On-line HPLC/ESI-MS	81
3.3 RESULTS	83
3.3.1 Ovalbumin characterization	83
3.3.2 NP-HPLC/ESI-MS	83
3.3.3 FACE	84
3.3.4 HPLC/ESI-MS studies of ANTS-labelled glycans	85
3.4 DISCUSSION	102
3.5 CONCLUSIONS	104
3.6 REFERENCES	105

4 A STUDY OF IMMUNOGLOBULIN G GLYCOSYLATION IN MONOCLONAL AND POLYCLONAL SPECIES BY ELECTROSPRAY AND MATRIX-ASSISTED LASER DESORPTION/IONIZATION MASS SPECTROMETRY	108
4.1 INTRODUCTION	108
4.2 EXPERIMENTAL	113
4.2.1 Preparation of IgG samples	113
4.2.2 N-deglycosylation	113
4.2.3 derivatization	114
4.2.4 FACE	114
4.2.5 HPLC/ESI-MS	114
4.2.6 ESI-MS	115
4.2.7 MALDI-TOF-MS and MALDI-QqTOF-MS	115
4.2.8 MALDI-QqTOF-MS/MS	115
4.3 RESULTS	116
4.3.1 Suitability of MALDI-MS	116
4.3.2 Comparative MALDI study	116
4.3.3 Qualitative characterization	117
4.3.4 Monoclonal murine IgG ₁ glycans	118
4.3.5 MALDI-MS/MS on prominent glycan compositions	119

4.4 DISCUSSION	140
4.4.1 Suitability of MALDI-MS	140
4.4.2 Comparative MALDI study	140
4.4.3 Qualitative characterization	142
4.4.4 Monoclonal murine IgG ₁ glycans	143
4.4.5 MALDI-MS/MS on prominent glycan compositions in IgG ₁	143
4.5 GLOBAL	143
4.6 CONCLUSIONS	144
4.7 REFERENCES	146
5 MALDI-MS/MS AND POST SOURCE DECAY STUDIES OF IgG GLYCANS	148
5.1 INTRODUCTION	148
5.2 EXPERIMENTAL	150
5.2.1 Preparation of IgG samples	150
5.2.2 <i>N</i> -deglycosylation	150
5.2.3 derivatization	150
5.2.4 MALDI-PSD and MALDI-MS/MS	150
5.3 RESULTS	151
5.4 DISCUSSION	162
5.4.1 Comparison of MALDI-MS/MS data between standards and IgG ₁ glycans	162
5.4.2 Comparison of MALDI-PSD and MALDI-MS/MS	164
5.4.3 Comparison of MS/MS data on <i>m/z</i> 1978 ions from IgG ₁	165
5.5 CONCLUSIONS	168
5.6 REFERENCES	169
6 SEQUENCING THE PRIMARY STRUCTURE OF ANIONIC POTATO PEROXIDASE	171
6.1 INTRODUCTION	171
6.2 EXPERIMENTAL	173
6.2.1 Plant material	173
6.2.2 Removal of heme groups	173
6.2.3 <i>N</i> -deglycosylation	173
6.2.4 Derivatization	173
6.2.5 Tryptic digestion	173
6.2.6 Glu-C digestion	174
6.2.7 ¹⁸ O isotopic labelling	174
6.2.8 Peptide fractionation	174
6.2.9 MALDI-MS and MALDI-MS/MS	174
6.3 RESULTS	175
6.3.1 MW measurement	175

6.3.2 Glycan characterization	175
6.3.3 Protein sequencing	175
6.3.4 Glycosylation sites	177
6.3.5 Peptide mapping	178
6.4 DISCUSSION	197
6.5 CONCLUSIONS	200
6.6 REFERENCES	201
7 CONCLUSIONS	203
7.1 CONCLUSIONS	203
7.2 FUTURE WORK	205

List of Figures

Figure 1.1 Monosaccharides encountered in mammalian glycoproteins.	22
Figure 1.2 (a) Trimannosyl core (b) Types of <i>N</i> -linked oligosaccharides.	26
Figure 1.3 Enzymatic deglycosylation.	27
Figure 1.4 Typical ESI source.	30
Figure 1.5. Charged droplet formation.	32
Figure 1.6 Positive ion electrospray process.	33
Figure 1.7 MALDI ionization process.	36
Figure 1.8 Quadrupole set up and applied potentials.	39
Figure 1.9 Tandem mass spectrometry.	41
Figure 1.10 Linear TOF.	44
Figure 1.11 Reflecting TOF.	45
Figure 2.1 Structures of the <i>N</i> -linked oligosaccharides used in this study.	65
Figure 2.2 ESI mass spectrum of native A1.	66
Figure 2.3 Reaction of <i>N</i> -linked oligosaccharides with 1-phenyl-3-methyl-5-pyrazolone.	67
Figure 2.4 ESI mass spectra of PMP-M3N2, acquired by on-line HPLC/MS.	68
Figure 2.5 ESI mass spectra of PMP-A1, acquired by on-line HPLC/MS.	69
Figure 2.6 On-line HPLC/ESI-MS traces, reconstructed from a full-scan experiment on a mixture containing 300 pmol each of PMP-A1, A2 and M3N2.	70
Figure 3.1 Labels used in this study.	87
Figure 3.2 ESI spectrum of hen ovalbumin glycans labelled with PMP.	88
Figure 3.3 On-line RP-HPLC/ESI-MS SICs obtained for PMP-labelled ovalbumin glycans.	89
Figure 3.4 NP-HPLC/ESI-MS of PMP-derivatized standards (tetraglucose and M3N2).	90
Figure 3.5 ESI spectra of NP-HPLC/MS separated standards at 60 V (tetraglucose and M3N2).	91
Figure 3.6 On-line NP-HPLC/ESI-MS SICs obtained for PMP-labelled Ovalbumin glycans.	92
Figure 3.7 Negative of a FACE gel, separation obtained for ANTS-labelled Ovalbumin glycans.	93
Figure 3.8 Calculated FACE migrations of ANTS-labelled glycans.	94
Figure 3.9 SICs obtained by on-line NP-HPLC/ESI-MS of ANTS-M3N2.	95
Figure 4.1 MALDI-QqTOF mass spectrum of an equimolar mixture of PMP-derivatized asialyl and sialylated <i>N</i> -linked oligosaccharides.	121
Figure 4.2 Asialyl and sialylated <i>N</i> -linked oligosaccharides standards.	123
Figure 4.3 MALDI-QqTOF mass spectrum of an equimolar mixture of PMP-derivatized asialyl <i>N</i> -linked oligosaccharides.	124
Figure 4.4 MALDI-QqTOF mass spectra obtained for PMP-derivatized polyclonal IgG glycans.	126
Figure 4.5 Suggested structures for bovine and human polyclonal IgG.	127
Figure 4.6 RP-HPLC/ESI-MS SICs of PMP-derivatized glycans	

	from polyclonal human IgG: (a) observed by MALDI-MS and (b) not observed by MALDI-MS.	128
Figure 4.7	MALDI-QqTOF-MS/MS spectrum of PMP-derivatized core-fucosyl asialyl digalactosyl biantennary glycan from murine monoclonal IgG glycan pool, obtained with 50% DO.	129
Figure 4.8	MALDI-QqTOF-MS/MS spectrum of PMP-derivatized core-fucosyl asialyl agalactosyl biantennary glycan from murine monoclonal IgG glycan pool, obtained with 50% DO.	131
Figure 4.9	MALDI-QqTOF-MS/MS spectrum of PMP-derivatized core-fucosyl asialyl digalactosyl biantennary glycan from murine monoclonal IgG glycan pool, obtained with 50% DO.	133
Figure 4.10	Comparison between (a) HPAEC-PAD, (b) FACE, and (c) MALDI- QqTOF-MS for the analysis of murine monoclonal IgG ₁ glycans.	135
Figure 5.1	MALDI-QqTOF-MS/MS spectrum of PMP-derivatized core-fucosylated asialyl agalactosyl biantennary glycan: [M+H] ⁺ ions of standard at <i>m/z</i> 1794.	153
Figure 5.2	MALDI-QqTOF-MS/MS spectrum of PMP-derivatized core-fucosylated asialyl agalactosyl biantennary glycans: [M+Na] ⁺ ions of standard at <i>m/z</i> 1816.	154
Figure 5.3	MALDI-QqTOF-MS/MS spectrum of PMP-derivatized core-fucosylated asialyl agalactosyl biantennary glycans: [M+Na] ⁺ ions at <i>m/z</i> 1816, from murine monoclonal IgG glycan pool, obtained with 50% DO.	154
Figure 5.4	MALDI-TOF-PSD spectrum of PMP-derivatized core-fucosylated asialyl agalactosyl biantennary glycans: [M+Na] ⁺ ions of standard at <i>m/z</i> 1816.	155
Figure 5.5	MALDI-TOF-PSD spectrum of PMP-derivatized core-fucosylated asialyl agalactosyl biantennary glycans: [M+Na] ⁺ ions at <i>m/z</i> 1816, from murine monoclonal IgG glycan pool, obtained with 50% DO.	155
Figure 5.6	MALDI-QqTOF-MS/MS spectrum of PMP-derivatized core-fucosyl asialyl digalactosyl biantennary glycans: [M+H] ⁺ ions of standard at <i>m/z</i> 2118.	156
Figure 5.7	MALDI-QqTOF-MS/MS spectrum of PMP-derivatized core-fucosyl asialyl digalactosyl biantennary glycan: [M+Na] ⁺ ions of standard at <i>m/z</i> 2140.	157
Figure 5.8	MALDI-QqTOF-MS/MS spectrum of PMP-derivatized core-fucosyl asialyl digalactosyl biantennary glycans: [M+Na] ⁺ ions at <i>m/z</i> 2140, from murine monoclonal IgG glycan pool, obtained with 50% DO.	157
Figure 5.9	MALDI-TOF-PSD spectrum of PMP-derivatized core-fucosyl asialyl digalactosyl biantennary glycans: [M+Na] ions of standard at <i>m/z</i> 2140.	158
Figure 5.10	MALDI-TOF-PSD spectrum of PMP-derivatized core-fucosyl asialyl digalactosyl biantennary glycans:	

	[M+Na] ⁺ ions at <i>m/z</i> 2140, from murine monoclonal IgG glycan pool, obtained with 50% DO.	158
Figure 5.11	MALDI-QqTOF-MS/MS spectrum of <i>m/z</i> 1978 ions, [M+Na] ⁺ corresponding to PMP-derivatized core-fucosyl asialyl monogalactosyl biantennary structures.	159
Figure 5.12	MALDI-PSD spectrum of <i>m/z</i> 1978 ions, [M+Na] ⁺ corresponding to PMP-derivatized core-fucosyl asialyl monogalactosyl biantennary structures.	160
Figure 5.13	MALDI-QqTOF-MS/MS spectra of <i>m/z</i> 1978 [M+Na] ⁺ ions of PMP-derivatized oligosaccharides released from different IgG species.	161
Figure 6.1	MALDI linear-TOF spectra of (a) glycosylated anionic potato peroxidase (b) deglycosylated anionic potato peroxidase.	179
Figure 6.2	MALDI-QqTOF mass spectrum obtained for PMP-derivatized anionic potato peroxidase glycans.	180
Figure 6.3	Suggested structures.	181
Figure 6.4	MALDI-QqTOF-MS/MS spectrum of PMP-derivatized glycan at <i>m/z</i> 1541.	182
Figure 6.5	Mass spectrum for the tryptic digest of anionic potato peroxidase.	183
Figure 6.6	Mass spectrum of the Glu-C digest of anionic potato peroxidase.	184
Figure 6.7	MALDI-QqTOF-MS/MS spectrum of <i>m/z</i> 842.7.	185
Figure 6.8	Spectra of fractionated Glu-C digest of anionic potato peroxidase.	187
Figure 6.9	Mass spectra of (a) C18 separated fraction at 30% ACN (b) Glu-C digest mixture.	188
Figure 6.10	Spectra of fractionated Glu-C digest of anionic potato peroxidase.	189
Figure 6.11	MALDI mass spectrum of tryptic digests of (a) glycosylated anionic potato peroxidase (b) deglycosylated anionic potato peroxidase.	190
Figure 6.12	MALDI-QqTOF-MS/MS spectrum of non-specific tryptic Glycosylated peptide.	191
Figure 6.13	Experimental peptide map of anionic potato peroxidase.	192
Figure 6.14	Comparison of the published sequence of anionic potato peroxidase with experimental peptide coverage.	193

List of Tables

Table 1.1 Glycosidic linkages encountered in mammalian glycoproteins and symbols used for monosaccharides.	24
Table 1.2. Carbohydrate fragmentation nomenclature.	48
Table 3.1 Assigned <i>Mr</i> and composition of oligosaccharides cleaved from ovalbumin derivatized with PMP (RP-HPLC/ESI-MS).	97
Table 3.2 Assigned <i>Mr</i> and composition of oligosaccharides cleaved from ovalbumin derivatized with PMP (normal-phase HPLC/ESI-MS).	100
Table 4.1 Comparison of MALDI signal intensities measured on five instruments, versus results from HPAEC-PAD analyses.	136
Table 4.2 Suggested compositions of oligosaccharides released from human and bovine polyclonal IgG, as detected by MALDI-MS and HPLC/ESI-MS.	137
Table 4.3 Suggested compositions of oligosaccharides released from murine monoclonal IgG ₁ , as detected by MALDI-MS and HPLC/ESI-MS.	138
Table 4.4 Comparison of relative abundances of oligosaccharides released from monoclonal murine IgG1 as measured by MALDI-QqTOF-MS, FACE, and HPAEC-PAD, for varying DO concentrations during cell growth.	139
Table 6.1 Suggested compositions of oligosaccharides released from anionic potato peroxidase, as detected by MALDI-MS.	194
Table 6.2 Glu-C digest of anionic potato peroxidase.	195
Table 6.3 Tryptic digest of anionic potato peroxidase.	196

List of Schemes

Scheme 1.1 Carbohydrate fragmentation nomenclature.	49
Scheme 4.1 General biantennary structure for IgG glycans.	120
Scheme 5.1 Scheme showing the nomenclature for describing the major fragment ions from core-fucosylated asialyl agalactosyl biantennary glycan.	153
Scheme 5.2 Scheme showing the nomenclature for describing the major fragment ions from core-fucosylated asialyl digalactosyl biantennary glycan.	156
Scheme 5.3 Possible alternative structures for (a) M_3N_4F and (b) $G_2M_3N_4F$ (M_5N_4F) from IgG. In (c), possible hybrid structure, with formula M_6N_4F .	166
Scheme 5.4 Formation of abundant fragment ions in the MS/MS spectra of $[M+Na]^+$ ions of PMP-derivatized IgG glycans.	167

Abstract

Alterations in glycan structures are associated with various developmental and pathological states of glycoproteins. The direct involvement of glycans in biological functions has been widely discussed and the generally accepted view suggests that they have two significant roles, one of which is to confer physiochemical properties onto proteins, and the other is to act as signals in cell-surface recognition phenomena. This thesis outlines the use of mass spectrometry, for the identification of protein-bound glycans. The methods described in this thesis improve on the derivatization of glycans by making use of state-of-the-art mass spectrometric resources, and extracting information from mass spectrometric spectra. To demonstrate their applicability, IgG and anionic potato peroxidase glycans are characterized.

Experiments were conducted on the high performance liquid chromatography (HPLC) and electrospray ionization mass spectrometry (ESI-MS) behaviors of 1-phenyl-3-methyl-5-pyrazolone (PMP)-labelled asialo and sialylated sugars vs. the native compounds. Suitability of 2-aminonaphthalene trisulfone (ANTS) derivatives for HPLC/ESI-MS was tested, in an attempt to include only one step of derivatization (ANTS) while allowing two types of analysis (FACE and HPLC/ESI-MS). We report on the use and comparison of derivatization (PMP vs. ANTS), HPLC, FACE and ESI-MS to characterize the glycans of ovalbumin.

N-linked oligosaccharides released from human and bovine polyclonal immunoglobulin G (IgG) obtained from commercial sources and also from a monoclonal IgG1 secreted by murine B-lymphocyte hybridoma cells (CC9C10) grown under different serum-free conditions (different steady-state dissolved oxygen concentrations) were characterized qualitatively by HPLC/ESI-MS and matrix assisted laser desorption ionization (MALDI-MS). MALDI-MS/MS as a quick and efficient method for comparing known and unknown structures with the same composition was explored.

Primary structure of anionic potato peroxidase, an enzyme that plays a key role in cell-suberization was characterized. Glycan structures and the glycosylation sites were determined.

ABBREVIATIONS

AA	amino acid	GFC	gel filtration chromatography
AA-Ac	3-(acetylamino)-6-aminoacridine	GlcNAc	<i>N</i> -acetylglucosamine
AB	2-aminobenzamide	HPAEC-PAD	high performance anion exchange chromatography pulsed amperometric detection
ABEE	4-aminobenzoic acid ethyl ester		
ACN	acetonitrile	HPLC	high performance liquid chromatography
AMAC	2-aminoacridone	IgGs	Immunoglobulins
ANTS	8-aminonaphthalene-1,3,5-trisulfonic acid	LC	liquid chromatography
CE	capillary electrophoresis	LIF	laser-induced fluorescence
CID	collision induced dissociation	mAb	monoclonal antibody
DHB	dihydroxybenzoic acid	MALDI	matrix assisted laser desorption ionization
DO	dissolved oxygen	Man	mannose
DP	degrees of polymerization	Mr	molecular weight relative to ¹² C
DTT	dithioreitol	MS	mass spectrometry
ESI	electrospray ionization	MS/MS	tandem mass spectrometry
Fab	antibody antigen-binding fragment	Neu5Ac	5(<i>N</i>)-acetylneuraminic acid
FACE	fluorophore assisted carbohydrate electrophoresis	Neu5Gc	5(<i>N</i>)-glycoylneuraminic acid
Fc	antibody C-terminal fragment	NMR	nuclear magnetic resonance
Gal	galactose		

NP	normal-phase
PA	2-aminopyridine
PMP	1-phenyl-3-methyl-5-pyrazolone
PNGaseF	peptide N-glycosidase F
PSD	post-source decay
QQQ	triple quadrupole
RP	reversed-phase
SDS-PAGE	sodium dodecyl sulfate polyacrylamide gel electrophoresis
SIC	selected ion chromatogram
SPAD	suberin poly(aliphatic) domain
SPPD	suberin poly(phenolic) domain
TIC	total ion chromatogram
TMAPA	trimethyl(<i>p</i> - aminoethyl)ammonium chloride
TOF	time-of-flight
UV	ultraviolet

1 INTRODUCTION

1.1 GLYCANS

Recent findings have demonstrated that alterations in glycan structures are associated with various developmental and pathological states of glycoproteins and have great biological significance [1]. The direct involvement of glycans in biological functions has been widely discussed and the generally accepted view suggests that they have two significant roles, one of which is to confer certain physiochemical properties onto proteins, and the other is to act as signals in cell-surface recognition phenomena [2].

Glycoproteins currently constitute an active area of research and, since the functional significance of the carbohydrate moieties has become increasingly apparent, there has been a need for rapid, reliable and sensitive methods for their determination. However, the problem with structural characterization of carbohydrates, in contrast to linear protein and nucleic acid biopolymers is that carbohydrates exhibit a wide structural variety due to different branching of the carbohydrate core and linkage of the monosaccharide subunits as well as derivatization of monomers by, e.g., sulfate or phosphate.

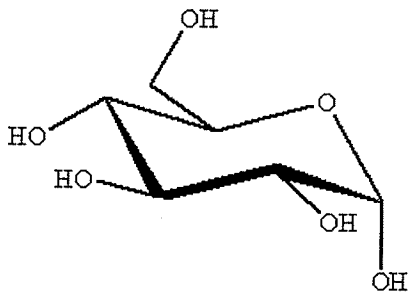
Several methods have been developed for this purpose including use of nuclear magnetic resonance (NMR) spectroscopy [3], high performance anion exchange chromatography with pulsed amperometric detection (HPAEC-PAD) [5,6], analysis with glycosidases in combination with efficient separation techniques [4], reversed phase high performance liquid chromatography (RP-HPLC) [7], capillary electrophoresis (CE) [8], electrospray ionization mass spectrometry (ESI-MS) [9], and matrix assisted laser desorption ionization mass spectrometry (MALDI-MS) [10].

1.1.1 Nomenclature and structural rules for oligosaccharides in glycoproteins

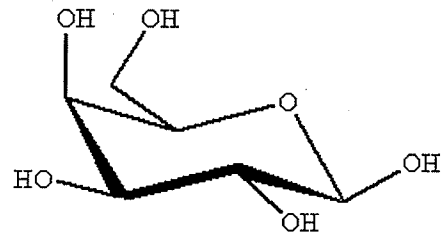
Glycoprotein oligosaccharides are polymers of monosaccharides (Figure 1.1). Oligosaccharides are generated by bond formation between the anomeric hydroxyl of one monosaccharide and a ring hydroxyl of another monosaccharide. This type of bond is called a glycosidic bond. Each of the ring hydroxyls on the monosaccharide is potentially available to form a glycosidic bond. The linkages occur between carbons 1-2, 1-3, 1-4, and 1-6 for neutral monosaccharides; carbons 2-3, 2-6, and 2-8 for sialic acids (Table 1.1). Each linkage may also have either an α - or β -anomeric configuration and more than one ring hydroxyl of a given monosaccharide constituent may be involved in a glycosidic bond, generating a branched, non-linear polymer.

1.1.2 Protein Glycosylation

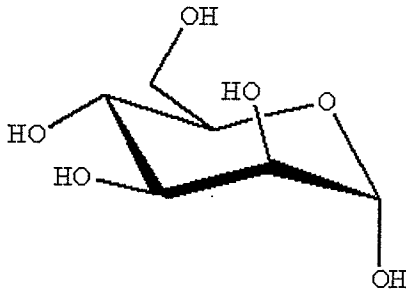
The complete analysis of a glycoprotein involves identification of the entire array of oligosaccharide structures attached to the protein as well as the assignment of each structure to its site(s) of attachment on the polypeptide chain. Structural analysis of glycoproteins is a formidable challenge due to the heterogeneity of oligosaccharide chains which are usually present on a glycoprotein. Different oligosaccharide structures are often attached to multiple different sites in a glycoprotein, and heterogeneity may exist not only among these different sites but also within the group of structures which occur at each single site of glycosylation. Classically molecules called glycoproteins are serum and cell membrane proteins which contain oligosaccharide substituents linked to asparagine (Asn, termed *N*-linked) in the Asn-Xxx-Ser/Thr sequence (where Xxx is any amino acid except proline), or to serine (Ser) or threonine (Thr) (Ser/Thr, termed *O*-linked) where no consensus sequence for attachment is known.



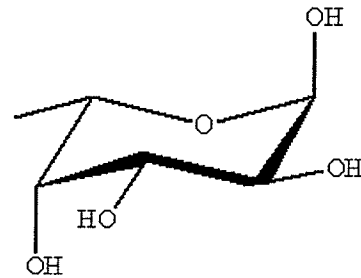
α -D-glucose



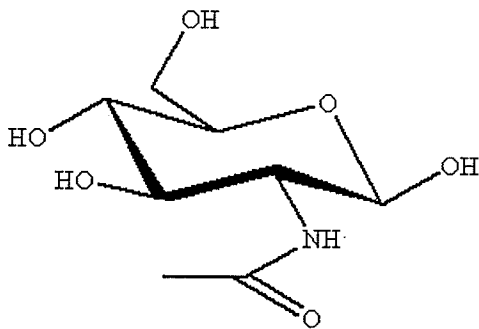
β -D-galactose



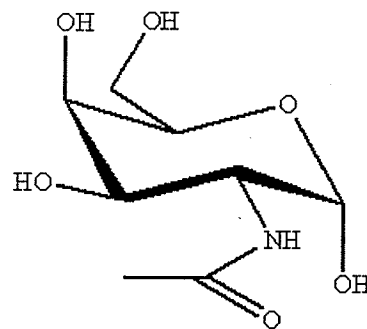
α -D-mannose



α -L-fucose

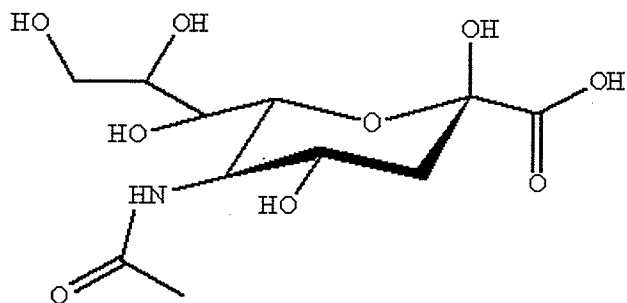


N-acetyl- β -D-glucosamine

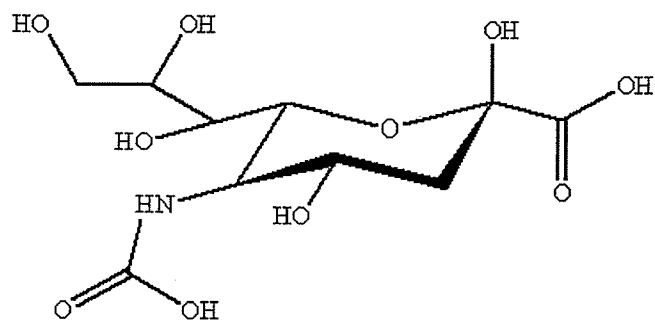


N-acetyl- α -D-galactosamine

Figure 1.1 Monosaccharides encountered in mammalian glycoproteins












N-acetyl- α -neuraminic acid



N-glycolyl- α -neuraminic acid

Figure 1.1 (cont'd)

Table 1.1 Glycosidic linkages encountered in mammalian glycoproteins and symbols used for monosaccharides

Monosaccharide	Abbreviation	Symbol	Anomers	Linkages
D-glucose	Glc		α	2,3
D-galactose	Gal		α β	3 3,4,6
D-mannose	Man		α β	2,3,6 4
L-fucose	Fuc		α	2,3,4,6
D-xylose	Xyl		β	2
<i>N</i> -acetyl-D-glucosamine	GlcNAc		β	2,3,4,6
<i>N</i> -acetyl-D-galactosamine	GalNAc		α β	3 4
5(<i>N</i>)-acetylneuraminic acid	Neu5Ac		α	3,6,8
5(<i>N</i>)-glycolylneuraminic acid	Neu5Gc		α	3,6,8

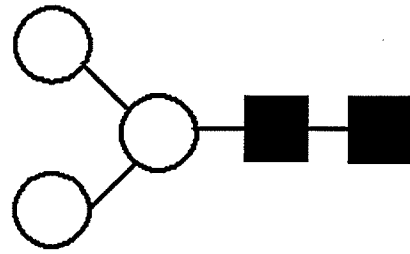
In order to isolate and analyze free oligosaccharides from a glycoprotein, they must be either chemically or enzymatically released. The released oligosaccharides can belong to one of three structural class; complex, hybrid or high-mannose type (Figure 1.2(b)). Chemical release of *N*-linked oligosaccharides is most often performed by hydrazinolysis, which cleaves the *N*-acetylglucosamine-asparagine (GlcNAc-Asn) linkage, leaving a glycosylamine residue as the reducing terminus [11].

For enzymatic release of *N*-linked oligosaccharides, the intact glycoprotein can be treated with either endo- β -*N*-acetylglucosaminidase (Endo H) or peptide-*N*-glycosidase F (PNGase F) (Figure 1.3) [12,13]. PNGase F releases most carbohydrates except those that contain α 1-3 linked fucose to the reducing terminal GlcNAc [14], then peptide-*N*-glycosidase A (PNGase A) is used. The enzyme cleaves the intact glycan as the glycosylamine and leaves aspartic acid in place of the asparagine at the *N*-linked site of the protein. The cleaved glycosylamine hydrolyses to form the reducing terminus of a glycan.

The analysis of oligosaccharides attached to glycoproteins by mass spectrometry has seen tremendous revolution in the past few years due to ESI-MS [9] and MALDI-TOF-MS [10]. The increased sensitivity and vastly extended mass range of the two techniques has permitted the analysis of large oligosaccharides which was previously difficult or even not possible. Significantly lower sample levels may now be characterized by these modern ionization methods.

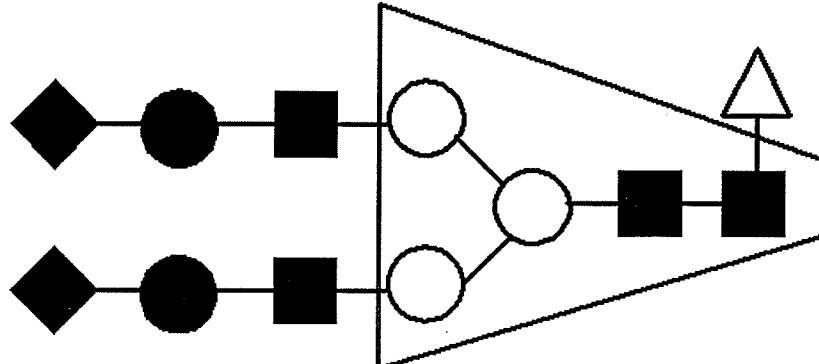
a

Trimannosyl core

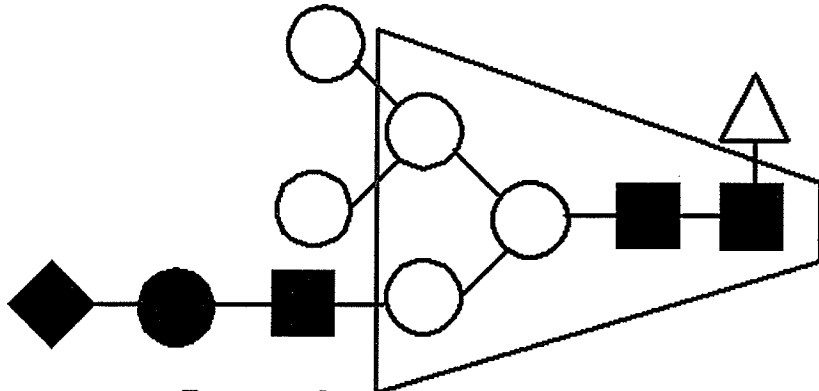


b

Complex



Hybrid



High-mannose

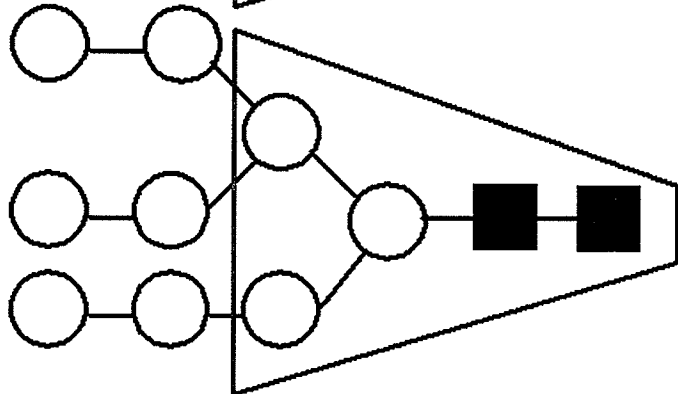


Figure 1.2. (a) Trimannosyl core (b) Types of *N*-linked oligosaccharides

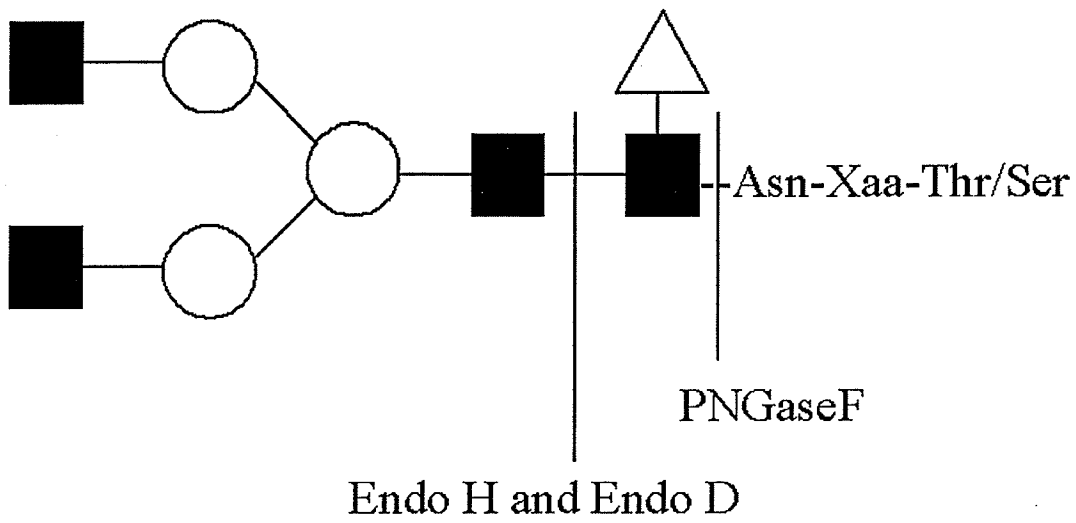


Figure 1.3 Enzymatic deglycosylation

1.2 MASS SPECTROMETRY

The focus of mass spectrometry is the “weighing of individual molecules”.

The weight of a molecule is determined by first ionizing the molecule, then measuring the response of the ion to both electric and magnetic fields. The formation of ions is essential because only those molecules that are charged can be measured by mass spectrometry. Early in the development of mass spectrometry, ions were produced in a variety of ways, from harsh ionization techniques, like electron impact (EI), to softer techniques such as chemical ionization (CI) and fast atom bombardment (FAB). The terms “hard” and “soft” refer to the propensity of an ionization technique to break apart the molecules. Hard ionization techniques, such as EI, lead to the development of many fragment ions. Often though, we are interested in the overall molecular mass of a species which is not always detected by EI for larger molecules. To observe the molecular ions for larger and more labile compounds, a softer method of ionization is required. Both CI and FAB are soft ionization techniques, than EI leading to the production of molecular ions, but even these techniques have their limitations when applied to large molecules.

1.2.1 ESI

The electrospray (ES) process dates to experiments by Zeleny [15]. However, it was Malcolm Dole’s experiments in the late 1960's and early 1970's which suggested that intact molecular ions could be introduced into the gas phase [16] but the potential of ESI was not realized until 1984 when ESI was coupled to a quadrupole mass analyzer [17]. In this mode, nonvolatile materials could be ionized without fragmentation using either positive or negative ionization. Again in 1984, Dole and co-workers, reported that ions bearing 1-3 positive charges were observed for lysozyme [18]. This

indicates that ESI of molecules leads to the phenomenon of multicharging, the placement of a number of either positive or negative charges on a molecule [19]. Multicharging leads to substantially lower mass-to-charge (m/z) ratios.

1.2.2 ESI Process [17]

The production of gas phase ions from electrolytes in solution involves three major steps: (1) production of charged droplets at the ES capillary tip; (2) charged droplet shrinkage by solvent evaporation and repeated droplet integrations leading ultimately to very small highly charged droplets capable of producing gas-phase ions, and (3) the actual mechanism by which gas-phase ions are produced from the very small and highly charged droplets.

1.2.2.1 Production of Charged Droplets at the ES Capillary Tip

As shown in the schematic representation (Figure 1.4), typically a voltage V_c , of 2-3 kV, is applied to the metal capillary (ESI source) and located 1-3 cm from the counter electrode. The counter electrode can typically be a plate with an orifice leading to the mass spectrometric sampling system or sampling capillary, mounted on a plate, which leads to the mass spectrometer. An analyte containing solution at flow rate 1-20 μL is passed through the capillary to its terminus where it is electrosprayed. The ESI process can be assisted pneumatically using a high velocity annular flow of gas (N_2) at the terminus. When turned on, the field E_c will penetrate the solution at the capillary tip. The influence of the electric field causes the positive and negative ions to move around in the solution until a charge distribution occurs. The charge distribution counteracts the electric field, leading to a field free condition. If for example, the capillary is the positive electrode, the positive ions in the solution will have drifted downfield in the solution,

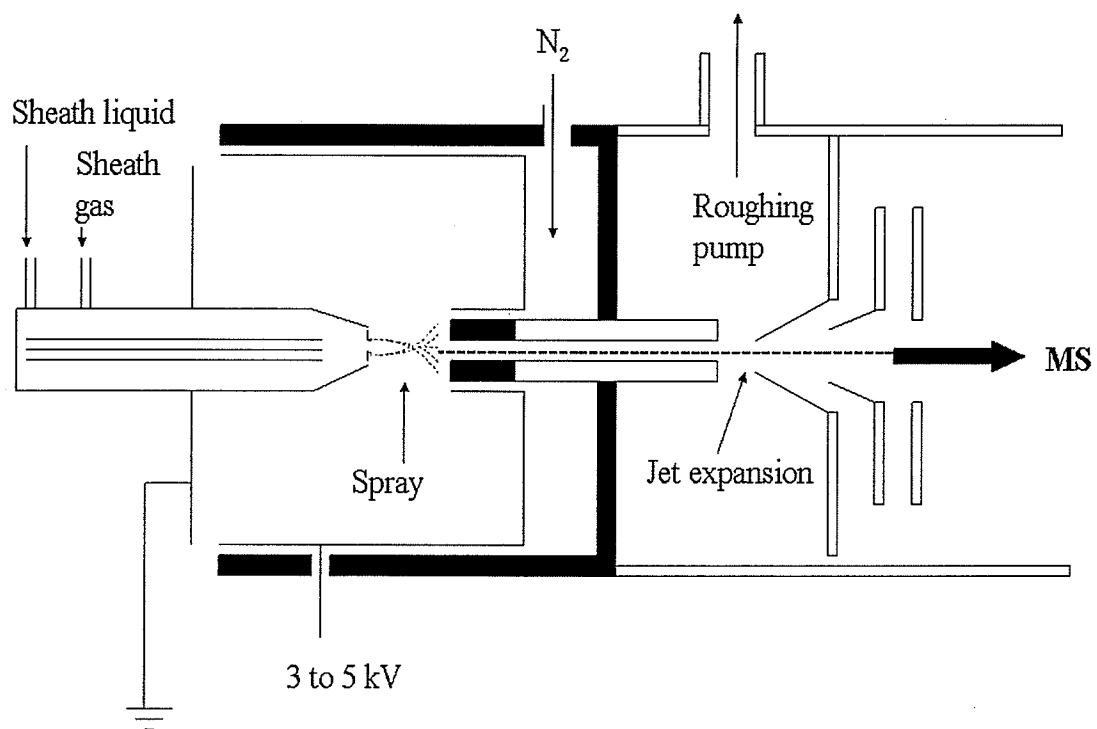


Figure 1.4. Typical ESI source

toward the meniscus of the liquid, and the negative ions will have drifted in the opposite direction. The accumulation of positive ions at the surface results in a mutual repulsion between the ions. This leads to destabilization of the liquid surface and resulting in surface expansion, allowing the positive ions and the liquid to move downfield. The described mechanism results in the formation of a Taylor cone. If the electric field that is applied is high enough, a fine jet emerges from the tip of the cone and breaks up into small charged droplets (Figure 1.5). These small droplets are positively charged due to the presence of excess positive ions at the surface of the cone and the cone jet. The droplets are drawn through space, via the potential gradient, towards the inlet of the mass spectrometer. The charged droplets that are produced by the cone jet shrink as a result of solvent evaporation while the charge remains constant. At a given radius the droplets approach the Rayleigh limit. The instability results in coulombic fission. These smaller droplets continue to evaporate until they too reach the Rayleigh limit and disintegrate or fission. A series of such evaporation-disintegration sequences ultimately leads to gas-phase ions (Figure 1.6).

One of the intrinsic advantages of ESI is its ability to place multiple charges on a particular species. The inherently unique characteristic of extensive multiple charging distinguishes ESI from all other ionization techniques. Multiple charging can occur by either proton or cation attachment in the positive ion mode and proton subtraction in the negative ion mode. The multiple charging effect makes the analysis of large molecules with M_r up to 100000 to 150000 Da possible using conventional mass analyzers with only modest m/z range. This is possible because by increasing the number of charges on a molecule, the m/z ratio is lowered, thus amenable to conventional mass

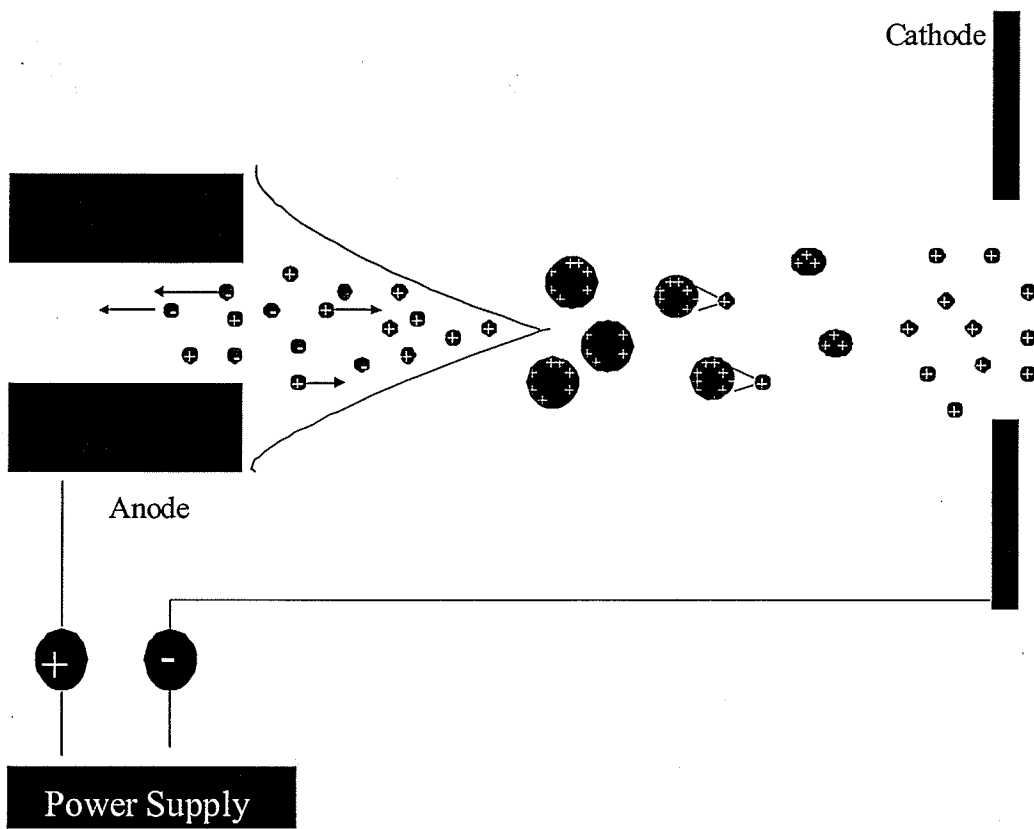
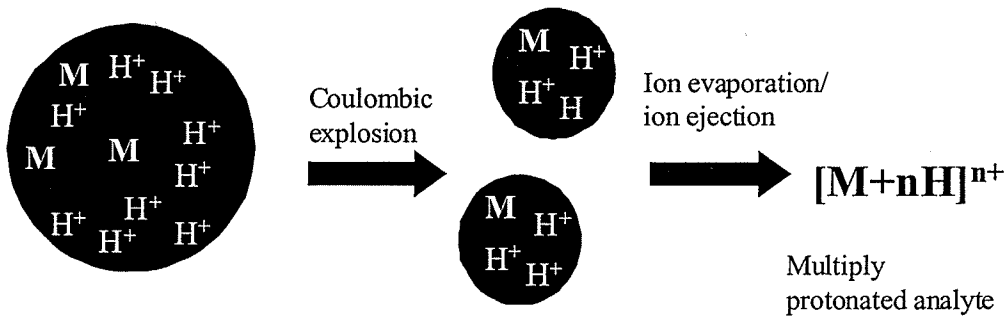


Figure 1.5. Charged droplet Formation



Droplet after evaporation

Figure 1.6. Positive ion electrospray process

spectrometers that have m/z ranges of 1000-3000 Da. For example, consider the protein dethiobiotin synthase, which has a MW of 24000. If 10 protons were placed on the protein, and thus 10 positive charges, it would be observed at m/z 2401 ($[24000 + 10] / 10 = 2401$) and appear within the conventional m/z range of most mass spectrometers.

1.2.3 Matrix-assisted laser desorption ionization (MALDI)

MALDI was initially introduced by Hillenkamp and Karas in the late 1980s [20]. It was first developed using ultraviolet (UV) lasers and now employs both UV and infrared (IR) lasers. MALDI has become a widespread analytical tool for peptides, proteins, and most other biomolecules (oligonucleotides, carbohydrates, natural products, and lipids). The efficient and directed energy transfer during a matrix assisted laser induced desorption process provides high ion yields of the intact analyte, and allows for the measurement of compounds with high accuracy and subpicomole sensitivity [21-23].

1.2.4 The MALDI Process

MALDI is an example of solid state sample introduction. In MALDI analysis, an analyte and a large molar excess of matrix, usually a UV-absorbing weak organic acid, are mixed together in an organic or aqueous solvent for mutual solubility. Once the solvent is removed, the matrix and analyte co-crystallize on the sample plate. Matrices are chosen based on their ability to co-crystallize with the analyte, their absorptivity for the laser radiation, and their ability to act as a proton donor and receptor to the analyte [24,25].

Once the analyte has co-crystallized with the matrix, it is placed in the mass spectrometer. Radiation from the laser is focused on the sample probe tip through

appropriate optics. The intensity of the laser should be sufficient to allow production of ions. Because the MALDI process is inherently a pulsed procedure, the most common mass spectrometers used are time-of-flight instruments, operated in either linear or reflectron mode.

The matrix absorbs the incident radiation and literally explodes, producing a thermal plume of excited matrix and analyte molecules/ions. In this plume, gas phase ion-molecule reactions occur, transferring a proton or cation from the matrix to the analyte [23,26]. Once the analyte is charged, it is accelerated into the mass spectrometer by applying a potential between the target and the acceleration grid (Figure 1.7).

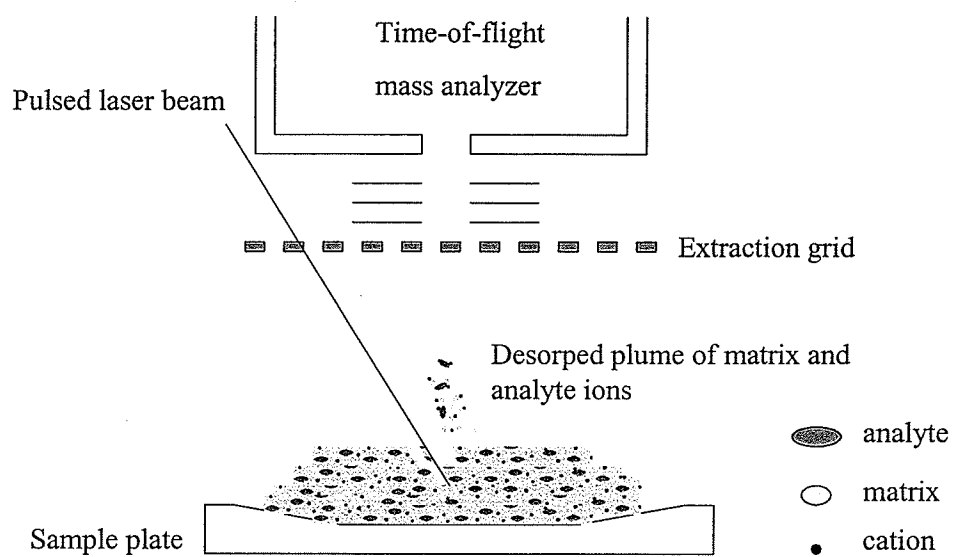


Figure 1.7 MALDI ionization process

1.3 MASS ANALYZERS

1.3.1 Triple Quadrupole Mass Analyzer

The principles of quadrupole mass analyzers were first introduced in the 1950's by Paul and Steinwedel [27]. These analyzers have now become part of most mass spectrometers because of ease, low cost and small size.

A quadrupole mass analyzer consists of four parallel rods through which the ions being separated are passed. Figure 1.8 shows a schematic diagram of a typical quadrupole consisting of 4 cylindrical rods. Ions enter through a series of focusing lenses along the z-axis and normal to the direction of the quadrupoles. The poles have a fixed DC and alternating RF voltages applied to them, generating an electric field:

$$\Phi = U - V\cos\omega t$$

where:

- Φ is the total potential applied
- U is the DC potential (500 to 2000 V)
- V is the "zero peak" amplitude of the RF voltage (0 to 3000 V)
- ω is the angular frequency in rads/s = $2\pi f$ where f is the RF frequency

At given values of U , V and ω only certain ions will have stable trajectories through the quadrupole. The range of ions of different m/z values capable of passing through the mass filter depends on the ratio of U to V . All other ions will have trajectories which are unstable (i.e., they move with large amplitudes in x- or y-direction) and will be lost (Figure 1.8). The equation of motion for a singly-charged particle can be expressed as a Mathieu equation [28] from which one can define expressions for the Mathieu parameters a_u and q_u ,

$$a_u = a_x = -a_y = \frac{4zU}{m\omega^2 r_0^2}$$

$$q_u = q_x = -q_y = \frac{2zV}{m\omega^2 r_0^2}$$

where:

r_0 is half the distance between two opposite rods

If u is less than the radius of the field, the ions will pass through the quadrupole to the detector. For a given quadrupole, r and $\omega = 2\pi f$ remain constant while U and V may be varied.

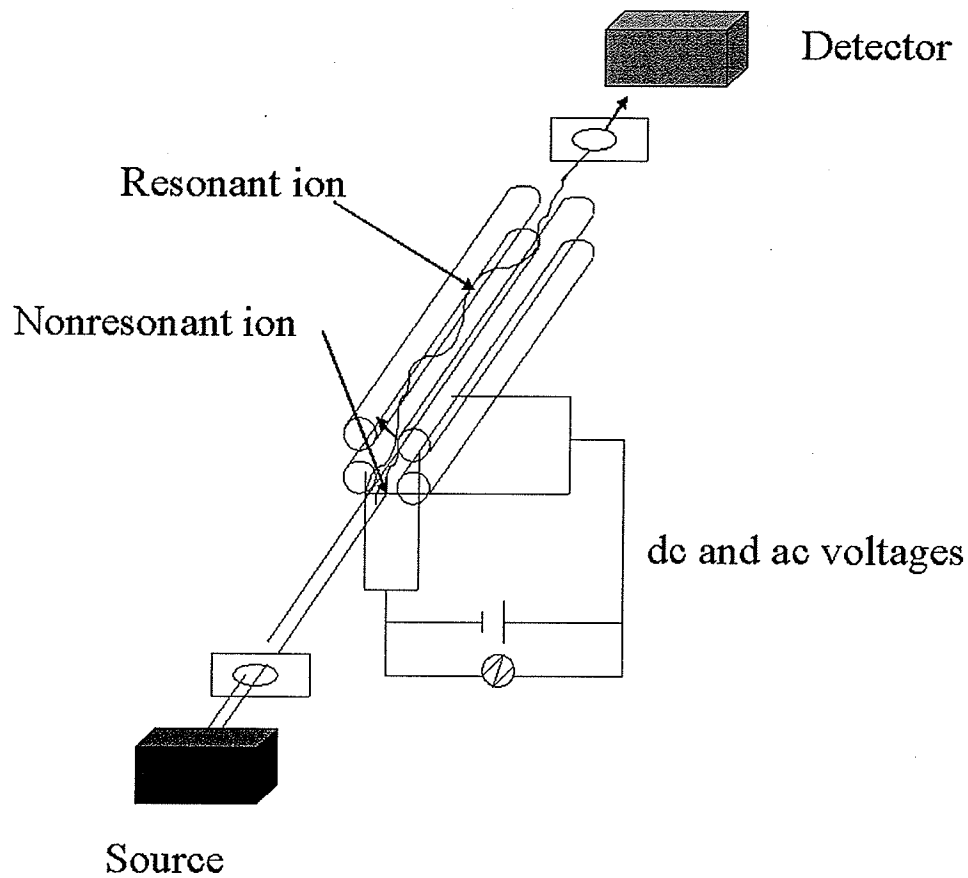


Figure 1.8. Quadrupole set up and applied potentials

1.3.1.1 Collision-Induced Dissociation

Collision-induced dissociation (CID) is most often performed by connecting two mass analyzers in tandem (tandem mass spectrometry, MS/MS) with a collision cell in between (Figure 1.9). Using the first mass analyzer, ions of a particular m/z value are selected as the analyte is being ionized. The selection of ions with the first mass analyzer (MS-1) also acts as a separation or purification step, since ions of all m/z values are rejected. The selected precursor ions then pass into the collision cell where they collide with a neutral gas such as helium. These collisions increase the internal energy of the ions (collisional activation), causing fragmentation of the precursor ions. The resulting fragment ions then pass into the second mass analyzer and onto the detector, creating a mass spectrum of the product ions from precursors of the particular selected mass.

Ions can be collisionally activated through high energy (keV) collisions or low energy (eV) collisions, depending on the mass analyzers employed. Most high energy CID experiments are performed on tandem four-sector instruments consisting of two double focusing mass spectrometers connected in tandem with a collision cell in between. Most low-energy CID experiments are performed on triple quadrupole instruments where the first and third quadrupoles are analogous to MS-1 and MS-2 of a four sector instrument, and the second quadrupole functions as the collision cell. As one might expect, high energy CID produces more types of fragment ions than low energy CID. The advantage of obtaining additional types of fragment ions is that more detailed structurally significant information may be obtained, such as those from ring cleavage processes in oligosaccharides [29].

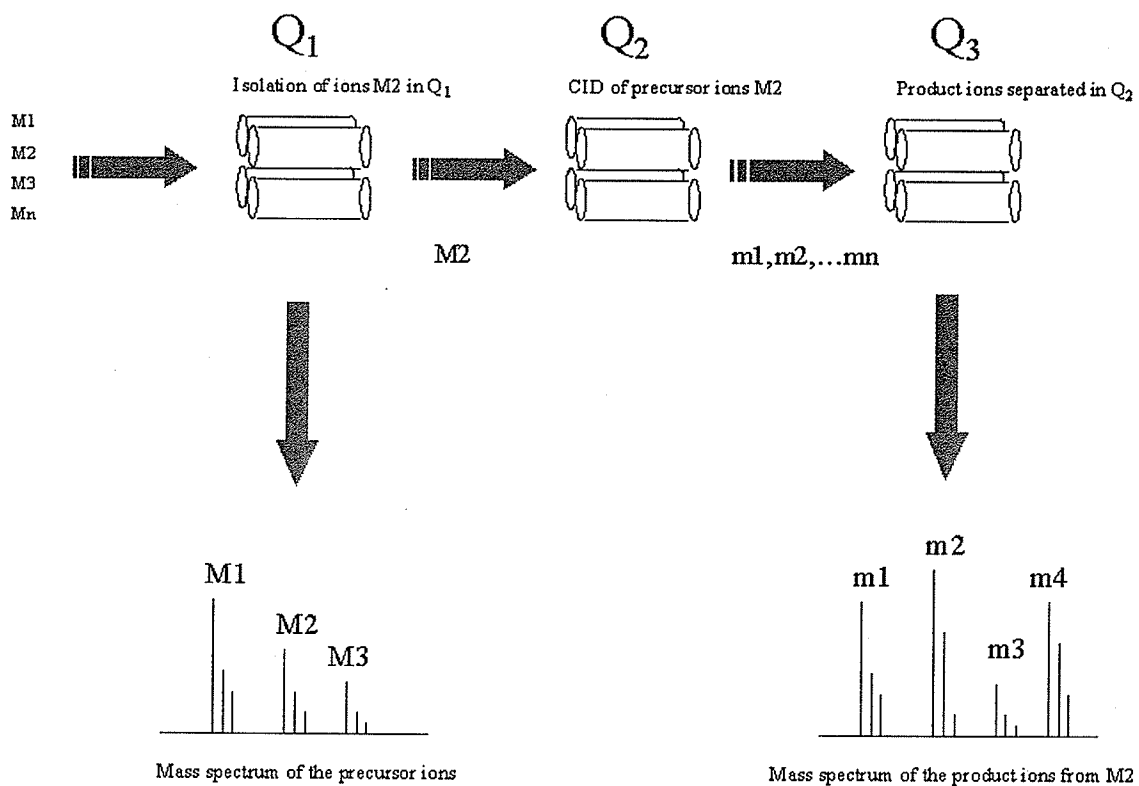


Figure 1.9. Tandem mass spectrometry

1.3.2 Time-of-flight mass spectrometry (TOF-MS)

TOF-MS was first successfully used to measure m/z values of ions in the 1950's [30,31]. The principle of mass analysis in a TOF analyzer involves accelerating a set of ions with different m/z values to a detector and giving all the ions the same kinetic energy (Figure 1.10). Because they have the same energy but differ in their masses, they reach the detector at different times. High mass ions require more time than low mass ions.

Thus,

$$KE = \frac{1}{2} m\nu^2 = qV$$

where,

KE is the kinetic energy of the ion
q is the charge where $q = ze$
 ν is velocity
m is mass of the ion
V is the applied acceleration potential

Ions will travel a given distance, d, within a time, t,

$$t = d/\nu$$

Combining equations yields the equation which relates the mass of the ion to its flight time:

$$t^2 = m/z (d^2/2Ve)$$

Early TOF instruments were not popular due to their limits in resolution as a result of the considerable spatial and kinetic energy spreads of the ions when introduced into the flight tube. The spread in kinetic energy can be partially compensated by a device called reflectron, which employs ion mirrors to solve the problem [32]. Ion mirrors produce electrostatic repeller fields into which ions of higher energy will penetrate deeper

than lower energy ions. High energy ions will be turned around and will arrive at the detector at the same time as ions of lower initial energy, which do not go as deep in the field. Thus, increasing the flight time by increasing the length of the drift tube would lead to higher resolution since Δt would remain the same but t would become greater (Figure 1.11).

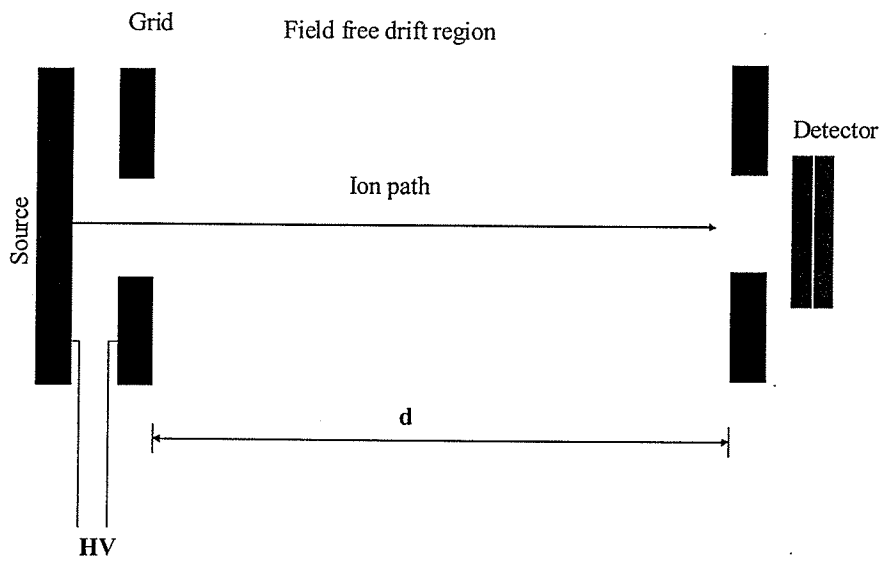


Figure 1.10 Linear TOF

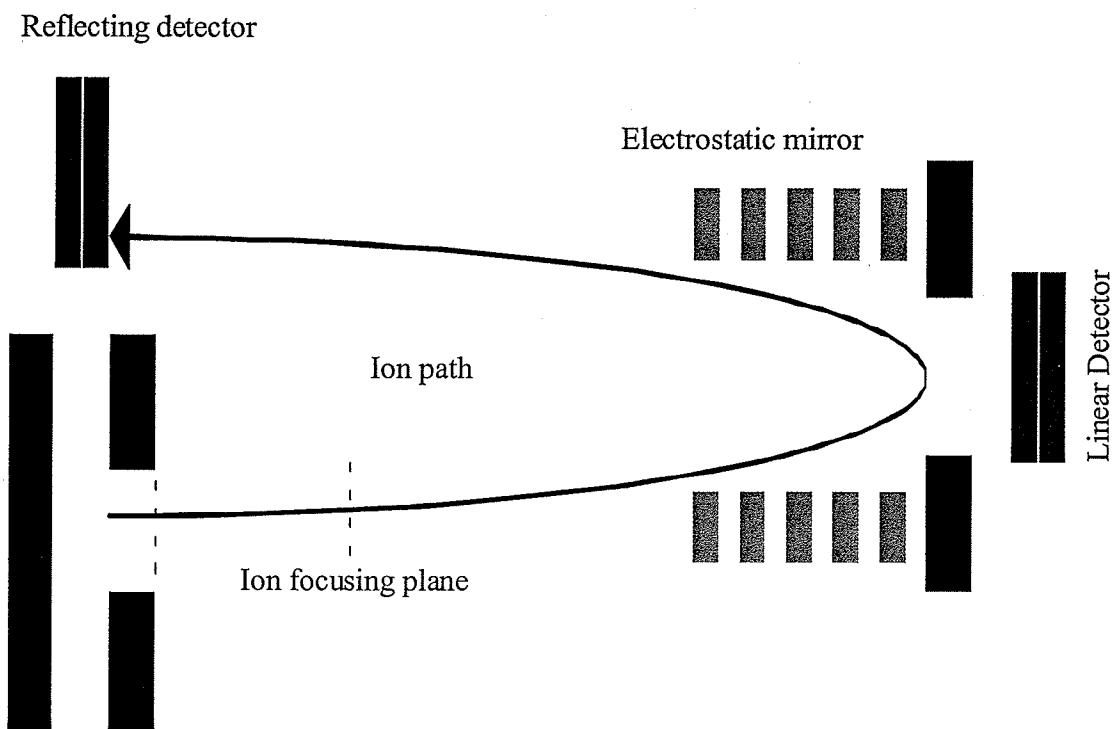


Figure 1.11 Reflecting TOF

1.4 CHEMICAL DERIVATIZATION FOR MASS SPECTROMETRIC ANALYSIS

Unlike the usual approach to proteins, the majority of mass spectrometry strategies in the carbohydrate area involve derivatization. Derivatized glycans fragment in a predictable manner, leading to abundant ions that can be assigned unambiguously. Underivatized samples, on the other hand, are less predictable in their fragmentation behavior and frequently give fragment ions that are derived from multiple cleavages and cannot, therefore, be attributed to a unique structure. Furthermore, due to the weak acidity or basicity of most *N*- and *O*-linked glycans, free oligosaccharides do not efficiently charge by protonation or deprotonation. It is necessary, therefore, to use derivatization techniques, except for acidic carbohydrates which already contain a negative charge.

Table 1.2 illustrates the types of fragment ions observed for derivatized as well as underivatized oligosaccharides [33,34]. Unfortunately, the carbohydrate community has not agreed on the use of a single systematic nomenclature, so Table 1.2 illustrates the nomenclature for the two most often described systems. The cleavage on the non-reducing side of glycosidic bonds to give oxonium ions are termed A-type cleavage ions by some researchers [33], while they are termed B_i -ions by others [34]. The subscript, *i*, represents the number of the glycosidic bonds cleaved, relative to the non-reducing terminus. *Y*- and *C*-ions, also referred to as β -cleavage ions, involve hydrogen transfer (or sometimes methyl or acetyl transfer in derivatized samples) to the glycosidic oxygen, as shown in Table 1.2. Finally, *X*- and *A*-ions, also referred to as ring cleavage ions, are believed to be formed by various types of fragmentation involving specific hydrogen transfers and resulting in the cleavage of sugar rings.

Scheme 1.1 illustrates the details of nomenclature proposed by Domon and Costello [33]. Fragments formed where the charge is retained on the non-reducing terminus of the molecule are termed *A*, *B*, and *C*, while fragments with charge retention on the reducing terminus are termed *X*, *Y*, and *Z*. The subscripts indicate the position of the cleavage relative to the termini and the superscripts indicate cleavages across a ring for *A*- and *X*-type fragments.

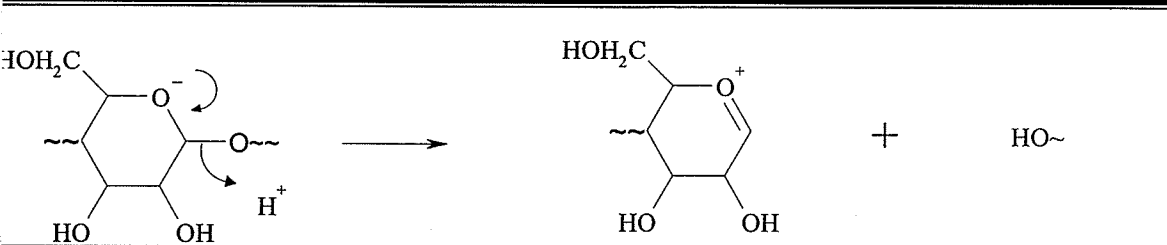
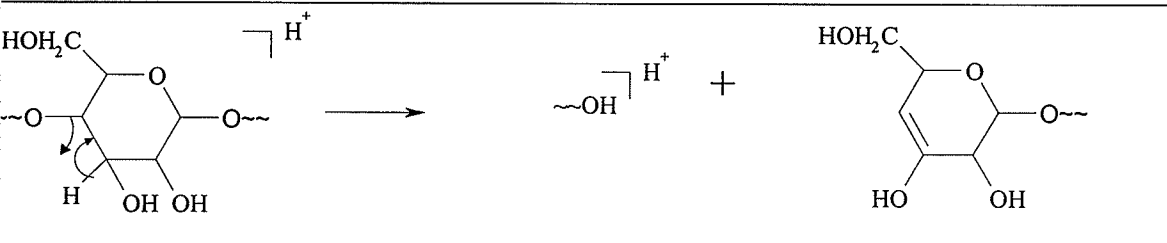
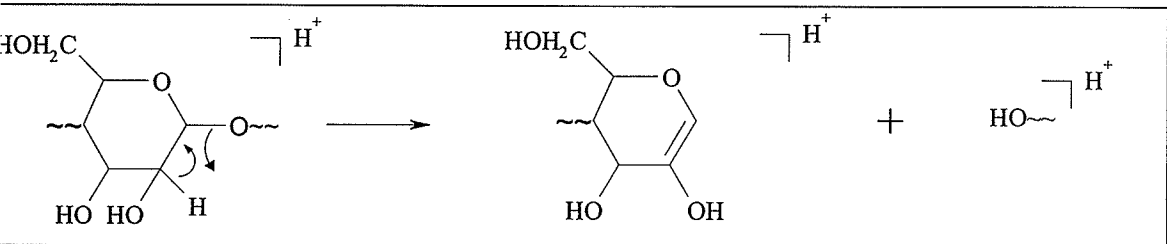
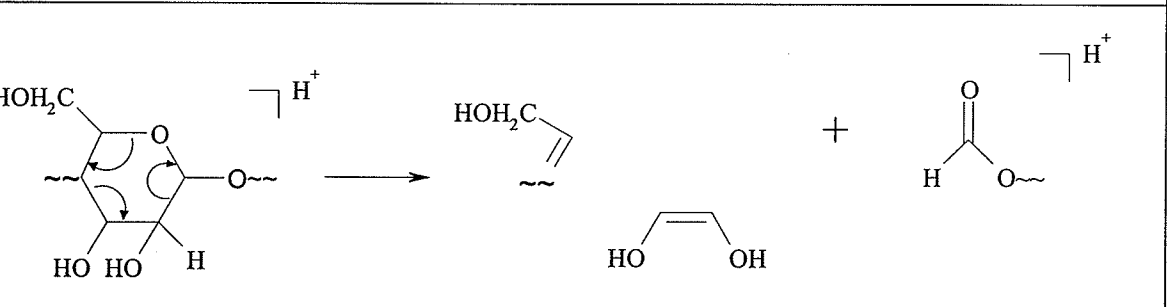
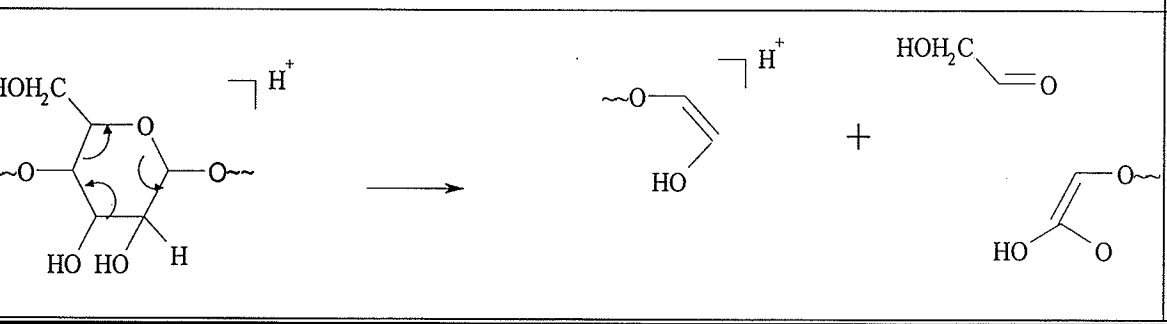
Besides enhancing fragmentation characteristics, derivatization enhances the volatility of samples as well as separability by chromatography. Other advantages of derivative include ease to free samples from salt impurities which may prejudice MS experiments, and enhancement of sensitivity due to the addition of hydrophobic labels. The precise choice of derivative depends on the particular problem under investigation. That is, it will depend mainly on the nature of mass spectrometry sample introduction, and ionization technique to be used.

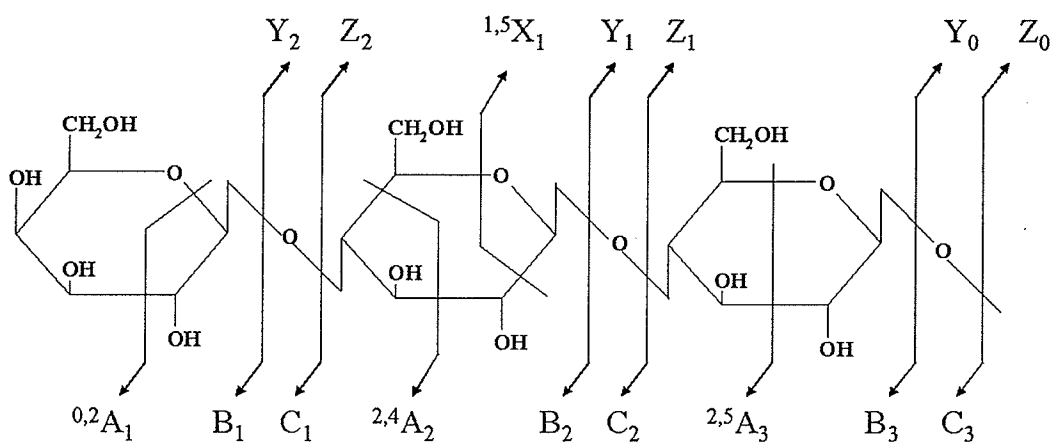
There are two fundamental reasons why derivatization is used for ESI-MS. First, if a sample is amenable to derivatization, the resulting less polar sample molecule becomes soluble in more volatile organic solvents, which in turn can provide a significant increase in detection sensitivity. Second, derivatization such as methylation brings unique insight to structures when glycans are analyzed by CID.

In general, derivatization methods can be classified into two categories:

(1) tagging of reducing ends, and (2) protection of most or all functional groups.

Table 1.2. Carbohydrate Fragmentation Nomenclature (described by Domon and Costello [15] and Dell and co-workers [16])

Proposed fragmentation pathway	Domon & Costello	Dell
	B-ions	A-type Oxonium cleavage
	C-ions	β -type (H-transfer)
	Y-ions	β -type (H-transfer)
	^{1,5} X-ions	ring cleavage
	Y-ions	ring cleavage



Scheme 1.1 Carbohydrate fragmentation nomenclature proposed by Domon and Costello [33].

Methods involving HPLC and ESI-MS have involved reductive amination to transform carbohydrates into UV-absorbent or fluorescent derivatives, which are detectable during chromatographic runs and yield improved sensitivity in ESI-MS. Recent reports on the use of such reducing end tags have shown that localization of the charge on the reducing end of oligosaccharides results in predominantly X, Y and Z fragmentations and thus greatly simplifies structure analysis of unknowns by MS [35-44].

Some of the derivatization agents tested are 2-aminopyridine (PA), [35,38] trimethyl(*p*-aminoethyl)ammonium chloride (TMAPA), [58] 4-aminobenzoic acid ethyl ester (ABEE) [36,45,46,58] and its amino ethyl version (ABDEAE), [47,37] 2-aminobenzamide (2-AB) [39] and 2-aminoacridone (2-AMAC). [48,40,49-51] Similar derivatives have been prepared by condensation with 1-phenyl-3-methyl-5-pyrazolone (PMP) [41,43,44,52] and its *p*-methoxy analogue (PMPMP). [42] Ahn and Yoo recently used malononitrile as a new derivatizing agent for ESI-MS and HPLC/ESI-MS of oligosaccharides, [53,54] and Charlwood *et al.* [55] introduced a novel fluorescent probe, 3-(acetylamino)-6-aminoacridine (AA-Ac), for *N*-linked glycans.

1.5 SAMPLE INTRODUCTION

An overlying concern in the use of mass spectrometry for biological studies is the method of introduction of samples into the instrument. Moving and manipulating small quantities of carbohydrate samples from the laboratory bench to the analytical instrument requires care and thought to minimize sample losses. Many approaches have been developed based primarily on the method of sample introduction into the ionization source. In general, biochemical experiments (e.g. gels and affinity columns) produce glycans for analysis in relatively dilute form and with variable content of buffers and

detergents. Mass spectrometry requires approaches tailored to a particular ionization technique.

1.5.1 Delivering Carbohydrates to ESI-MS

Carbohydrates are introduced in an ESI source in liquid solution.

Consequently, ESI allows samples to be manipulated on-line in conjunction with many separation or solution delivery methods. The two most widely used separation methods are HPLC and CE. Both of these techniques combine analyte preconcentration and purification. At low flow rates ($< 100 \mu\text{l}/\text{min}$), ESI behaves as a concentration dependent device, thus minimization of the column elution volume maximizes the concentration of the glycans subjected to ESI. Low flow rate separation techniques such as microcolumn HPLC and CE are ideal for integration with ESI to maximize sensitivity of analysis.

1.5.2. The effect of detergents on glycan analysis

Detergents or surfactants are widely used in glycoprotein chemistry. They aid solubilization as well as stabilization of glycoprotein complexes. In particular, membrane-bound proteins frequently require detergent treatment in order to dissolve. Detergents are also commonly employed in analytical techniques used for characterizing these glycoproteins, e.g. PAGE and CE. They are also used to enhance peptide and protein recoveries from synthetic membranes in electroblotting and in electroelution of proteins from gels. Detergents have the reputation of being completely unsuitable for ESI-MS of glycans; in reality some, but not all detergents, are unsuitable and that these are cases where it is possible to choose a surfactant that will still allow suitable ESI conditions. It is still suggested to mass spectrometrists to avoid detergents whenever possible; they add interfering ions and rarely improve signal-to-noise ratios.

1.5.3. General Detergent Properties

Detergents are surface-active agents (surfactants) containing a hydrophobic portion which is more soluble in non polar systems, and a hydrophilic portion, which is soluble in water. Detergents will migrate to the interface of the solvent, reducing its surface tension. At low concentration, detergents will form monolayers; at higher concentration, i.e. equal or higher than the critical micellar concentration (CMC), they tend to aggregate to form micelles or clusters. Detergents are characterized by their physiochemical properties. The properties must be carefully considered when choosing a detergent for purification or analysis.

Three interfering effects have to be considered if detergents are used during spectral analysis: 1) background ions which can obscure signal, 2) suppression of the sample signal, and 3) adduct formation. In addition, during ESI-MS, a shift of the charge envelope can take place. Extensive work has been done to evaluate the compatibility of a variety of detergents on ESI-MS [56]. Nonionic saccharide detergents yielded strong ESI signals without much chemical background. In contrast, sodium dodecyl sulfate (SDS) performed poorly. The study showed that careful selection of the detergent and proper concentration can enhance mass spectral analysis. As expected, ionic detergents can suppress the analyte signal due to competition between detergent and analyte ions for ESI current [56].

The combination of ESI and liquid chromatography (LC) does not necessarily solve the problem of detergent interference with the ionization process. Most of the neutral detergents (RTX-100, Tween-20, and NP-40) are complex mixtures of polymeric molecules that are fractionated by reversed phase (RP)-HPLC and, coupled

with efficient ionization by ESI-MS, result in many of the spectra in an ESI-MS being obscured with detergent related ions [57].

The presence of SDS should always be avoided, or dramatically reduced, where possible. The detergent problem can be addressed by substituting the polymeric detergents with essentially monomeric detergents with one specific mass and possibly only one retention time in chromatography. Then, the known mass of the detergent can simply be ignored or subtracted as constant background noise.

1.6 REFERENCES

1. O. P. Bahl, in *Glycoconjugates: Composition, Structure, and Function*, H. J. Allen and E. C. Kisailius, (Eds), Marcel Dekker Inc., pp. 1–12 (1992).
2. Oxford Glycosystems Ltd., *Tools for Glycobiology, Catalog and Technical Notes*, Rosedale, NY (1992).
3. Halbeek, H.V., *Meth. Enzymol.* **230**, 132 (1994).
4. Edge, C.J., Rademacher, T.W., Wormald, M.R., Parehk, R.B., Butters, T.D., Wind, D.R. and Dwek, R.A. *Proc. Natl. Acad. Sci. USA* **89**, 6338 (1992).
5. Lee, Y.C. *J. Chromatogr. A* **720**, 137 (1996).
6. Kunkel, J.P., Chan, D.C.H., Jamieson, J.C. and Butler, M. *Biotechnol.* **62**, 55 (1998).
7. Suzuki, S., Kakehi, H. and Honda, S. *Anal. Biochem.* **68**, 2073 (1996).
8. Olechno, J.D. and Nolan J.A. in *Handbook of Capillary Electrophoresis*, 2nd Edn, Landers, J.P. (Ed.), CRC Press, pp. 297-378 (1997).
9. Reinhold, V.N., Reinhold, B.B. and Chan, S. *Meth. Enzymol.* **271**, 377 (1996).
10. Mechref, Y. and Novotny, M.V. *Anal. Chem.* **70**, 455 (1998).
11. Takasaki, S., Mizuochi, T. and Kobata, A. *Methods Enzymol.* **83**, 263 (1982).
12. Trimble, R.B. and Maley, F. *Anal. Biochem.* **141**, 515 (1984).
13. Tarentino, A.L., Gomez, C.M. and Plummer, T.H. *Biochem.* **24**, 4665 (1985).
14. Tretter, V., Altmann, F. and März, L. *Eur. J. Biochem.* **199**, 647 (1991).
15. Zeleny, J., *Phys. Rev.* **10**, 1 (1917).
16. Dole, M., Mack, L.L. and Hines, R.L., *J. Chem. Phys.* **49**, 2240 (1968).
17. Yamashita, M. and Fenn, J.B. *J. Phys. Chem.* **88**, 4451 (1984)
18. Clegg, G. and Dole, M. *Biopolymers* **10**, 821 (1971).
19. Gieniec, J., Mack, L., Nakamae, K., Gupta, C., Kumar, V. and Dole, M. *Biomed. Mass Spectrom.* **11**, 259 (1984).

20. Karas, M. and Hillenkamp, F. *Anal. Chem.* **60**, 2299 (1988).
21. Cotter, R.J. *Anal. Chem.* **64**, A1027 (1992).
22. Chait, B.T. and Kent, S.B.H. *Science* **257**, 1885 (1992).
23. Hillenkamp, F., Karas, M., Beavis, R.C. and Chait, B.T. *Anal. Chem.* **63**, A1193 (1991).
24. Beavis, R.C. and Chait, B.T. *Rapid Commun. Mass Spectrom.* **3**, 432 (1989).
25. Beavis, R.C., Chaudhary, T. and Chait, B.T. *Org. Mass Spectrom.* **27**, 156 (1992).
26. Wang, B.H., Dresewerd, K., Bahr, U., Karas, M. and Hillenkamp, F. *J. Amer. Soc. Mass Spectrom.* **4**, 393 (1993).
27. Paul, W. and Steinwedel, H.S.Z. *Naturforsch* **8a**, 448 (1953).
28. March, R.E. and Hughes, R.J. *Quadrupole Storage Mass Spectrometry*, Wiley, New York, NY, 1989.
29. Harvey, D.J., Bateman, R.H. and Green M.R. *J. Mass Spectrom.* **32**, 167 (1997)
30. Cameron, A.E. and Eggers Jr., D.F. *Rev. Sci. Instrum.* **19**, 605 (1948).
31. Wiley, W.C. and McLaren, J.B. *Rev. Sci. Instrum.* **26**, 1150 (1955).
32. Mamyrin, B.A., Karateav, V.I., Schmickk, D.V. and Zagulin, V.A. *Sov. Phys. JETP* **37**, 45 (1973).
33. Domon, B. and Costello, C.E. *Glycocon. J.* **5**, 397 (1988).
34. Kondo A., Suzuki J., Kuraka N., Hase S., Kato I. and Ikenaka J. *Agric. Biol. Chem.* **54**, 2169 (1990).
35. Dell A., Carman H., Tiller P.R. and Thomas-Oates J.E. *Biomed. Environ. Mass Spectrom.* **16**, 19 (1988).
36. Wang W.T., LeDonne N.C. and Ackerman B. *Anal. Biochem.* **141**, 366 (1984).
37. Yoshino K.I., Takako T., Muruta H. and Shimonishi Y. *Anal. Chem.* **67**, 4028 (1995).
38. Okafo, G., Langridge, J., North, S., Organ, A., West, A., Morris, M. and Camilleri, P. *Anal. Chem.* **69**, 4985 (1997).

39. Guile G.R., Rudd P.M., Wing D.R., Prime S.B. and Dwek R.A. *Anal. Biochem.* **240**, 210 (1996).
40. Okafo G.N., Burrow L.N., Carr S.A., Roberts G.D., Johnson W. and Camilleri P. *Anal. Chem.* **68**, 4424 (1996).
41. Honda S., Akao E., Suzuki S., Okuda M., Kakehi K. and Nakamura J. *Anal. Biochem.* **180**, 351 (1989).
42. Kakehi K., Suzuki S., Honda S. and Lee Y.C. *Anal. Biochem.* **199** 256 (1991).
43. Shen X. and Perreault H. *J. Mass Spectrom.* **34**, 502 (1999).
44. Saba J.A., Shen X., Jamieson J.C. and Perreault H. *Rapid Commun. Mass Spectrom.* **13**, 704 (1999).
45. Li D.T. and Her G.R. *J. Mass Spectrom.* **33**, 644 (1998).
46. Khoo K.H. and Dell A. *Glycobiology* **1**, 83 (1990).
47. Mo W., Sakamoto H., Nishikawa A., Kagi N., Langridge J.I., Shimonishi Y. and Takao T. *Anal. Chem.* **71**, 4100 (1999).
48. North S., Birrell H. and Camilleri P. *Rapid Commun. Mass Spectrom.* **12**, 349 (1998).
49. Okafo G., Langridge J., North S., Organ A., West A., Morris M. and Camilleri P. *Anal. Chem.* **69**, 4985 (1997).
50. Charlwood J., Langridge J., Tolson D., Birrell H. and Camilleri P. *Rapid Commun. Mass Spectrom.* **13**, 107 (1999).
51. Charlwood J., Birrell H., Bouvier E.S.P., Langridge J. and Camilleri P. *Anal. Chem.* **72**, 1469 (2000).
52. Shen X. and Perreault H. *J. Chromatogr. A* **811**, 47 (1998).
53. Ahn Y.H. and Yoo J.S. *Rapid Commun. Mass Spectrom.* **12**, 2011 (1998).
54. Ahn Y.H. and Yoo J.S. *Rapid Commun. Mass Spectrom.* **13**, 855 (1999).
55. Charlwood J., Birrell H., Gribble A., Burdes V., Tolson D. and Camilleri P. *Anal. Chem.* **72**, 1453 (2000).
56. Ogorzalek Loo, R. R., Dales, N. and Andrews, P. C. *Protein Science* **3**, 1975 (1993).

57. Cano, L., Swiderek, K.S. and Shively, J.E. 1994. *In Techniques in Protein Chemistry VI*, Crabb, J.W. ed. (Academic Press, San Diego), 21-30.
58. Okamoto, M., Takahashi, K., Doi, T. and Takimoto, Y. *Anal. Chem.* **69** 2919 (1997).

2 EFFECT OF 1-PHENYL-3-METHYL-5-PYRAZOLONE LABELLING ON THE FRAGMENTATION BEHAVIOUR OF ASIALO AND SIALYLATED N-LINKED GLYCANS UNDER ELECTROSPRAY IONIZATION CONDITIONS

2.1 INTRODUCTION

Historically, HPLC and mass spectrometry studies have employed reductive amination to transform carbohydrates into UV-absorbent or fluorescent derivatives for improved detection during chromatographic runs and increased sensitivity in mass spectrometric analysis. Some of the reductive amination derivatization agents tested have been TMAPA [1], ABEE [2] and its amino ethyl version ABDEAE [3], PA [4], 2-AB [5], and 2-AMAC [6]. Similar derivatives have been prepared by condensation with 1-phenyl-3-methyl-5-pyrazolone (PMP) [7], and its *p*-methoxy analog (PMPMP) [8].

Mass spectrometric studies on native [9,10] and permethylated (methylated) [11] oligosaccharides have shown that fragmentation occurs at either end of the molecules and that structure determination of unknown oligosaccharides would be difficult without labelling the reducing end with a proton/cation attracter. Reports on the use of 2-AMAC, [12,13] TMAPA [14] PA, [15,16] ABDEA [3] and PMP [17,18] have shown that localization of the charge on the reducing end of oligosaccharides results in predominant X, Y and Z fragmentations [19] and thus greatly simplifies structural analysis of unknowns by MS.

Electrospray studies of maltopentanose [14], high-mannose and dextran ladder [12] derivatives have shown that in order to obtain informative ESI spectra, post-

derivatization desalting by on- or off-line HPLC was necessary. Even in these cases, some ESI spectra contained $[M+Na]^+$ and/or $[M+H+Na]^{2+}$ ions, and these could lead to ambiguous assignments if combined with $[M+nH]^{n+}$ ions during the analysis of an unknown oligosaccharide sample. Direct infusion or loop injection of PMP-tetraglucose (and smaller sugars) without desalting yielded good quality spectra with $[M+H]^+$ (predominant) and $[M+Na]^+$ present [17,18]. The latter disappeared with the use of HPLC, and almost no fragmentation was observed in either case. Interestingly, variation of the cone voltage had a very restricted effect on the extent of fragmentation. When the PMP derivatization method was first applied to commercially obtained *N*-linked oligosaccharides, it became obvious that desalting was necessary in order to acquire clean ESI spectra, much more so than in the case of PMP-tetraglucose. Suzuki-Sawada and co-worker [15] have shown that the ESI solvent composition has a profound influence on the nature of PA *N*-linked oligosaccharide ions observed. For example, a 5 mM phosphate buffer produced only $[M+Na]^+$ ions, whereas an acetic acid containing solution produced mainly $[M+2H]^{2+}$ ions. The presence of PMP moieties in molecules already containing GlcNAc groups did not improve the ESI-MS sensitivity as much as in the case of tetraglucose, a neutral oligosaccharide.

In the first part of the chapter investigations into the use of PMP derivatization for asialo and sialylated *N*-linked oligosaccharides are described. The latter have not been studied in great detail to date, and are important since numerous sialylated glycoproteins exist and need to be characterized. The PMP reaction safely prevents losses of sialic acid (SA) moieties, enhances reversed-phase HPLC retention and separation according to the number of SA residues present, and yields better ESI-MS sensitivity than

PA labelling [17]. Moreover, either protonated molecules or fragment ions of PMP sugars can be observed, depending on the adjustment of the cone voltage.

The second part of the chapter describes the use of PMP derivatives in RP-HPLC separations. The hydrophobic interactions of RP-HPLC have been the most popular means of HPLC for a long time. However, appreciation for this separation mode in the analysis of oligosaccharides came relatively late [20,21]. Due to the polarity of underivatized oligosaccharides, only weak interactions are experienced with typical reversed-phase packings. Derivatization has been used as a means of increasing retention with the stationary phase. Typically derivatization with labels containing single aromatic group (e.g. PA) does not significantly increase retention on C-18 stationary phases [17] unless buffered polar mobile phases are used [15] which are in turn not suitable for hydrophobic derivatives. Camilleri and co-workers reported on efficient reversed-phase retention of the 2-AMAC derivatives [12,22]. The aminocridone group, as the bis-PMP label, contains two aromatic rings and thus confers more non-polar character onto an oligosaccharide than would, for instance, PA, hence the increased retention.

2.2 EXPERIMENTAL

2.2.1 Materials

N-Linked standards M3N2, NGA3, A1 and A2, whose structures are given in Figure 2.1, were obtained from Oxford Glycosystems (Rosdale, NY, USA) and used as received. The PMP reagent was purchased from ICN Biomedicals Inc. (Aurora, OH, USA). All solvents were glass-distilled, HPLC-grade and obtained from Mallinkrodt (Paris, KY, USA). Distilled, deionized water was obtained from a Barnstead Nano-Pure™ filtration system supplied by a reverse-osmosis feedstock.

2.2.2 PMP-derivatization

The solutions of individual sugars (20 μg each) were evaporated to dryness and samples were re-dissolved in 0.3 M NaOH in water (20 μL). A 0.5 M methanolic solution (20 μL) of PMP was added to these solutions. The mixtures were sealed and heated at 70°C for 30 min. The mixtures were then neutralized by adding 20 μL of HCl solution (0.3 M), and extracted repeatedly with chloroform. The aqueous layer was evaporated to dryness, and the PMP-sugars were re-dissolved in 50:50 ACN-water for analysis by MS.

2.2.3 ESI-MS

The instrument used for these experiments was a Quattro-LC from Micromass (Manchester, UK) equipped with a Z-Spray™ electrospray ionization source and a triple quadrupole analyzer. Direct injections were performed with a 20 μL Rheodyne loop, and the carrying solvent was 50:50 ACN/water at a flow rate of 10 $\mu\text{L}/\text{min}$. The samples were sprayed using a 3.5-kV needle voltage, and the cone voltage (declustering voltage) was set according to the needs of the experiment (from 20 to 60 V). The source block and desolvation temperatures were maintained at 110 and 130°C, respectively, during direct injection analyses. Mass spectra were recorded in the positive ion mode at a scan rate of 300 μ/sec .

2.2.4 ESI-MS/MS

The argon pressure in the cell was 2×10^{-3} Torr and the CID energy was set at 90 eV to break down sodium containing clusters. The scan rate was again 300 μ/sec .

2.2.5 On-line HPLC/ESI-MS

The HPLC system used was an Ultra-Plus pump module from Microtech Science Inc. (Sunnyvale, CA, USA). A 250 x 4.6 mm Vydac 218TP54 Protein & Peptide Column was used (The Separations Group, Hesperia, CA, USA). Injections were made through a 20- μ L Rheodyne loop. A constant flow rate was set at 1.00mL/min, and the composition of the mobile phase was programmed as follows: The initial composition of 20% of Eluent B (2:1 *t*-butyl alcohol/ACN) in water (Eluent A) was kept for 10 min, then linearly modified to 95% over 25 min, and kept at 95% for 10 min. Trifluoroacetic acid (TFA) was kept at a constant concentration of 0.05% throughout the separation. The source block and desolvation temperatures of the Quattro-LC Z-Spray™ source were set at 130 and 250 °C, respectively. The scan rate was increased to 600 u/sec.

2.3 RESULTS

Initial work on *N*-linked oligosaccharides consisted of characterizing the positive mode ESI-MS behavior of native asialo oligosaccharides (A1). Figure 2.2 shows a spectrum obtained at 60 V, significant extent of fragmentation was observed. Abundant low mass diagnostic fragments ions were observed (m/z 366, 528, 657); however, the rest of the spectrum at $m/z > 900$ was of very low intensity. Therefore, it did not seem possible to produce predominantly protonated molecules for A1 with our ESI instrument. Mixture analysis requires the production of predominantly molecular ions.

PMP derivatization method (global reaction shown in Figure 2.3) was applied to asialo M3N2 and NGA3, and to sialylated A1 and A2 glycans. On-line RP-HPLC was used to remove most of the salt content, prior to spectrum acquisition. Figure 2.4(a) shows a spectrum of PMP-M3N2 acquired at a cone voltage of 20 V. Predominant

$[M+2H]^{2+}$ ions were observed, as would be desired for mixture analysis. Increase of cone voltage to 60 V resulted in a spectrum (Figure 2.4(b)) that contained reducing end (Y- and Z-type) ions, which is favorable for structural determination with its clear fragmentation pattern. Figure 2.4(a) shows predominant Y_1 ions, as had been observed for PMP-NGA3 [18]. Even though on-line HPLC was used for this experiment, $[M+Na]^+$ ions were still observed in the spectrum but did not interfere with the study. Since the latter require more internal energy to fragment than $[M+H]^+$, they remained intact in the source, while protonated molecules were dissociated. The observation of only sodium-exempt fragment ions favoured proper spectral interpretation.

HPLC/ESI-MS experiments were extended to sialylated compounds, specifically PMP derivatized A1 and A2. Figure 2.5(a) shows a spectrum of PMP-A1 acquired at cone voltage of 20 V. The spectrum contained doubly and triply protonated molecular ions with little or no fragmentations. The desialylated product, whose molecular ions should have appeared at m/z 658 (3+) and 987 (2+), was not obtained from the PMP derivatization reaction. Higher cone voltage (60 V) produced informative fragmentation pattern favoring Y-type ions at $m/z > 700$. The abundant ions at m/z 204, 366, and 657, originating from the nonreducing end of the molecule, were also observed in the spectrum of native A1 (Figure 2.2). These ions can be used as 'fingerprints' for sialylated *N*-linked oligosaccharides. The spectra of PMP-A2 (not shown) were similar to those of Figure 2.5, i.e. the same type of molecular ions and fragments were observed, and no loss of sialic acid arising from the derivatization reaction was observed.

Enzymatic digestion with PNGase F [23] and chemical digestion via hydrazinolysis [24] produce non-reduced *N*-linked oligosaccharides containing the

common trimannosyl core, $(\text{Man})_3(\text{GlcNAc})_2$. A simple and efficient analytical approach to structural elucidation of such oligosaccharides is to perform on-line HPLC/MS. Due to the relatively high polarity of these compounds, normal-phase or anion exchange HPLC give the best results. Since both these HPLC modes are difficult to interface with MS, reversed-phase (RP) HPLC is a better option to consider.

A mixture containing PMP-derivatized M3N2, A1 and A2 was characterized by on-line HPLC/ESI-MS. The cone voltage was kept low (20 V), as to maximize the production of protonated molecules in the spectrum. The elution of profile of each compound was monitored by following their selected ion chromatogram (SIC) (Figure 2.6). A similar experiment was repeated at 60 V, but it was more difficult to identify the individual species because some of the abundant fragment ions (e.g. m/z 552) are common to all three species, and other important ions (e.g. m/z 204, 366, 657) are common to A1 and A2. An advantageous feature of our instrument is the ability to alternate the cone voltages from 20 to 60 V and back to 20 every second scan, which makes it possible to obtain both molecular weight and fragmentation information in one chromatographic run.

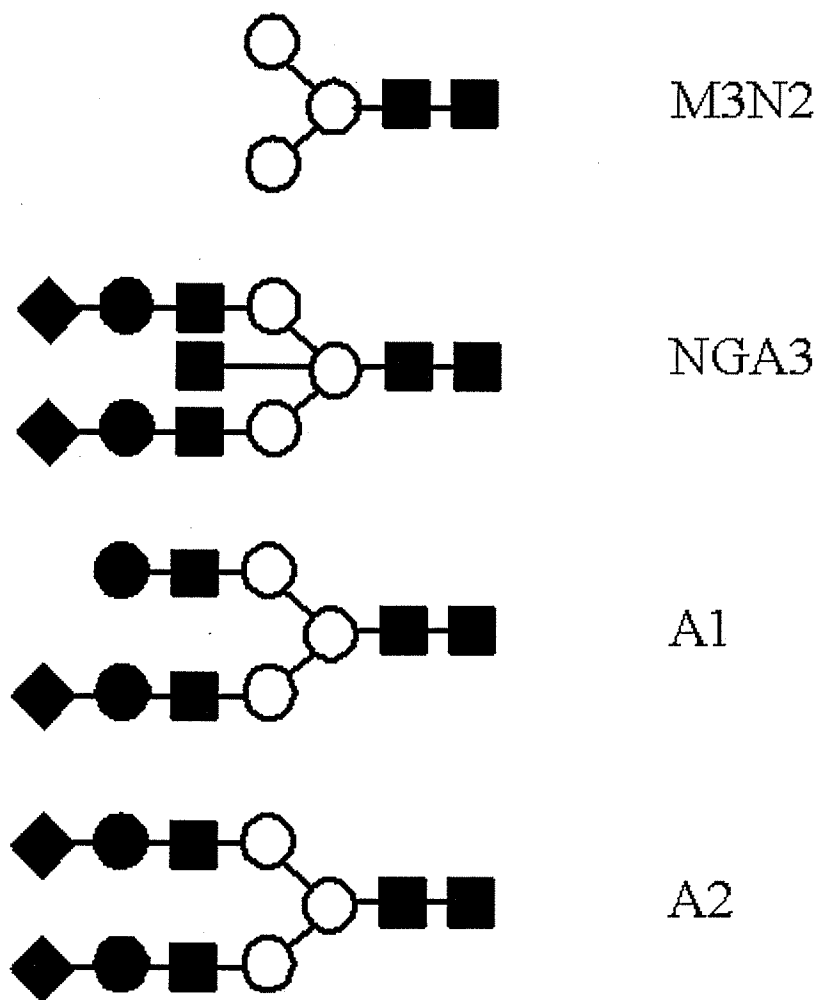


Figure 2.1 Structures of the *N*-linked oligosaccharides used in this study.

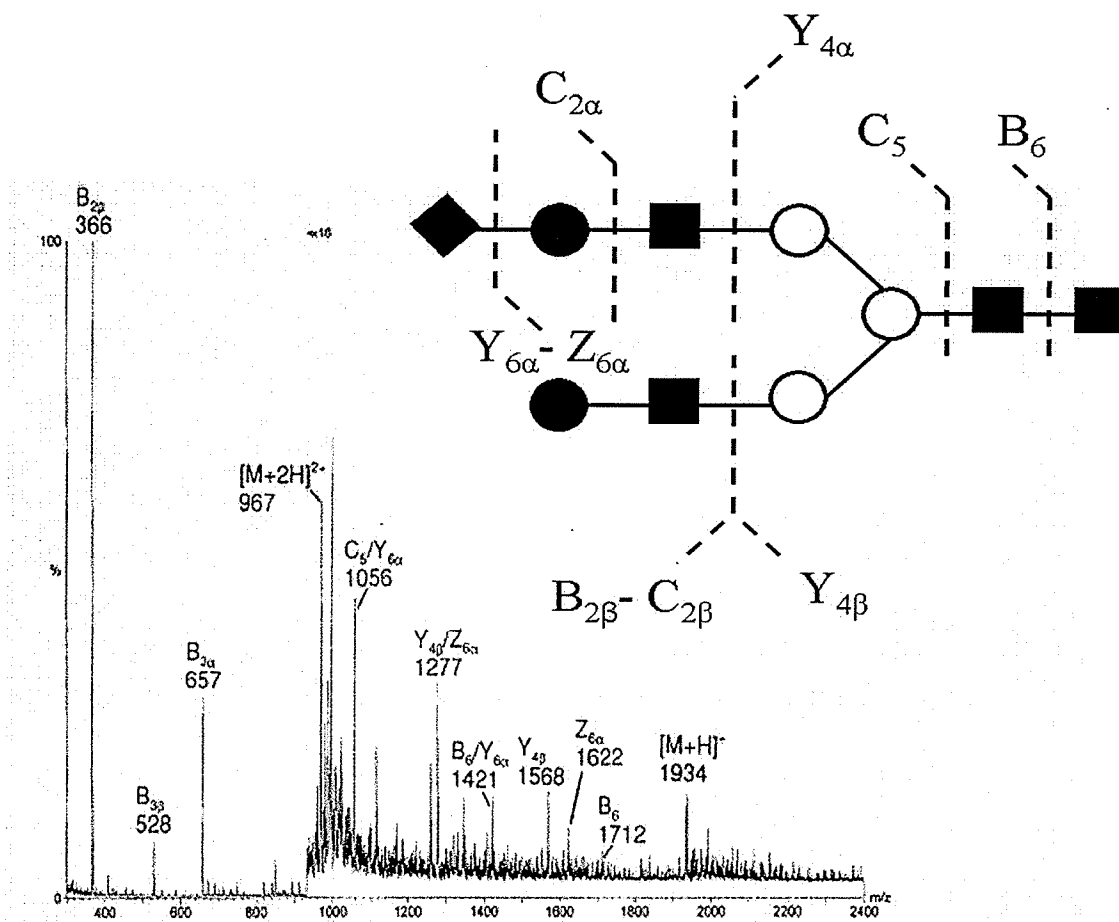


Figure 2.2 ESI mass spectrum of native A1, acquired with a cone voltage of 60 V.

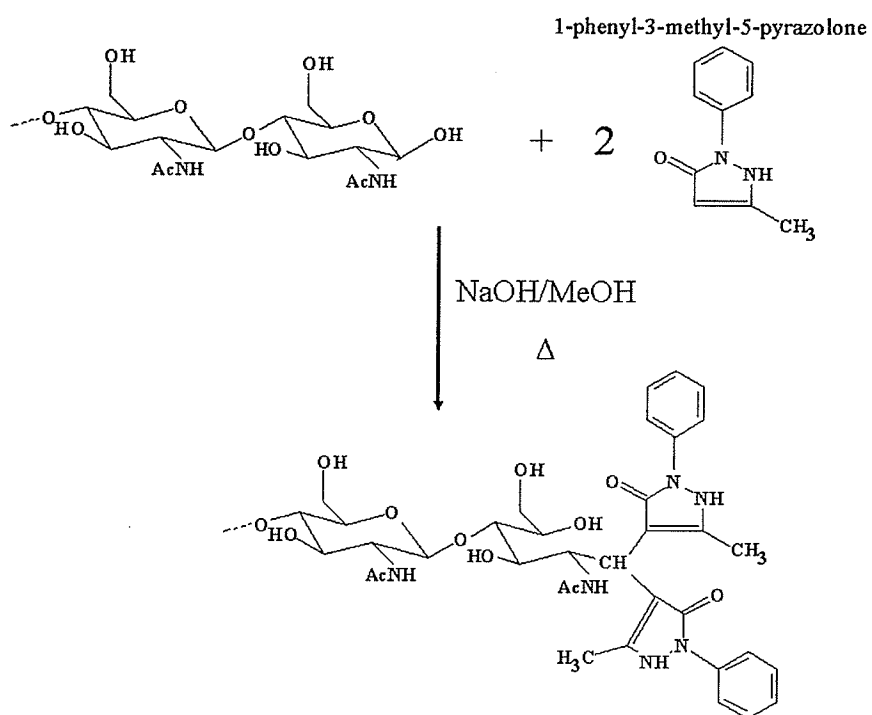


Figure 2.3 Reaction of *N*-linked oligosaccharides with 1-phenyl-3-methyl-5-pyrazolone (PMP).

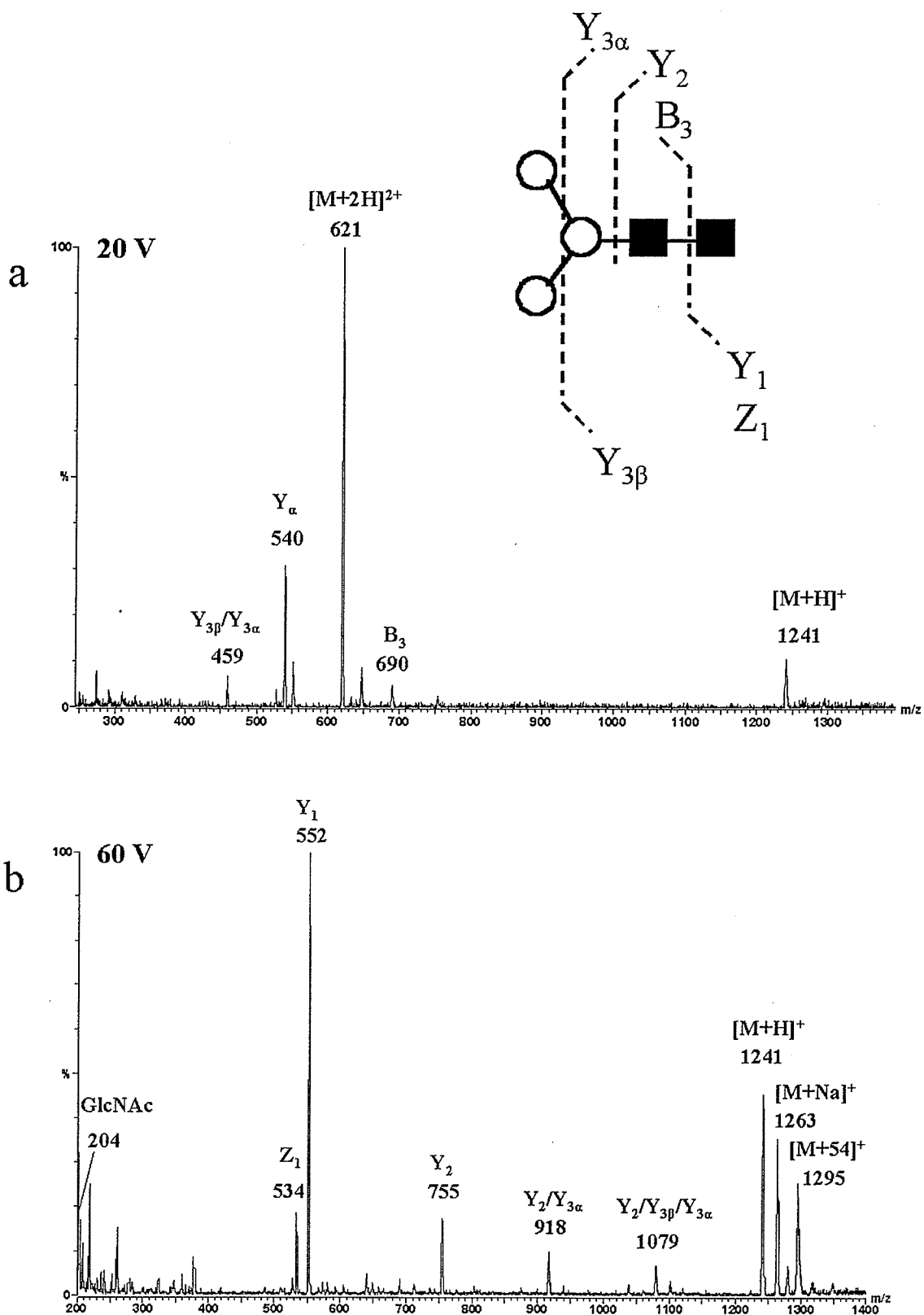


Figure 2.4 ESI mass spectra of PMP-M3N2, acquired by on-line HPLC/MS, (a) acquired at 20 V cone voltage, and (b) at 60 V.

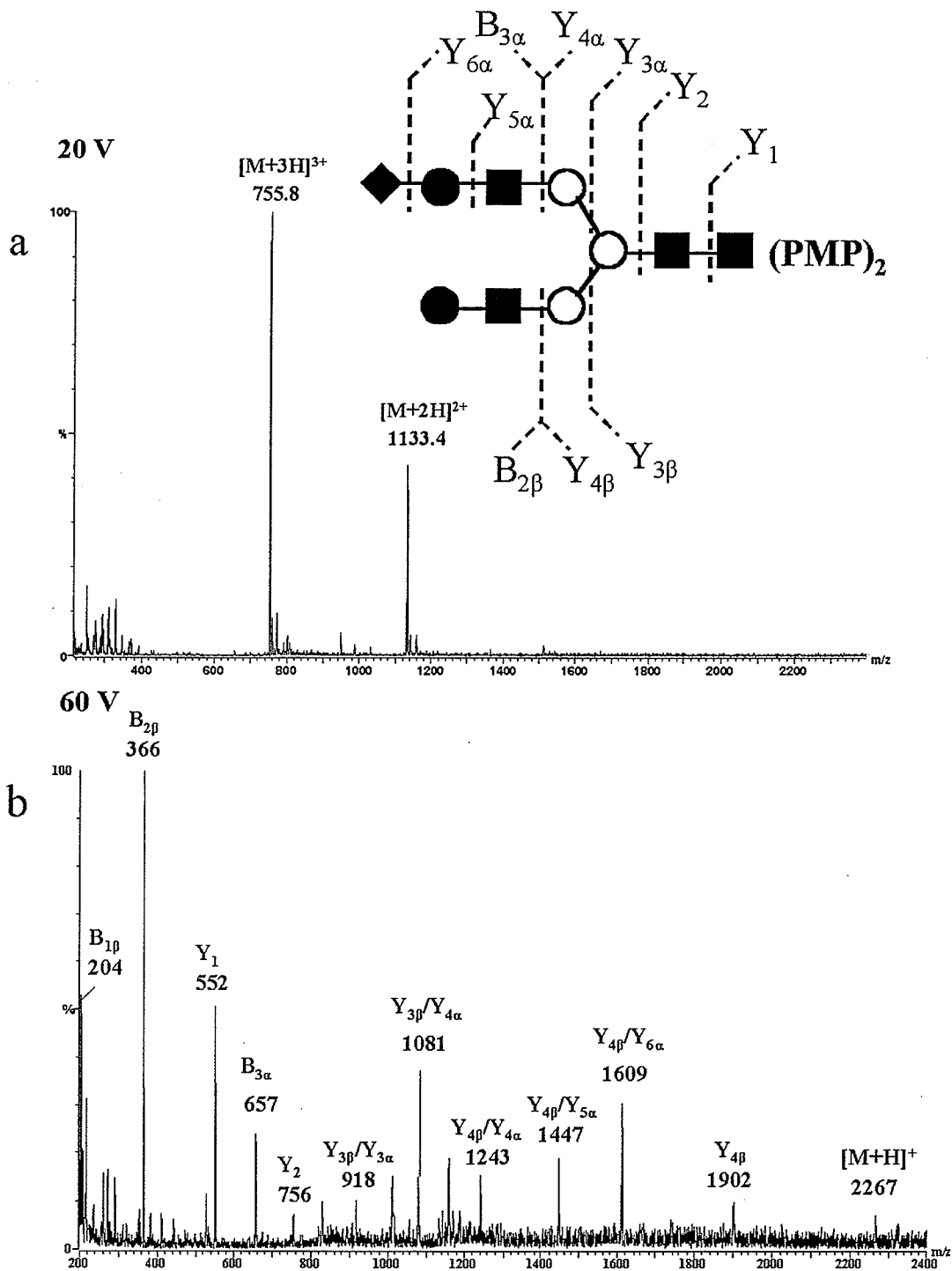


Figure 2.5 ESI mass spectra of PMP-A1, acquired by on-line HPLC/MS, (a) acquired at 20 V cone voltage, and (b) at 60 V.

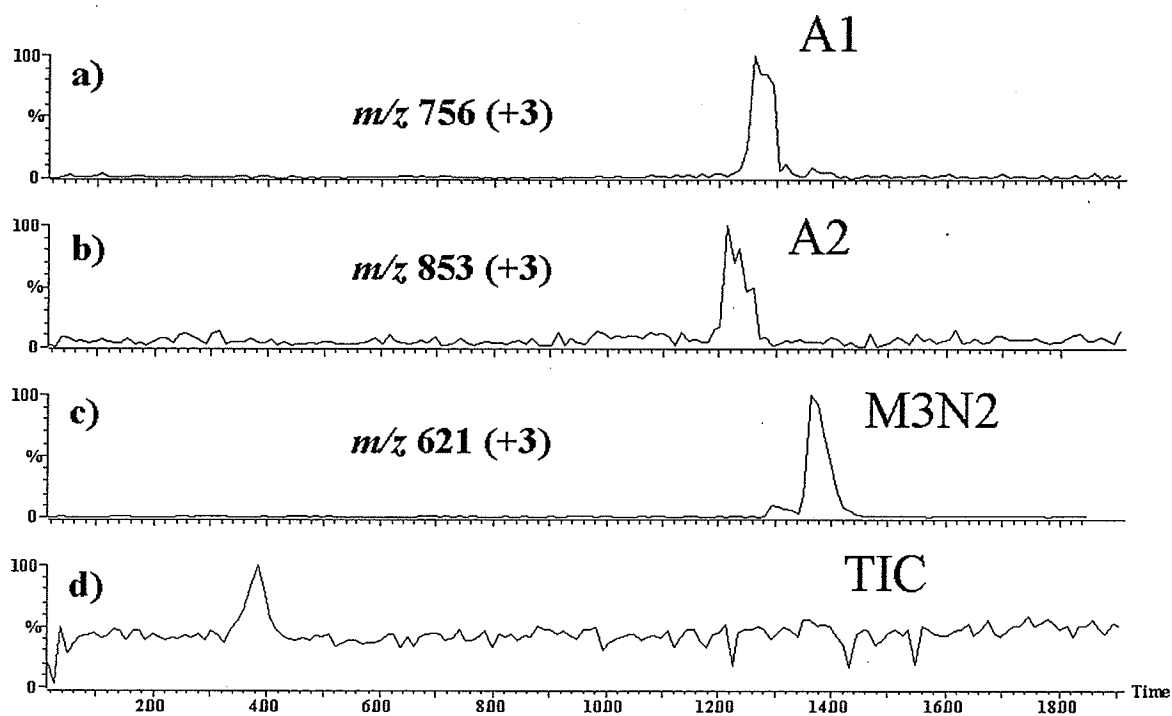


Figure 2.6 On-line HPLC/ESI-MS traces, reconstructed from a full-scan experiment on a mixture containing 300 pmol each of PMP-A1, A2 and M3N2. Cone voltage: 20 V. (a) m/z 756 trace for $[M+3H]^{3+}$ of PMP-A1, (b) m/z 853 trace for $[M+3H]^{3+}$ of PMP-A2, (c) m/z 621 trace for $[M+2H]^{2+}$ of PMP-M3N2, and (d) total ion chromatogram.

2.4 DISCUSSION

Native asialo oligosaccharides yield good ESI-MS sensitivity, although they are very susceptible to in-source CID, and the fragments are produced from any of the branches of the molecules, i.e. do not give specific structural information. A recent report briefly discusses the acquisition of two full-scan ESI spectra, recorded using 200 pmol of NGA3 in solution [18]. The first spectrum was obtained with a cone voltage of 60 V, under typical ionization conditions yielding only $[M+nH]^{n+}$ ions for peptides with their Z-Spray™ source. This spectrum was a good example of in-source CID and contained complete sequence information. Although the spectrum contained fragments that indicated the monosaccharide sequence, they occurred non-preferentially from either branch of the molecule, making spectral interpretation difficult in the case of an unknown oligosaccharide. The second spectrum [18] was acquired using 30 V cone voltage, and showed predominant $[M+2H]^{2+}$ ions. The observed fragmentation was considerably less abundant, making composition analysis easier than the higher cone voltage spectrum, where extensive non-selective fragmentation was observed.

Sialylated *N*-linked oligosaccharides have not been studied in great detail to date, and are important since numerous sialylated glycoproteins exist and need to be characterized. Attempts at obtaining signal from the analyte at low cone voltage was unsuccessful. Increasing the cone voltage (60 V) provides better results, but the observed fragmentation pattern is not feasible. The fragmentation pattern of A1 (Figure 2.2) shows cleavages from three branches of the molecule, with no selectivity producing low mass diagnostic fragments that are characteristic of most *N*-linked oligosaccharides, making identification of an unknown oligosaccharide impossible. Negative mode offers better

sensitivity than positive mode for native sialylated compounds but asialo oligosaccharides remain more sensitive under positive mode conditions owing to the presence of *N*-acetylated residues [10]. It is more practical to conduct the analysis of all glycans under investigation in the same mode or polarity, and for this reason we discuss below the impact of adding PMP groups to sialylated oligosaccharides for positive mode ESI-MS. Furthermore, derivatization improves sensitivity and simplifies fragmentation pattern.

Typically HPAEC-PAD [25,26] and NP-HPLC are used in the separation of native *N*-linked oligosaccharides. As expected attempts at RP-HPLC separation of the two native sugars (NGA3 and M3N2) showed that they have no affinity for the C-18 column. They co-eluted within one minute of the solvent when regular mobile phase conditions were used, i.e. as described in the experimental part or when using water/ACN gradients. Shen *et al.* [17,18] have studied the effect of PMP-labelling on RP-HPLC and ESI-MS behaviors of neutral carbohydrates. This same derivatization method [7,27] (global reaction shown in Figure 2.3) was applied to asialo M3N2 and NGA3, and to sialylated A1 and A2 glycans. As indicated in Figure 2.3, a basic environment is required for PMP-derivatization, thus making it difficult to eliminate sodium ions from solutions that are to be analyzed by MS. This is not a hindrance when characterizing neutral glycans such as tetraglucose, i.e. $[M+H]^+$ ions could always be observed in spite of a high sodium ion concentration. With *N*-linked sugars, the situation was different. A spectrum was obtained for a non-desalted aliquot of a solution of PMP-NGA3, it contained only low abundance $[M+2Na]^{2+}$ ions, which had to be fragmented at 90 eV collisionally induced energy in order to provide any meaningful structural information [18]. The

fragmentation pattern observed showed cleavages occurring from either branch of the molecule, as well as the presence of one or two sodium adduct ions, making interpretation of the spectrum difficult. Attempts at desalting PMP derivatives with Sep-Pak cartridges proved to be futile, yielding irreproducible results due to sample loss. On-line RP-HPLC/ESI-MS was therefore performed next, and direct injections were not used further for these derivatives. Only one RP-HPLC experiment was necessary to remove most of the salt content.

The ESI spectrum of PMP-NGA3 after desalting with on-line HPLC has been published recently [18]. The spectrum was obtained at a cone voltage of 60 V using 100 pmol of material. PMP-NGA3 showed extensive fragmentation as observed for native NGA3, although Y-type fragment ions were predominant. B₃ cleavages, either by themselves or combined with Y-type, did occur; however, the resulting fragment ions were not abundant, and Y-type ions prevailed [18]. Interestingly, PMP-tetraglucose did not produce fragments to any significant extent under the same conditions. Neutral sugars and their derivatives appear to be more stable under ESI conditions than sugars with hybrid structures, which undergo extensive fragmentation, more in the native form than in the derivatized form.

Typically derivatization with labels containing single aromatic group (e.g. PA) does not significantly increase retention on C-18 stationary phases [17] unless buffered polar mobile phases are used [15] which are in turn not suitable for hydrophobic derivatives. The data in Fig. 2.6 show that retention of the carbohydrates on the C-18 column has been greatly enhanced by addition of the bis-PMP labels. The bis-PMP label, contains two aromatic rings and thus confers more non-polar character onto an

oligosaccharide than would, for instance, PA, hence the increased retention. The HPLC conditions reported here still require some optimization, but the method is promising.

2.5 CONCLUSIONS

The PMP derivatization method is simple to use and prevents the loss of sialic acid moieties from carbohydrates. PMP derivatives of typical *N*-linked oligosaccharides undergo extensive in-source fragmentation under conditions that are routinely used for exclusive production of molecular ions from peptides. The fragments produced are, however, useful for structural determination, as they mostly contain the reducing end (bis-PMP label) of the molecule. If only molecular weight determination is desired, the cone voltage may be lowered to 20 V (instead of 60 V), to produce mainly protonated molecules. The preliminary results presented here also show that these derivatives are separable to a useful extent by reversed-phase HPLC. Combining separability and usefulness of in-source fragmentation patterns results in a method with considerable potential for carbohydrate analysis. As most LC/MS software packages feature the possibility of alternating functions during the course of a run, both molecular weight information and fragmentation patterns may be obtained for each component of a mixture.

2.6 REFERENCES

1. Dell, A., Carman, H., Tiller, P.R. and Thomas-Oates, J.E. *Biomed. Environ. Mass Spectrom.* **16**, 19 (1988).
2. Wang, W.T., LeDonne Jr., N.C. and Ackerman, B. *Anal. Biochem.* **141**, 366 (1984).
3. Yoshino, K.I., Takako, T., Muruta, H. and Shimonishi, Y. *Anal. Chem.* **67**, 4026 (1995).
4. Kondo, A., Suzuki, J., Kuraka, N., Hase, S., Kato, I. and Ikenaka, J. *Agric. Biol. Chem.* **54**, 2169 (1990).
5. Guile, G.R., Rudd, P.M., Wing, D.R., Prime, S.B. and Dwek, R.A. *Anal. Biochem.* **240**, 210 (1996).
6. Okafo, G.N., Burrow, L.N., Carr, S.A., Roberts, G.D., Johnson, W. and Camilleri, P. *Anal. Chem.* **68**, 4424 (1996).
7. Honda, S., Akao, E., Suzuki, S., Okuda, M., Kakehi, K. and Nakamura, J. *Anal. Biochem.* **180**, 351 (1989).
8. Kakehi, K., Suzuki, S., Honda, S. and Lee, Y.C. *Anal. Biochem.* **199**, 256 (1991).
9. Naven, T.J.P., Harvey, D.J., Brown, J. and Critchley, G. *Rapid Commun. Mass Spectrom.* **11**, 1681 (1997).
10. Duffin, K.L., Welply, J.K., Huang, E. and Henion, J.D. *Anal. Chem.* **64**, 1440 (1992).
11. Solouki, T., Reinhold, B.B., Costello, C.E., O'Malley, M., Guan, S. and Marshall, A.G. *Anal. Chem.* **70**, 857 (1998).
12. Camilleri, P., Tolson D. and Birrell, H. *Rapid Commun. Mass Spectrom.* **12**, 144 (1998).
13. North, S., Okafo, G., Birrell, H., Haskins, N. and Camilleri, P. *Rapid Commun. Mass Spectrom.* **11**, 1635 (1997).
14. Okamoto, M., Takahashi, K.I. and Doi, T. *Rapid Commun. Mass Spectrom.* **9**, 641 (1995).
15. Suzuki-Sawada, J., Umeda, Y., Kondo, A. and Kato, I. *Anal. Biochem.* **207**, 203 (1992).
16. Gu, J., Hiraga, T. and Wada, Y. *Biol. Mass Spectrom.* **23**, 212 (1994).

17. Shen, X. and Perreault, H. *J. Chromatogr. A* **811**, 47 (1998).
18. Shen, X. and Perreault, H. *J. Mass Spectrom.* *in press* (1999).
19. Domon, B. and Costello, C.E. *Glycoconjugate J.* **5**, 397 (1988).
20. Morelle, W. and Strecker, G. *J. Chromatogr. B* **706**, 101 (1998).
21. Cheetham, N. W. H., Sirimanne, P. and Day W. R. *J. Chromatogr.* **207**, 439 (1981).
22. North, S., Birrell, H. and Camilleri, P. *Rapid Commun. Mass Spectrom.* **12**, 349 (1998).
23. Takasaki, S., Mizuochi, T. and Kobata, A. *Meth. Enzymol.* **83**, 263 (1982).
24. Hirani, S., Bernasconi, R.J. and Rasmussen, J.R. *Anal. Biochem.* **162**, 485 (1987).
25. Lee, Y.C. *J. Chromatogr. A* **720**, 137 (1996).
26. Kunkel, J.P., Chan, D.C.H., Jamieson, J.C. and Butler, M. *J. Biotechnol.* **62**, 55 (1998).
27. Fu, D. and O'Neill, R.A. *Anal. Biochem.* **227**, 377 (1995).

3 INVESTIGATION OF DIFFERENT COMBINATIONS OF DERIVATIZATION, SEPARATION METHODS AND ELECTROSPRAY IONIZATION MASS SPECTROMETRY FOR STANDARD OLIGOSACCHARIDES AND GLYCANS FROM OVALBUMIN

3.1 INTRODUCTION

In contrast to the sequencing of linear protein and nucleic acid biopolymers, structural characterization of complex glycans from glycoproteins remains very challenging. Structural elucidation involves characterization of sugar sequence, branching, linkage, anomeric configuration and localization of possible sulfate and phosphate groups [1].

In 1990 Jackson reported on the use of polyacrylamide gel electrophoresis (PAGE) for the separation of fluorophore-labelled carbohydrates, and thereby introduced the technique of fluorophore-assisted carbohydrate electrophoresis (FACE) [2-4]. This method replaces the use of a detergent such as sodium dodecyl sulfate (SDS) by a negatively charged label, e.g. a trisulfone. 2-aminonaphthalene trisulfone (ANTS) [5] and aminopyrene-3,6,8-trisulfonate (APTS) [6] labelled oligosaccharides have been separated by CE by number of groups. APTS derivatives were also characterized by negative ion MALDI-MS. Li *et al.* [7] performed CE/MS on three types of oligosaccharide derivatives (ABEE, *p*-aminobenzoic acid, *m*-aminobenzoic acid). Harvey published a review on MALDI-MS of oligosaccharides [8] which lists a wide range of derivatization agents available for MS.

So far, two CE/ESI-MS studies on ANTS derivatives of neutral oligosaccharides have been reported, [9,10] and our initial attempts to obtain satisfactory ESI spectra on ANTS-labelled *N*-linked oligosaccharides without CE have indicated limited success [11]. Che *et al.* [10] characterized ANTS-derivatized dextran products from partial hydrolysis, i.e. neutral oligosaccharides with different degrees of polymerization (DP). They observed mainly $[M-H]^-$ and $[M-2H]^{2-}$ for $1 \leq DP \leq 6$. With *N*-linked oligosaccharides, our limited success so far may be due to competition between the acidic character of sulfone groups and the basic properties of GlcNAc residues for ionization.

Complete characterization of glycoproteins requires an oligosaccharide analysis of the sugars associated with the protein. In this chapter, we report on method development toward the MS characterization of the glycan content of a model glycoprotein, ovalbumin. Ovalbumin is a molecule whose carbohydrate portion (3.5%) by weight [12] is mostly non-sialylated [13]. Characterization of ovalbumin glycans has been the object of extensive studies over the past 20 years [14-29]. There is only one *N*-glycosylation site, and no *O*-linked glycans are present [14,18,30]. So far, more than 30 different oligosaccharides have been reported. Until 1992, only high-mannose and hybrid types had been listed [14,18,20]. Recently, complex-type oligosaccharides have also been found, and all these *N*-linked glycans have been shown to contain neutral sugars without sialic acid [15,23-25,29]. Charlwood *et al.* [31] recently proposed three sialylated structures among 24 ovalbumin oligosaccharides detected by MALDI-TOF-MS. Harvey *et al.* [16] performed MALDI-TOF-MS on ovalbumin glycans detached by hydrazinolysis, with no derivatization. They reported 36 glycan compositions, none of

which contained sialic acid residues. This model glycoprotein was chosen because of the wide availability of data in the literature pertaining to its structural characterization.

We report on the use and comparison of derivatization, HPLC, FACE and ESI-MS to characterize the molecular masses of glycoforms and glycans of this biomolecule. These experiments follow up on studies by our group, [32-34] where the PMP derivatives of standard sugars were characterized by LC and MS. ANTS derivatization was used for FACE analysis. We also tested the suitability of ANTS derivatives for HPLC/ESI-MS, in an attempt to include only one step of derivatization (ANTS) while allowing two types of analysis (FACE and HPLC/ESI-MS). The characterization of extremely complex glycan structures with microheterogeneity present at each glycosylated site constitutes a difficult task and in most cases, one single method cannot provide sufficient information to perform satisfactory characterization of these biologically important carbohydrates. Thus, using only one type of label, rather than two is attractive in the design of an analytical protocol. For example, the use of ANTS for both FACE and HPLC/ESI-MS would constitute a good time-saving measure. Novelty aspects of this work include the use of PMP for *N*-linked glycans of ovalbumin and the on-line reversed- and normal-phase HPLC/ESI-MS separation of these, plus the use of ANTS derivatization of *N*-linked glycans and detection of ANTS-labelled standards by normal-phase HPLC/MS. The results confirm those found in the literature, and emphasize the greater specificity of on-line HPLC/ESI-MS analysis than FACE analysis alone.

3.2 EXPERIMENTAL

3.2.1 Materials

PMP was purchased from ICN Biomedicals (Aurora, OH, USA) and used as obtained. Peptide-N-glycosidase-F (PNGase F) deglycosylation kits and ANTS derivatization kits were obtained from Glyko (Novato, CA, USA). Tetraglucose {4-O-[4-O-(6-O- α -D-glucopyranosyl- α -Dglucopyranosyl)- α -D-glucopyranosyl]-D-glucopyranose} and ovalbumin (albumin, chicken egg, Grade V) were purchased from Sigma (St Louis, MO, USA). *N*-Linked oligosaccharide standards NGA2 (asialo-, agalacto-, biantennary), NA2 (asialo-, galactosylated, biantennary) and M3N2 (conserved trimannosyl core) were obtained from Oxford GlycoSystems (Rosedale, NY, USA) and used as received. All solvents were glass distilled, HPLC grade and obtained from Mallinckrodt (Paris, KY, USA). Deionized, filtered water was obtained from a Barnstead Nano-Pure water filtration system supplied by a reverse osmosis feedstock.

3.2.2 Preparation of PMP derivatives

Tetraglucose, NGA2 and NA2 (10 μ g) were subjected to PMP derivatization. The mixture of *N*-glycans from ovalbumin was subjected to the same procedure. Typically, the sugars were dissolved in a 0.3 M NaOH solution (10 μ L). A 0.5 M methanolic solution of PMP (10 μ L) was added. The samples were sealed in tubes and heated at 70 °C for 30 min. After cooling, they were neutralized with 10 μ L of 0.3 M HCl. Then, 0.5 mL of water and 1 mL of chloroform were added. The organic phase was discarded. The extraction was repeated twice. The aqueous portion was evaporated to dryness, leaving a residue of PMP-sugar(s). A schematic diagram of PMP labelling is shown in Figure 2.3.

3.2.3 Preparation of ANTS derivatives

These fluorescent derivatives were prepared using the ANTS labeling kit as purchased from Glyko, based on the method described by Jackson [24]. The structure of the ANTS oligosaccharide is shown in Figure 3.1.

3.2.4 Enzymatic release of asparagines-linked oligosaccharides from ovalbumin

Ovalbumin (200 μg) was dissolved in 100 μL of water in a microcentrifuge tube. An equal volume of 2X Profiling Enzyme Buffer (C3) from the Glyko deglycosylation kit was added. Ovalbumin was then denatured by boiling in a hot water-bath. OLIGO profiling enzyme (C1) from Glyko (5 μL) was added to the glycoprotein, and the mixture was mixed and centrifuged. Following 16 h of incubation at 37 °C, the protein was precipitated by adding three volumes of cold absolute ethanol, and the mixture was kept in an ice-bath. The protein was centrifuged down to a pellet, and the supernatant containing the oligosaccharides was removed. The supernatant was dried in a centrifuge vacuum evaporator to a translucent pellet.

3.2.5 FACE profiling

The released oligosaccharides were labelled with fluorophore by the addition of 0.015 M disodium ANTS in 15% acetic acid followed by an equal volume of 1 M NaBH_3CN . The labelled oligosaccharides were then separated by electrophoresis in a 21% precast polyacrylamide gel (Glyko) and imaged and analysed using the fluorophore-assisted carbohydrate electrophoresis (FACE2) image software (Glyko).

3.2.6 On-line HPLC/ESI-MS

The mass spectrometer used was a Quattro-LC from Micromass (Manchester, UK) equipped with a Z-spray™ ESI source. Samples were sprayed using a

3.60 kV needle voltage, and the declustering (cone) voltage was set at values between 20 and 60 V, depending on the experiment conducted. The source block and desolvation temperatures were set at 110 and 250 °C, respectively. Spectra were recorded in both the positive and negative ion modes, with a scan rate of 300 u/sec. For most experiments, 5 μ L aliquots were injected and contained material obtained from ca 200 μ g of the glycoprotein. The HPLC instrument used was a Hewlett-Packard 1100 quaternary delivery system (Agilent Technologies, Mississauga, Ontario, Canada). The columns were (i) a 250 x 4.6 mm i.d. Vydac 218TP54 Protein & Peptide C18 (The Separations Group, Hesperia, CA, USA) for reversed-phase HPLC and (ii) a 250 x 4.6 mm i.d. Ultremex 5 NH2 (Phenomenex, Torrance, CA, USA) for normal-phase experiments. The chromatograph was equipped with a Rheodyne injector (20 μ L loop). A constant flow-rate of 1 mL min⁻¹ was kept, and the composition of the mobile phase was programmed as follows: (i) for reversed-phase HPLC, the initial composition (5%) of ACN in water was kept for 5 min, then increased to 60% over 10 min, and kept at 60% for 20 min. TFA was kept at a constant concentration of 0.04% throughout the separation. (ii) For normal-phase experiments on ANTS derivatives and PMP standards, eluent A was a mixture of ACN and water in proportions varying from 0:10 to 5:5 (v/v) and eluent B was an ACN–water mixture in proportions varying from 2:8 to 7:3 (v/v), with the pH adjusted to 3.5 with formic acid. The gradient consisted of 100% A for 10 min, to 100% B over 10 min, and 100% B for 10 min. This method was based on a gradient developed by Yang and Butler [35] for the separation of benzamide sugar derivatives.

3.3 RESULTS

3.3.1 Ovalbumin characterization

Figure 3.2 shows an ESI mass spectrum obtained for glycans detached from ovalbumin using PNGase F and derivatized with PMP. The glycan mixture was desalted using on-line reversed-phase HPLC/MS, the cone voltage was kept low (20 V) to maximize the production of protonated molecular ions. The solution produced mainly $[M+2H]^{2+}$ ions. The peaks were observed reproducibly over four independent analyses. Due to limited sample size, stress was put on tuning the instrument for increased sensitivity, thus decreasing resolution. The low resolution yielded poor definition of the isotopic clusters and therefore average M_r values were used for comparison. Table 3.1 presents a list of possible compositions of the PMP-glycans detected for the deglycosylated glycan. Most of the glycan compositions have already been reported, [14-16, 31] but using different protocols than the ones reported here.

. Using a reversed-phase gradient, separation of the ovalbumin glycans derivatized with PMP was undertaken. Figure 3.3 shows the SICs of four glycans. As seen from their elution profile the separation was not very efficient. All PMP-sugars eluted within the same range, i.e. over less than 6 min. Attempts to improve the separation by modifying the gradient to a shallower increase of ACN concentration, were met with limited success.

3.3.2 NP-HPLC/ESI-MS

Initial experiments were undertaken for NP-HPLC of PMP derivatives with labelled standard oligosaccharides (tetraglucose and M3N2). The experiment was conducted using 20 V cone voltage, so as to maximize production of protonated

molecules. The results are shown in Figure 3.4, where SICs are used to follow the elution of each compound. The elution of the compounds were monitored through their $[M+H]^+$ signals. We were able to observe good separation. PMP-tetraglucose tended to stay adsorbed on the column longer than PMP-M3N2, and therefore produced wider peaks with extensive tailing. These ions were the most abundant in the mass spectra, with 60 V as the cone voltage (Figure 3.5). No fragmentation was observed at 60 V, and lower cone voltages resulted in similar spectra, but with weaker signals. Under reversed-phase conditions, the nature of ions observed for PMP-oligosaccharides changed with cone voltage. At low voltages of ca 20 V, $[M+2H]^{2+}$ and $[M+3H]^{3+}$ ions were observed with no fragmentation, and at 60 V, $[M+H]^+$ ions and their in-source fragments would appear [33].

The ESI-MS sensitivity achieved in normal-phase conditions was not as good as those under reversed-phase conditions. The detection limits under normal-phase conditions were ca 2 nmol for PMP-tetraglucose and 20 nmol for PMP-M3N2. Some normal-phase SICs obtained for ovalbumin PMP-sugars appear in Figure 3.6. Oligosaccharides were detected (as $[M+H]^+$), and 18 possible compositions were detected, as listed in Table 3.2. All compositions, except for glycans 22–24, were listed in Table 3.1.

3.3.3 FACE

Figure 3.7 shows a picture of a FACE gel with separated ANTS-labelled oligosaccharides from ovalbumin, which have been tentatively identified according to a detailed method based on the DP of ANTS-carbohydrates. Numbers next to the proposed compositions refer to those used in Tables 3.1–3.3, indicating that all sugars detected by

FACE were also detected by at least one method involving MS. FACE is not a definitive identification method, rather it provides informative maps which can be compared to results from other techniques. Figure 3.8 compares calculated migration positions of glycans 1–24 with those of glycans tentatively identified directly from the gel.

Comparison of these diagrams suggests that one band may easily be interpreted as one or two sugars as in the central diagram, while in fact other sugars could also have migrated to similar positions on the gel (left-side diagram).

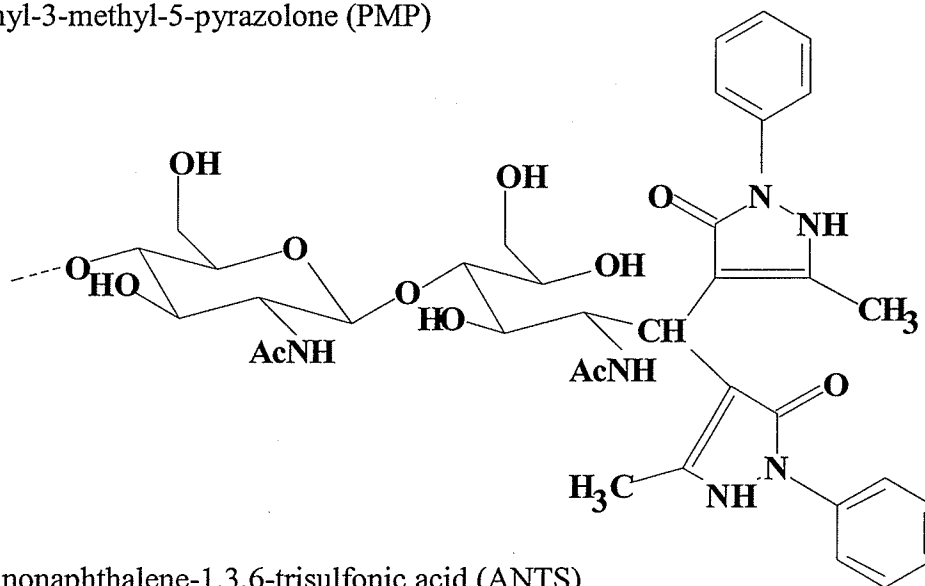
3.3.4 HPLC/ESI-MS studies of ANTS-labelled glycans

The present study was undertaken with a focus to develop an HPLC/MS method for the analysis of ANTS-derivatives of oligosaccharides detached from glycoproteins. Optimization of ESI conditions with the presence of excess ANTS is difficult. Direct loop injection of ANTS-labelled oligosaccharides results in the spectra being dominated by the excess ANTS. Sep-Pak methods using either normal-or reversed-phase packings failed to eliminate all the excess ANTS reagent. On-line HPLC/MS was a better option for the detection of these derivatives. Because there is no significant retention of ANTS and its sugar derivatives by RP-HPLC, a normal-phase column was used. At high pH, negatively charged species would adhere to the column and cause lengthy retention with extensive band broadening. A low pH eluent was therefore used, made up of water, ACN and formic acid at pH 3.5. The gradient was operated as to increase concentration of formic acid over time, while decreasing the polarity of the solvent itself, i.e. decreasing the proportion of ACN in water. The initial portion of the experiment involved optimizing the chromatographic conditions using ANTS-labelled standards (M3N2, NGA2 and NA2). Figure 3.9 compares the SIC signals and mass

spectra obtained for ANTS-M3N2 with cone voltages of 20 V [(a) and (c)] and 60 V [(b) and (d)]. At 20 V, the strongest analyte related signal was produced by $[M-4H+Na]^{3-}$ ions at m/z 431. At 60 V, the ANTS-labelled molecule breaks down and abundant Z_1 ions (m/z 571) are produced. For M3N2 and other ANTS-labelled standards, separation is observed (not shown), but the poor sensitivities obtained at a 20 V cone voltage [Figure 3.9(c)] and the breakdown of the analytes at higher cone voltages [e.g. Figure 3.9(d)] hamper the significance of the experiment. Similar experiments were repeated in the positive ion mode, without observing any significant analyte signals.

The last experiment discussed consists of using normal-phase HPLC combined with negative mode ESI-MS to study ovalbumin glycans derivatized with ANTS. Owing to the low concentration of each labelled glycan combined with co-elution of excess ANTS, high levels of background noise were observed. The results obtained were inconclusive as only six glycans were positively identified. In our hands HPLC/ESI-MS of ANTS derivatives of neutral oligosaccharides does not show promise and is better suited for CE/ESI-MS [46,47]. Therefore, the combination of ANTS derivatization, normal-phase HPLC and ESI-MS on a Quattro-LC system did not allow for the successful identification of *N*-linked glycans from a glycoprotein, whereas the use of PMP derivatization leads to more useful results.

1-phenyl-3-methyl-5-pyrazolone (PMP)



8-aminonaphthalene-1,3,6-trisulfonic acid (ANTS)

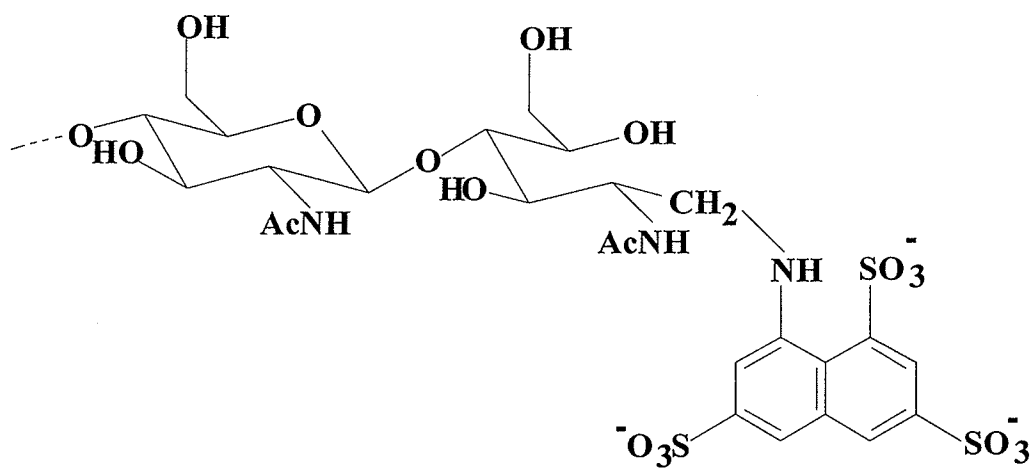


Figure 3.1 Labels used in this study.

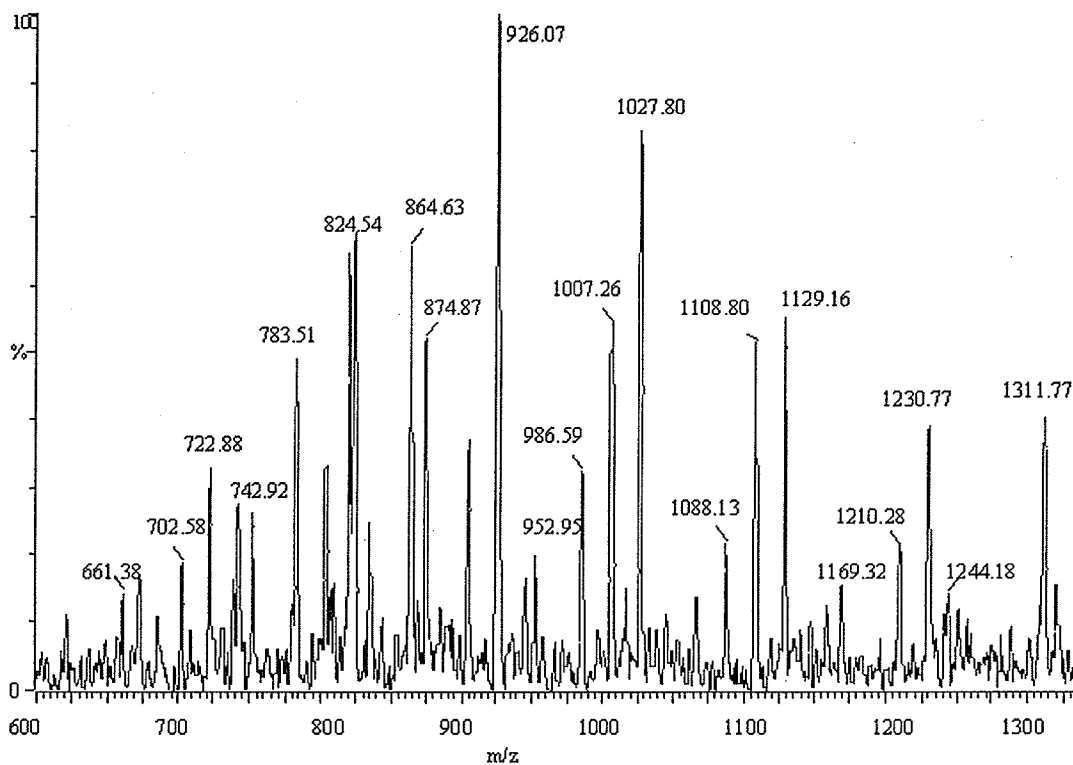


Figure 3.2 Electrospray spectrum of hen ovalbumin glycans labelled with PMP (see Figure 3.1), detached using PNGase F and run by on-line reversed phase HPLC/MS. See Table 3.1 for proposed assignments.

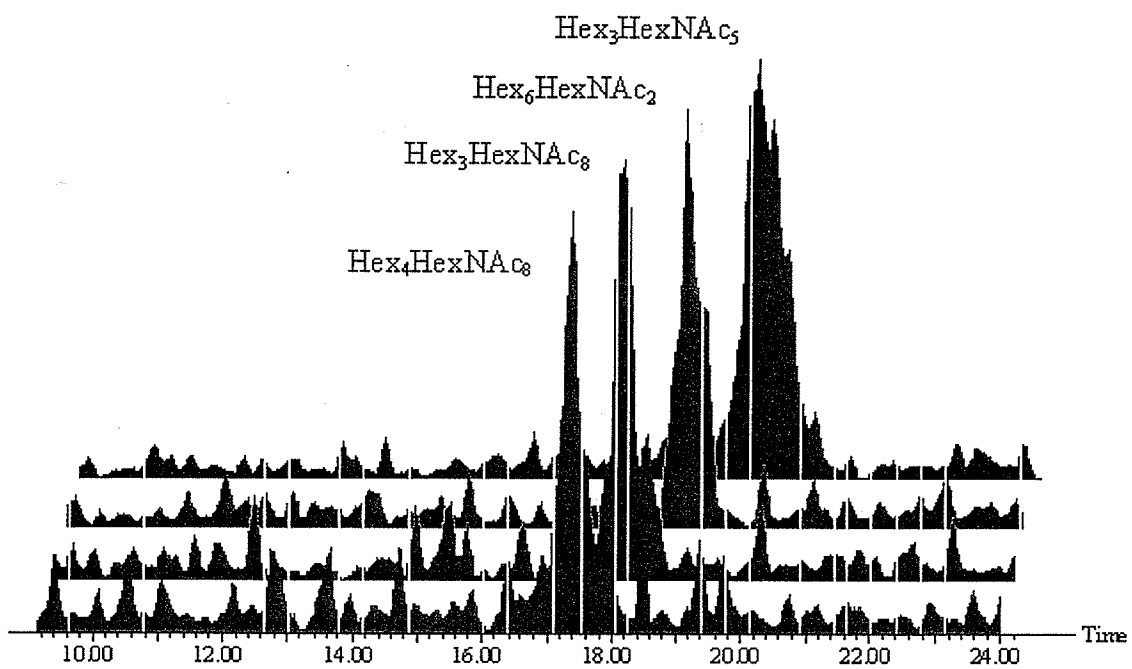


Figure 3.3 On-line reversed phase HPLC/ESI-MS selected ion chromatograms obtained for PMP-labelled ovalbumin glycans, detached with PNGase F. See Table 1 for proposed assignments.

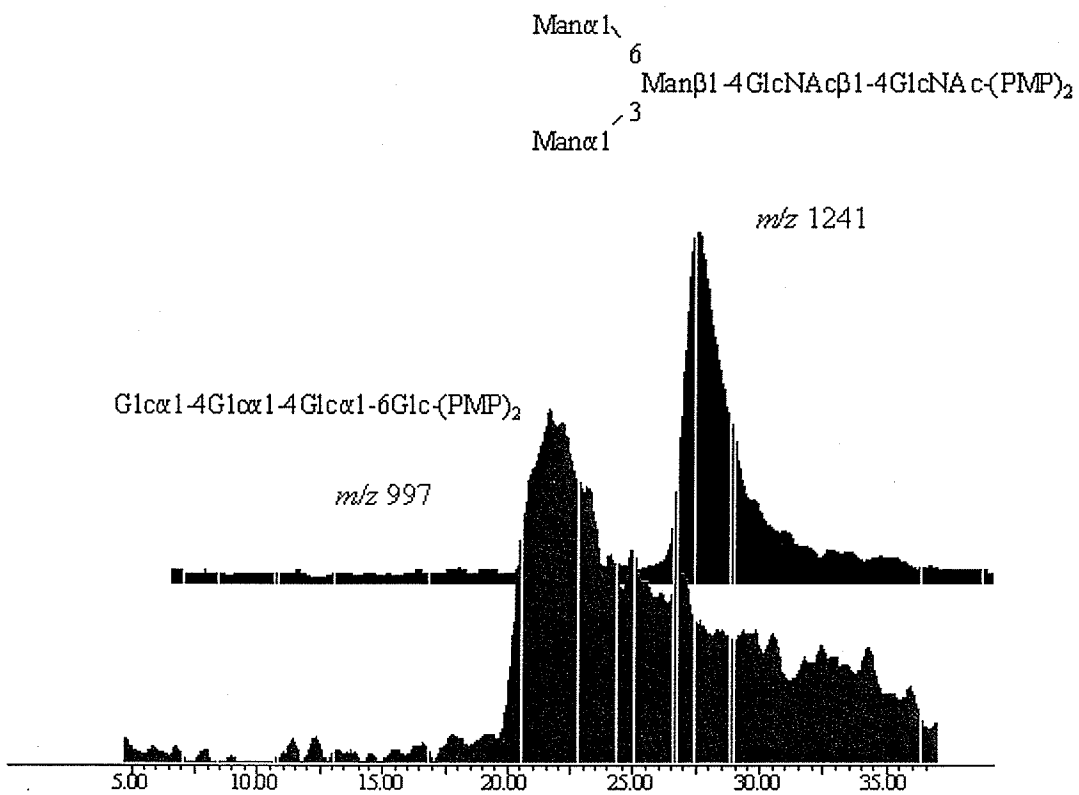


Figure 3.4 NP-HPLC/ESI-MS of PMP-derivatized standards (tetraglucose and M3N2).

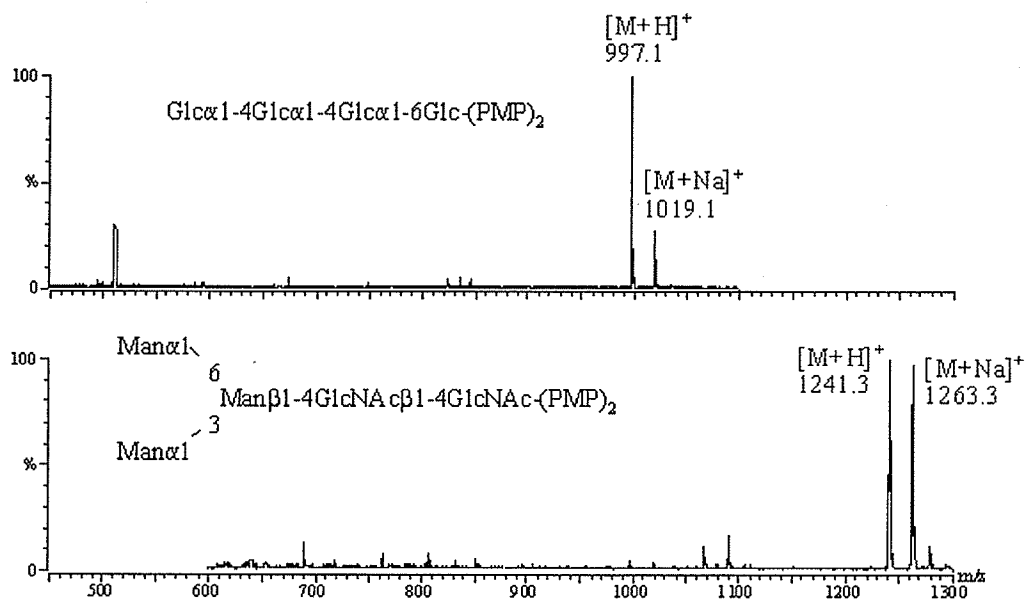


Figure 3.5 ESI spectra of NP-HPLC/MS separated standards at 60 V (tetraglucose and M3N2).

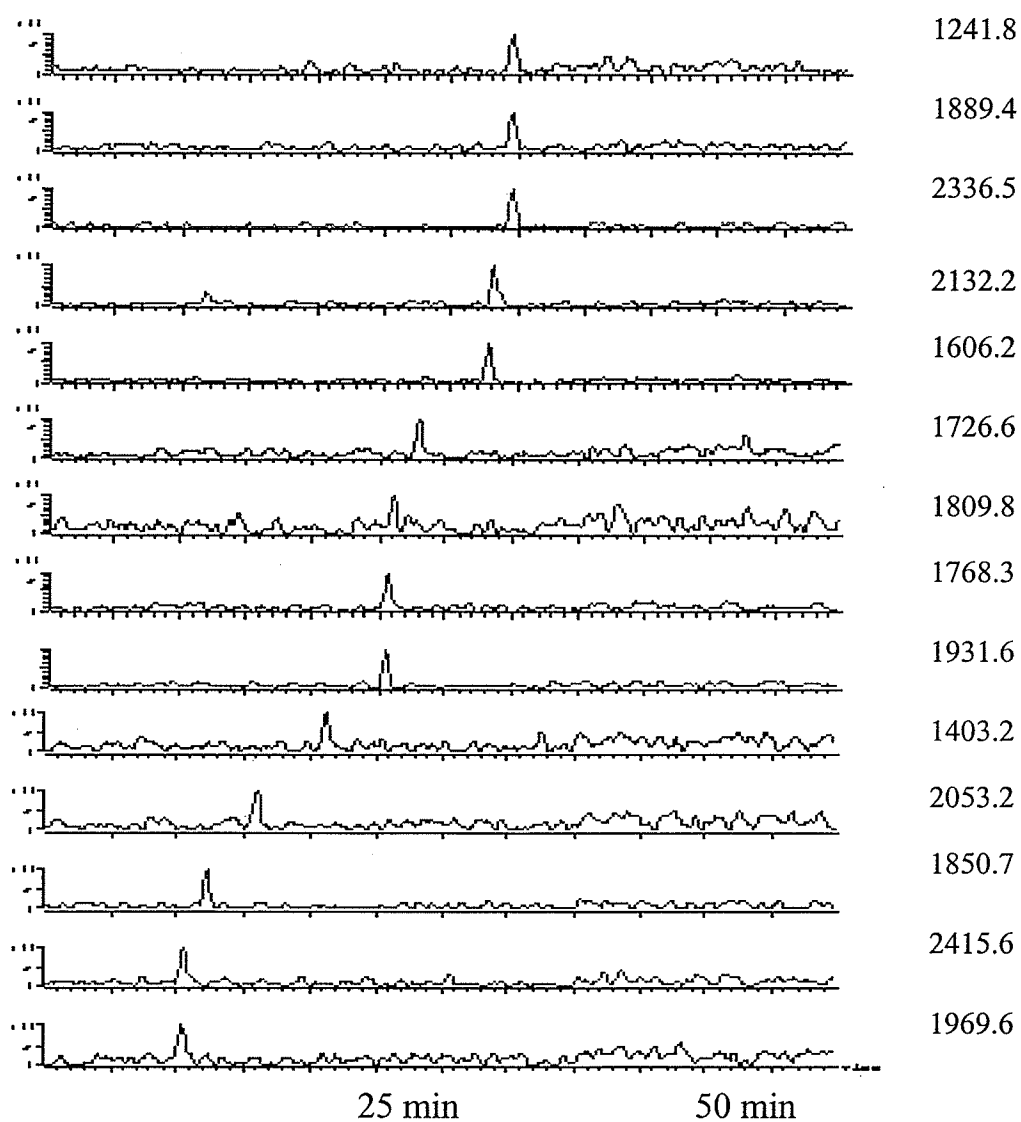


Figure 3.6 On-line normal phase HPLC/ESI-MS selected ion chromatograms obtained for PMP-labelled ovalbumin glycans, detached with PNGase F. Numbers on the right indicate the selected m/z values. See Table 3.2 for proposed assignments.

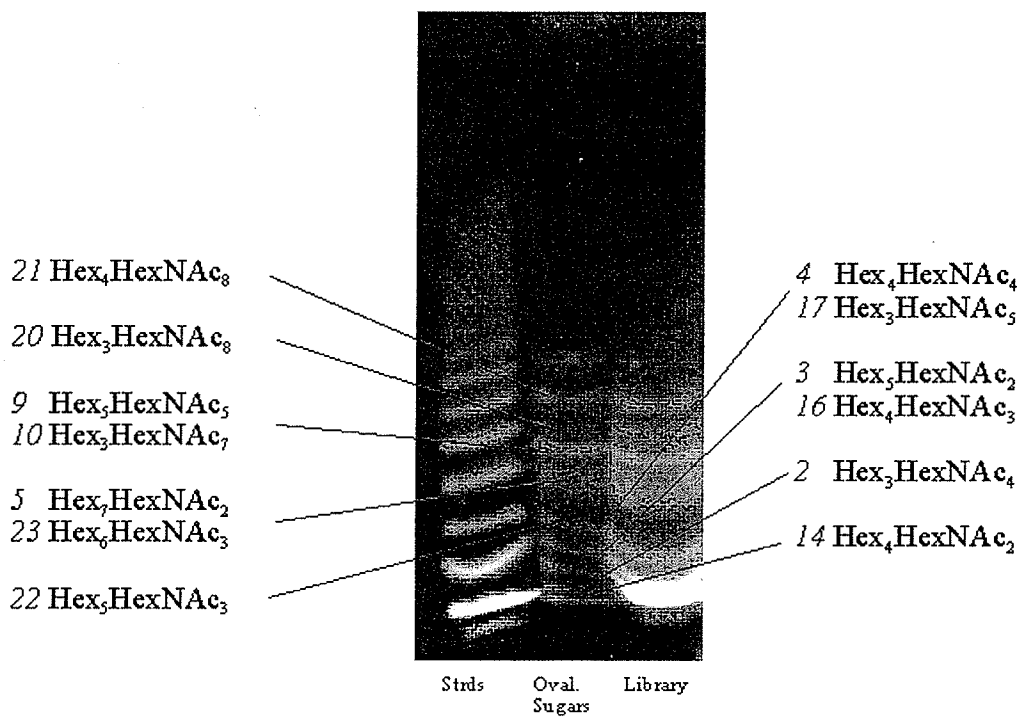


Figure 3.7. Negative of a fluorophore-assisted carbohydrate electrophoresis (FACE) gel, separation obtained for ANTS-labelled ovalbumin glycans, detached with PNGase F.

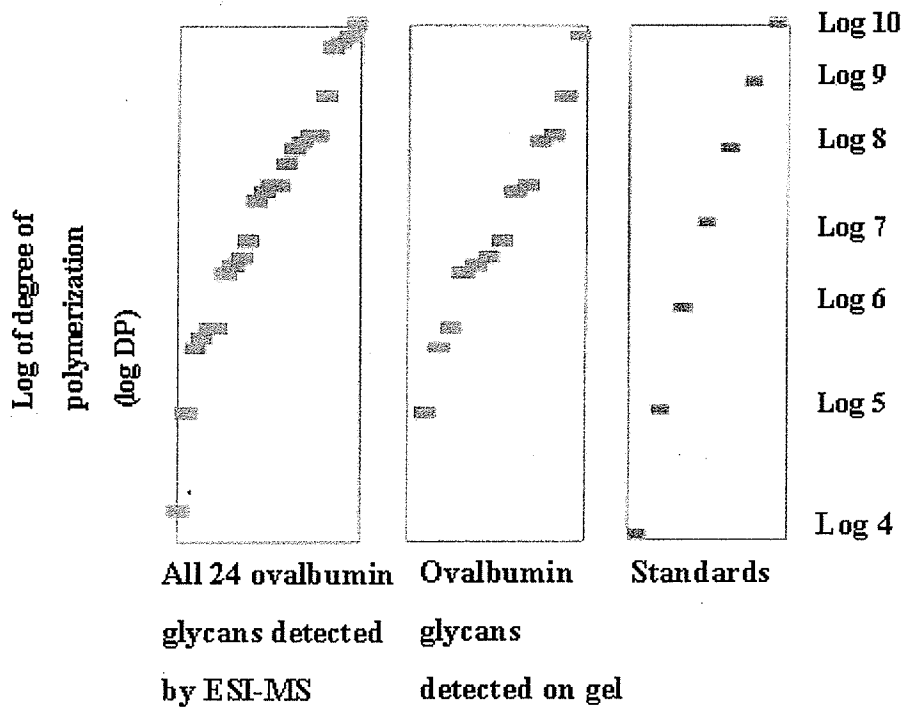


Figure 3.8. Calculated FACE migrations of ANTS-labelled glycans.

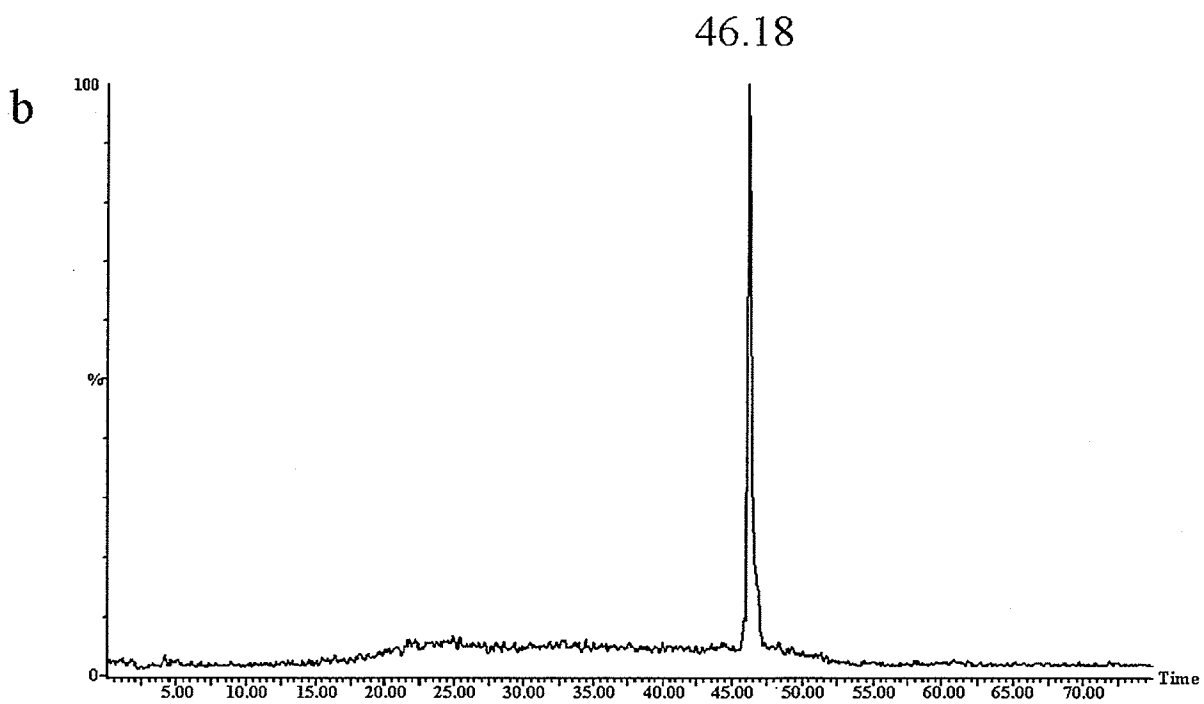
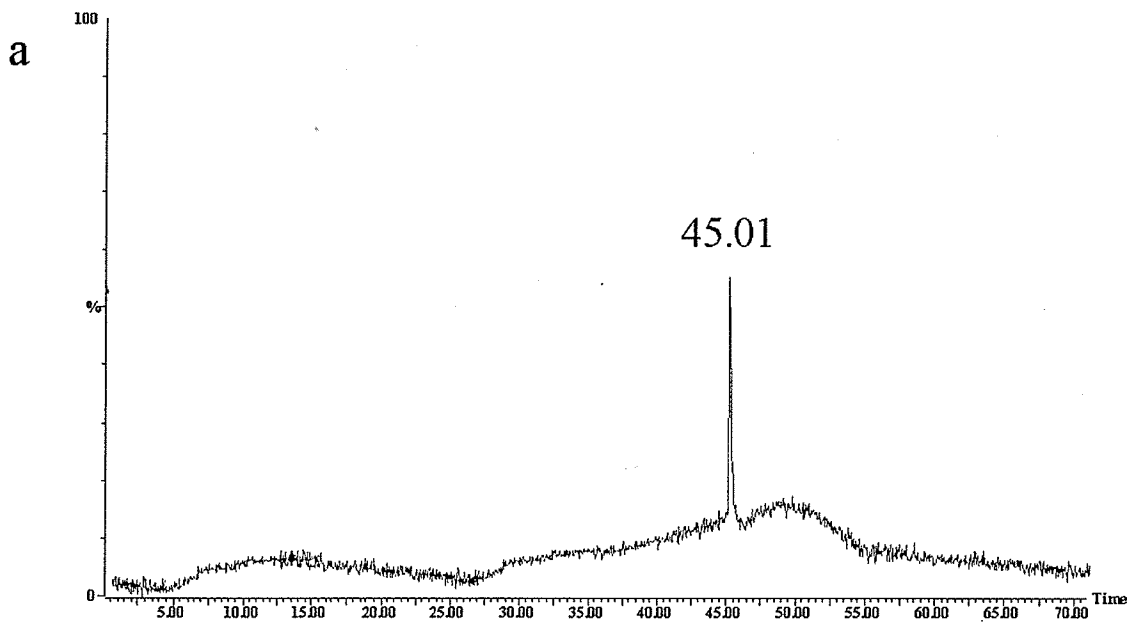


Figure 3.9 Selected ion chromatograms obtained by on-line normal-phase HPLC/ESI-MS of ANTS-M3N2. (a) SIC of m/z 431 ions at a cone voltage of 20 V; (b) SIC of m/z 571 ions at a cone voltage of 60 V.

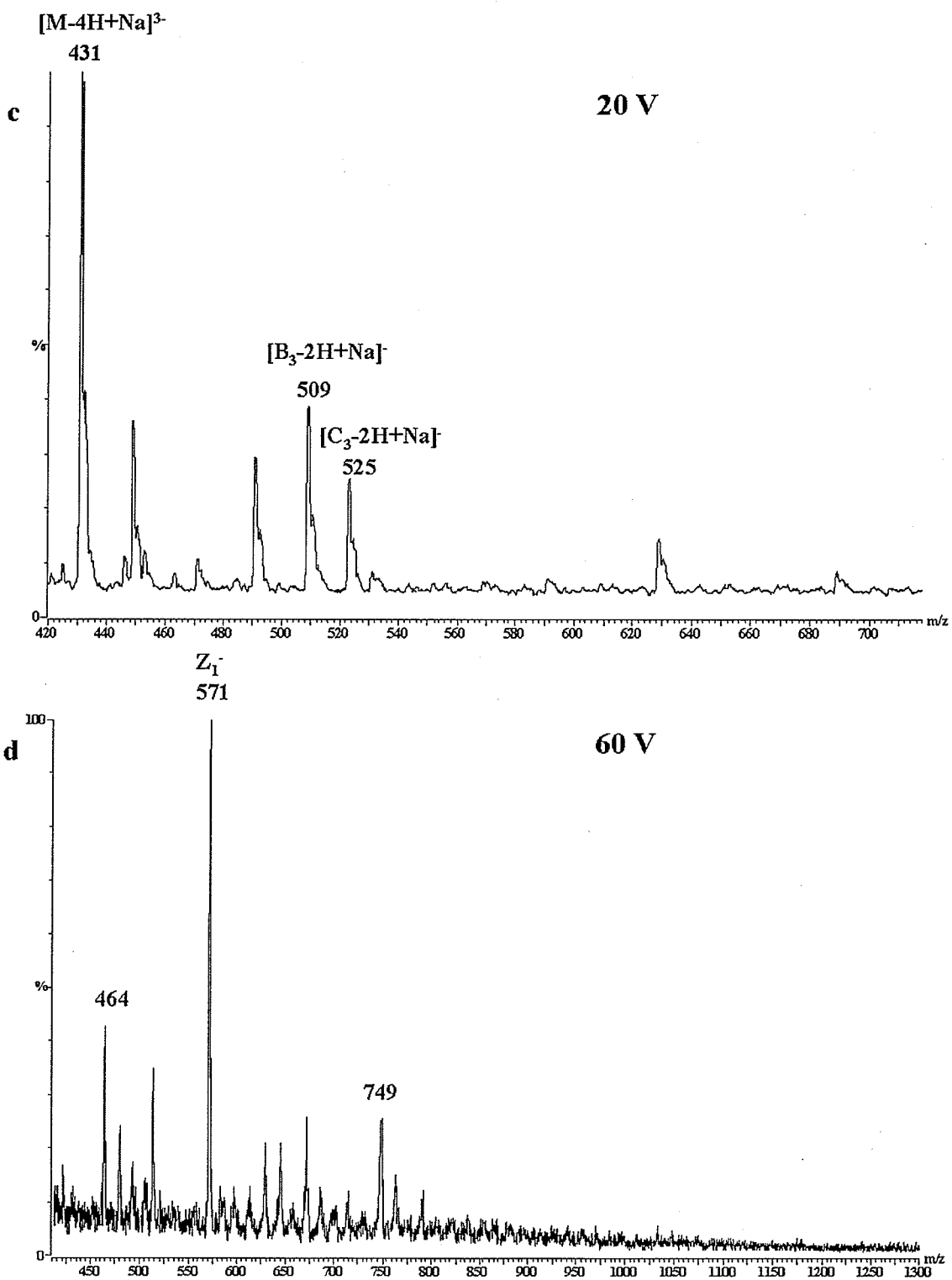
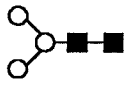
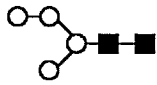
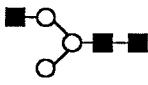
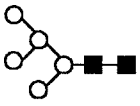
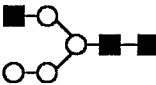
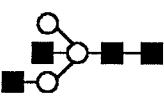
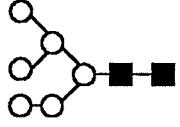
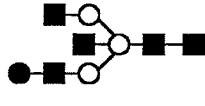
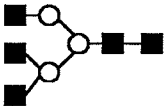
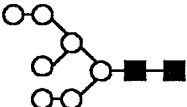
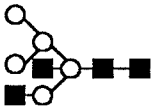
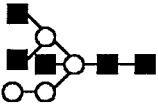
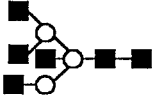
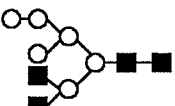
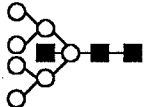
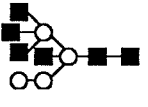
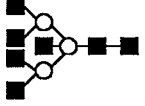
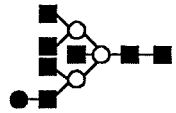
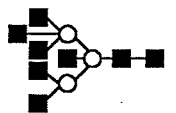
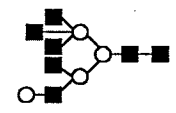


Figure 3.9 Mass spectra obtained by on-line normal-phase HPLC/ESI-MS of ANTS-M3N2. (c) mass spectrum at 20 V; (d) mass spectrum at 60 V.

Table 3.1 Assigned M_r and composition of oligosaccharides cleaved from ovalbumin with PNGase F and derivatized with PMP (reversed-phase HPLC/ESI-MS).

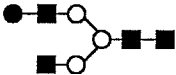
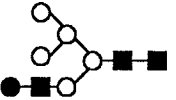
Observed m/z of PMP-oligosaccharide (2+)	M_r of oligosaccharide (Da) ^a	Composition (calculated M_r of oligosaccharide)	Suggested Structure ^{18,21,23,38}	No.
621.5	911	$H_3N_2(911)$		13
702.6	1073	$H_4N_2(1073)$		14
722.9	1114	$H_3N_3(1114)$		15
783.5	1235	$H_5N_2(1235)$		1
804.2	1276	$H_4N_3(1073)$		16
824.5	1317	$H_3N_4(1317)$		2
864.6	1397	$H_6N_2(1397)$		3
905.5	1479	$H_4N_4(1479)$		4


926.1	1520	$H_3N_5(1520)$		17
945.5	1559	$H_7N_2(1559)$		5
986.6	1641	$H_5N_4(1641)$		6
1007.3	1682.6	$H_4N_5(1682.5)$		18
1027.8	1724	$H_3N_6(1724)$		7
1067.5	1803	$H_6N_4(1804)$		8
1088.1	1844	$H_5N_5(1845)$		9
1108.8	1886	$H_4N_6(1886)$		19
1129.2	1926	$H_3N_7(1927)$		10

1169.3	2007	H ₆ N ₅ (1317)		11
1210.3	2089	H ₄ N ₇ (2089)		12
1230.8	2130	H ₃ N ₈ (2130)		20
1311.8	2292	H ₄ N ₈ (2292)		21

^a Obtained by subtracting the mass of the PMP portion from the observed *Mr* of PMP derivatives.

Table 3.2 Assigned M_r and composition of oligosaccharides cleaved from ovalbumin with PNGase F and derivatized with PMP (normal-phase HPLC/ESI-MS)

Observed m/z of PMP-oligosaccharide (+)	M_r of oligosaccharide (Da) ^a	Composition (calculated M_r of oligosaccharide)	Suggested Structure ^{18,21,23,38}	No.
1241.8	911	H ₃ N ₂ (1073)	See Table 3.1	14
1403.2	1072	H ₄ N ₂ (1072)	See Table 3.1	15
1566.	1235	H ₃ N ₃ (1235)	See Table 3.1	1
1605.4	1274	H ₅ N ₂ (1275)	See Table 3.1	13
1648.2	1317	H ₄ N ₃ (1317)	See Table 3.1	2
1726.6	1396	H ₃ N ₄ (1396)	See Table 3.1	3
1768.3	1437	H ₆ N ₂ (1434)		22
1809.8	1479	H ₄ N ₄ (1478)	See Table 3.1	4
1850.7	1520	H ₃ N ₅ (1520)	See Table 3.1	17
1889.4	1558	H ₇ N ₂ (1558)	See Table 3.1	5
1931.6	1601	H ₅ N ₄ (1600)		23
1969.6	1639	H ₄ N ₅ (1640)	See Table 3.1	6
2053.2	1722	H ₃ N ₆ (1723)	See Table 3.1	7
2132.2	1801	H ₆ N ₄ (1803)	See Table 3.1	8
2215.6	1885	H ₄ N ₆ (1885)	See Table 3.1	19
2257.1	1926	H ₃ N ₇ (1926)	See Table 3.1	10

2336.5	2005	H ₆ N ₅ (2006)	See Table 3.1	11
2415.6	2085	H ₄ N ₇ (2087)	See Table 3.1	12
2539.5	2209	H ₆ N ₆ (2209)		24

^a Obtained by subtracting the mass of the PMP portion from the observed *Mr* of PMP derivatives.

3.4 DISCUSSION

Ovalbumin has only one glycosylation site (Asn-292), containing variety of non-sialylated glycans [36]. However, recently the presence of 3 sialylated glycans for ovalbumin has been reported [31]. The present study did not show the presence of any sialylated glycans, this may be due to the experimental conditions used. Even though PMP derivatization prevents desialylation, there exists a possibility that they are eliminated during extraction with NaOH. Furthermore, these investigations were performed in the positive mode contrast to the above mentioned study, as they used negative mode MALDI-MS for their detection of sialylated glycans.

The M_r values measured through ESI-MS experiments can only suggest possible [(Hex)_x (GlcNAc)_y] structures. More specific information on carbohydrate structure has, however, been obtained in other laboratories by MALDI-TOF-MS, with detection in the post-source decay (PSD) mode, [17,37,38] or by ESI-CID-MS/MS [31,39,40].

Our laboratory [33] has shown the separation of sialylated *N*-linked glycans and the separation of sialylated from asialylated *N*-linked glycans by RP-HPLC/ESI-MS. Using a similar reversed-phase gradient, separation of the ovalbumin glycans derivatized with PMP was undertaken. As seen from their elution profile (Figure 3.3) the separation was not very efficient. The findings were disappointing given that we had shown earlier that it was possible to separate sialylated from asialylated *N*-linked carbohydrates, and carbohydrates with different numbers of sialic acid residues using a similar reversed-phase gradient [33].

The present study was undertaken with a focus to develop an HPLC/MS method for the analysis of ANTS-derivatives of oligosaccharides detached from glycoproteins. ANTS-labelled oligosaccharides have been separated by FACE [2–4] and CE [5]. The two aromatic rings of ANTS allow detection either by UV absorption at 226 nm or by LIF using a helium-cadmium laser with excitation at 325 nm and the three sulfonate groups provide the required charged groups for the separation. The characterization of extremely complex glycan structures with microheterogeneity present at each glycosylated site constitutes a difficult task and in most cases, one single method cannot provide sufficient information to perform satisfactory characterization of these biologically important carbohydrates. Thus, using only one type of label, rather than two is attractive in the design of an analytical protocol. For example, the use of ANTS for both FACE and HPLC/ESI-MS would constitute a good time-saving measure. The need to establish a suitable chromatographic/mass spectrometric procedure for ANTS derivatives still exists, and is the focus of the following discussion. The derivatization of glycans involves the use of excess ANTS. The excess ANTS is difficult to eliminate from the derivatized sugar using chromatographic methods owing to its high mobility relative to ANTS-labelled large sugars.

North *et al.* [15] and Charlwood *et al.* [31] have shown the separation of AMAC-derivatized ovalbumin glycans by hydrophilic interaction liquid chromatography (HILC). The mobile phase used in both studies [15,31] was similar to that used by Yang and Butler [35] for normal-phase separations, and we decided to use a similar approach with an amino column. The ESI-MS sensitivity achieved in normal-phase conditions was not as good as those under reversed-phase conditions. Shen *et al.* [32] had previously

shown the detection limit to be 2 pmol for PMP-tetraglucose and 1 nmol for PMP-NGA3 (asialo-, agalacto, triantennary). The detection limits under normal-phase conditions were ca 2 nmol for PMP-tetraglucose and 20 nmol for PMP-M3N2.

The results obtained were inconclusive as only six glycans were positively identified. In our hands HPLC/ESI-MS of ANTS derivatives of neutral oligosaccharides does not show promise and is better suited for CE/ESI-MS [9,10]. Therefore, the combination of ANTS derivatization, normal-phase HPLC and ESI-MS on a Quattro-LC system did not allow for the successful identification of *N*-linked glycans from a glycoprotein, whereas the use of PMP derivatization leads to more useful results.

3.5 CONCLUSIONS

Electrospray of an intact glycoprotein with a low glycosylation level, such as ovalbumin, provided reliable qualitative information on the sugar content of the molecule. The ESI-MS sensitivity associated with ANTS-derivatized *N*-linked sugars was really poor if intact molecular ions were detected. It was enhanced by detection of abundant fragment ions at higher cone voltages. For these types of sugars, ANTS is a better label for electrophoresis and fluorescence than it is for mass spectrometry. Characterization of the PMP-derivatized pool of *N*-linked glycans from ovalbumin by full-scan reversed-phase and normal-phase HPLC/ESI-MS confirmed some of the sugar compositions found by ESI of the intact glycoprotein. Comparison of results obtained using more than one method was important here, because although they produced overlapping data, the methods did not yield identical fingerprints.

3.6 REFERENCES

- 1 Bahr U., Pfenninger A., Karas M. and Stahl B. *Anal. Chem.* **69**, 4530 (1997).
2. Jackson P. *Biochem. J.* **270**, 705 (1990).
3. Jackson P. and Williams G.R. *Electrophoresis* **12**, 94 (1999).
4. Jackson P. *Anal. Biochem.* **196**, 238 (1991).
5. Klockow A., Amado R., Widmer H.M. and Paulus A. *J. Chromatogr. A* **716**, 241 (1995).
6. Suzuki H., Müller O., Guttman A. and Karger B.L. *Anal. Chem.* **69**, 4554 (1997).
7. Li D.T., Sheen J.F. and Her G.R. *J. Am. Soc. Mass Spectrom.* **11**, 292 (2000).
8. Harvey D.J. *Mass Spectrom. Rev.* **18**, 349 (1999).
9. Delaney J., Gennaro L. and Vouros P. In *Proceedings of the 48th ASMS Conference on Mass Spectrometry and Allied Topics, 2000*.
10. Che F., Song J.F., Zeng R., Wang K.Y. and Xia Q.C. *J. Chromatogr. A* **858**, 229 (1999).
11. Saba J.A., Jamieson J.C. and Perreault H. In *Proceedings of the 48th ASMS Conference Mass Spectrometry and Allied Topics, 2000*.
12. Tomiya N., Awaya J., Kurono M., Endo S., Arata Y. and Takahashi N. *Anal. Biochem.* **171**, 73 (1988).
13. Sottani C., Fiorentino M. and Minoia C. *Rapid Commun. Mass Spectrom.* **11**, 907 (1997).
14. Duffin K.L., Welply J.K., Huang E. and Henion J.D., *Anal. Chem.* **64**, 1440 (1992).
15. North S., Birrell H. and Camilleri P. *Rapid Commun. Mass Spectrom.* **12**, 349 (1998).
16. Harvey D.J., Wing D.R., Kuster B. and Wilson I.B.H. *J. Am. Soc. Mass Spectrom.* **11**, 564 (2000).
17. Harvey D.J. *J. Am. Soc. Mass Spectrom.* **11**, 572 (2000).
18. Yet M.G., Chin C.C.Q. and Wold F. *J. Biol. Chem.* **263**, 111 (1988).
19. Chen L.M., Yet M.G. and Shao M.C. *FASEB J.* **2**, 219 (1988).

20. Honda S., Makino A., Suzuki A. and Kakehi K. *Anal. Biochem.* **191**, 228 (1990).
21. Kakehi K. and Honda S. *Appl. Biochem. Biotechnol.* **43**, 55 (1993).
22. Tai T., Yamashita K., Ito S. and Kobata A. *J. Biol. Chem.* **252**, 6687 (1977).
23. Corradi Da Silva M.L., Stubbs H.J., Tamura T. and Rice K.G. *Arch. Biochem. Biophys.* **318**, 465 (1995).
24. Kuster B., Naven T.J.P. and Harvey D.J. *J. Mass Spectrom.* **31**, 1131 (1996).
25. Mechref Y. and Novotny M.V. *Anal. Chem.* **70**, 455 (1998).
26. Tai T., Yamashita K., Ogata-Arakawa M., Koide N., Muramatsu T., Twashita S., Inoue Y. and Kobata, A. *J. Biol. Chem.* **250**, 8569 (1975).
27. Yamashita K., Tachibana Y. and Kobata A. *J. Biol. Chem.* **253**, 3862 (1978).
28. Ashton D.S., Beddell C.R., Cooper D.J. and Lines A. *Anal. Chim. Acta* **306**, 43 (1995).
29. Naven T.J.P. and Harvey D.J. *Rapid Commun. Mass Spectrom.* **10**, 1361 (1996).
30. Patel T., Bruce J., Merry A., Bigge C., Wormald M., Jaques A., and Parekh R. *Biochemistry* **32**, 679 (1993).
31. Charlwood J., Birrell H., Bouvier E.S.P., Langridge J. and Camilleri P. *Anal. Chem.* **72**, 1469 (2000).
32. Shen X. and Perreault H. *J. Mass Spectrom.* **34**, 502 (1999).
33. Saba J.A., Shen X., Jamieson J.C. and Perreault H. *Rapid Commun. Mass Spectrom.* **13**, 704 (1999).
34. Shen X. and Perreault H. *J. Chromatogr. A* **811**, 47 (1998).
35. Yang M. and Butler M. *Biotechnol. Bioeng.* **68**, 370 (2000).
36. Sutton C.W., O'Neill J.A. and Cottrell J.S. *Anal. Biochem.* **218**, 34 (1994).
37. Talbo G. and Mann M. *Rapid Commun. Mass Spectrom.* **10**, 103 (1996).
38. Harvey D.J., Naven T.J.P., Kuster B., Bateman R.H., Green M.R. and Critchley G. *Rapid Commun. Mass Spectrom.* **9**, 1556 (1995).

39. Reinhold V.N., Reinhold B.B. and Costello C.E. *Anal. Chem.* **67**, 1772 (1995).

40. Reinhold V.N., Reinhold B.B. and Chan S. *Methods Enzymol.* **271**, 377 (1996).

4 A STUDY OF IMMUNOGLOBULIN G GLYCOSYLATION IN MONOCLONAL AND POLYCLONAL SPECIES BY ELECTROSPRAY AND MATRIX-ASSISTED LASER DESORPTION/IONIZATION MASS SPECTROMETRY

4.1 INTRODUCTION

The glycoproteins called immunoglobulins G (IgG) form the most prevalent class of antibodies found in blood serum and in lymph. They account for about 75% of total serum immunoglobulins and about 15% of all serum proteins [1,2]. IgGs are secreted by activated B lymphocytes and malignant myelomas. They are present both in plasma and in interstitial fluid and are the only immunoglobulins to cross the placenta in significant volume. IgGs are involved in the humoral immune response, binding to antigens to inactivate them or triggering an inflammatory response which results in their clearance.

IgGs are the least glycosylated of the immunoglobulins, containing 2–3% carbohydrate by mass in mammals. More specifically, murine IgGs contains 2.3 asparagine-linked (*N*-linked) biantennary oligosaccharide chains per molecule [3], and human IgGs, 2.8 [4]. Two of these represent glycosylation at the conserved sites at Asn-297 in the heavy-chain C_H2 domains of the Fc portion [4]. The remaining 0.3 or 0.8 glycans are contained in the hypervariable regions of the Fab section, with position and frequency of occurrence dependent on the presence of the consensus sequence Asn-Xaa-Thr/Ser for *N*-glycosylation. Parekh *et al.* [4] reported about 30 variants of biantennary chains in human IgG, the majority of which are core fucosylated, as are murine IgG oligosaccharides [3]. Fc glycans tend to be core fucosylated and their extent of

galactosylation is variable (0 to 2 galactosyl residues). Galactosylated glycans may also be monosialylated, but not disialylated, due to internal hindrance between the C_{H2} domains. Fab glycans are similar to those in Fc, with higher extents of galactosylation and higher incidence of mono- and disialylated structures [5]. Bisecting *N*-acetylglucosamine (GlcNAc) residues are uncommon in murine IgG [3], have a low incidence in human IgG Fc glycans, and have a higher incidence in human Fab glycans [6]. The Fc glycans of IgG are important for the antibody to maintain its structure and functions [7]. In the hypervariable regions, Fab *N*-linked glycosylation has been reported to influence the binding affinity of antigens [8]. Reports have shown that IgG forms containing Fab oligosaccharides may have preferential roles in IgG self-association, aggregation, and cryoprecipitation [9].

Raju *et al.* [10] showed that for neutral oligosaccharides from polyclonal IgGs, the extent of terminal galactosylation, core-fucosylation, and/or presence of bisecting *N*-acetylglucosamine varies among species (human, rhesus, dog, cow, guinea pig, sheep, goat, horse, rat, mouse, rabbit, cat, and chicken). They also found acidic oligosaccharides to contain *N*-acetylneuraminic acid (human and chicken), *N*-glycolylneuraminic acid (rhesus, cow, sheep, goat, horse, and mouse), or both types of sialic acids (dog, guinea pig, rat, rabbit, and cat).

Kunkel *et al.* [11] were able to observe similar results for bovine and human polyclonal IgG. They were able to show that predominant *N*-linked structures were core fucosyl asialyl biantennary chains with varying galactosylation. There were also some minor amounts of afucosyl, bisected, and monosialyl oligosaccharides. *N*-linked glycans from human and bovine IgG had approximately the same incidences of

core-fucosylation (85–90%), bisecting *N*-acetylglucosamine (5–15%), and the presence of at least one terminal galactose (75–85%). The incidence of sialylation was low and consisted almost entirely of 5(*N*)-acetylneuraminic acid in human IgG and solely of 5(*N*)-glycolylneuraminic acid in bovine IgG. The characterization and quantification were performed using HPAEC-PAD. Although HPAEC-PAD is now a well established technique in carbohydrate analysis, it does not provide structural details in regards to the compounds observed and is limited by the complexity of the glycan mixtures released from glycoproteins. Furthermore, identification of glycans is possible only if the proper standards are available to establish their elution position [12]. And even if this is the case the peak in question must represent single structure.

Mass spectrometry on the other hand provides more reliable qualitative determination and has exhibited quantitative capabilities, as discussed in the next paragraphs.

Recent reports have highlighted the semi-quantitative properties offered by the MALDI technique. Harvey *et al.* [13] have shown that the general spectral peak heights or areas will reflect the amount of oligosaccharides in a sample providing that the correct matrix is chosen. A study by Raju *et al.* [10] has shown that the relative *pKa* values of analytes in a mixture has an effect on ionization efficiency in MALDI, thus the use of negative ion-mode MALDI would be suitable than the positive mode for the analysis of acidic *N*-linked oligosaccharides. The quantitative capability of MALDI strongly relies on similar chemical properties among analytes in a mixture, e.g., carbohydrates different in composition by one GlcNAc residue will have different ionization efficiencies in the positive ion mode, whereas a difference of one Gal instead

would not be as influential. Also, the presence of sialic acid residues greatly enhances negative ion production, but will decrease the number of ions observed in the positive mode. Competition for ion formation between analytes in mixtures is also controlled by relative pK_a values to a certain extent. The higher the pK_a , higher the efficiency of ionization in the positive mode for analytes of the same class. The same ideas are also applicable to ESI-MS measurements.

The polyclonal IgG glycans have been extensively characterized. In the first part of the chapter we tested mass spectrometry as a potential quantitative and qualitative tool in the determination of glycan structures from polyclonal IgG, specifically for human and bovine. Quantitative studies to date have been done with CE-LIF and HPAEC-PAD [10,11]. Although both methods have been established in carbohydrate analysis as precise analytical methods, they are limited by complexity of the sample involved. Mass spectrometry provides more reliable qualitative information and we will show that it can be used quantitatively as well for the characterization of IgG glycans. Furthermore MS/MS methods will provide quicker analysis time and require minimum sample size, this is of importance when dealing with biological samples when sample sizes are small. We have used a combination of derivatization, HPLC/ESI-MS, and MALDI-MS to characterize the glycans released from human and bovine polyclonal IgG. The polyclonal IgG were characterized qualitatively by HPLC/ESI-MS. Structural elucidation involved derivitization of the glycans with PMP [14] and the use of a prototype double quadrupole time-of-flight (QqTOF) mass spectrometer [15]. The MALDI mass spectrometer used allowed acquisition of MS and tandem MS, which were useful for structural investigations at a more detailed level.

The second portion of this study is aimed at characterizing glycans from monoclonal species. Monoclonal antibodies (mAbs) are becoming increasingly useful as diagnostic reagents and pharmaceuticals [10]. Typically, mAbs belong to the IgG class and thus produced in hybridoma or recombinant cell cultures. Different aspects of the cell culture conditions can have an effect on the glycosylation of mAbs and recombinant proteins. Thus functional consequences resulting from improper glycosylation may be significant if IgG is to be used in products for human therapeutic and diagnostic use. Earlier work performed at our university examined the effect of varying the dissolved oxygen (DO) concentration (10 to 100%) on the structure of the *N*-linked oligosaccharides of mAb [5,10,16]. The murine B-lymphocyte hybridoma was grown in chemostat culture in two different bioreactors. A link was established between steady-state DO concentration and the structure of *N*-linked oligosaccharide chains of the antibody produced by the cells in two different bioreactors, establishing that the trend was not bioreactor specific [5]. Overall, the extent of galactosylation decreased with reduced DO concentration and all *N*-linked glycans were associated with the heavy chains of the IgG₁ produced, most probably in the Fc at Asn-297 [10,17]. Monoclonal antibody oligosaccharides had the same incidence of core-fucosylation (~95%) and bisecting *N*-acetylglucosamine (~5%) as polyclonal murine IgG [10]. The same study had shown that an increase in the level of DO concentration in hybridoma cell culture on mAb glycosylation, could increase the level of galactosylation of the chains. At 10% DO, the chains were mainly agalactosyl (~45%) or monogalactosyl (~45%), with little digalactosyl (10%) chains. At higher DO concentrations, there was a significant reduction in the amount of agalactosyl chains (~20%) and an increase in the amount of

monogalactosyl (~50–55%) and digalactosyl (~25–30%) chains. The glycans were characterized with FACE and HPAEC-PAD. Scheme 1 shows a general biantennary structure for these glycans.

In the second part of the chapter we extended the quantitative studies to glycans released from mAbs. Similar to the polyclonal studies we compared the quantitative capability of MALDI-MS with HPAEC-PAD and FACE. Additional qualitative studies were done with HPLC/ESI-MS and MALDI-MS to characterize the extent of glycosylation in the mAbs.

4.2 EXPERIMENTAL

4.2.1 Preparation of IgG samples

Bovine and human polyclonal IgG were obtained from Sigma (St. Louis, MO). The murine B-lymphocyte hybridoma cell line, CC9C10, was obtained from the American Type Culture Collection (ATCC HB-123). These cells, derived from Sp2/0 myeloma, secrete a IgG_{1k} mAb against insulins and proinsulins [16]. They were grown as chemostat cultures in DO concentrations of 10, 50, and 100%, as previously described [10]. Monoclonal antibody was purified from these cells also as described [10]. *N*-linked oligosaccharide standards as models of IgG glycans (e.g., core-fucosyl asialyl digalactosyl biantennary) were obtained from Oxford GlycoSciences (Oxford, UK).

4.2.2 *N*-deglycosylation

Samples of mAb and polyclonal IgG (1 mg) were subjected to PNGase F digestion using recombinant PNGase F (Glyko, Novato, CA) and accompanying protocol as described [5]. No detergent was used for this deglycosylation process.

4.2.3 Derivatization

The oligosaccharide pools obtained from monoclonal and polyclonal IgG samples were separated into three portions, one of which remained underivatized for HPAEC-PAD analysis; another was labeled using the charged fluorophore ANTS and earlier described in the literature [18]. The third aliquot was derivatized with PMP for MS [14].

4.2.4 FACE

These analyses were performed according to previously published methods [5, 10]. Polaroid photographs of the FACE gels were scanned and quantitated using the public-domain software NIH Image, Version 1.62 (U.S. National Institutes of Health, Bethesda, MD) as described [19].

4.2.5 HPLC/ESI-MS

Analytical scale NP and RP separations were effected online with ESI-MS. For RP experiments, a 250 X 4.6-mm Vydac 218TP54 Protein & Peptide column was used (The Separations Group, Hesperia, CA), and for NP we used a 250 X 4.60-mm Ultremex 5 NH₂ (Phenomenex, Torrance, CA). The flow rate was kept constant at 1.00 mL/min, and about 50 μ L/min was fed into the mass spectrometer via a T-junction. Solvent programs were as follows: for RP, a composition of 5% ACN in water was kept constant for 10 min, brought up to 100% ACN over 30 min, and kept at 100% for an additional 10 min. For NP, eluents A and B were water:ACN mixtures with compositions varying from 0:10 to 5:5 and 2:8 to 7:3 (v/v), respectively. The percentage of A was kept at 100% for 10 min, and the percentage of B was linearly increased to 100% over 30 min and kept at 100% for 10 min.

4.2.6 ESI-MS

The mass spectrometer used was a Quattro-LC (Micromass, UK) equipped with a Z-Spray™ source and a triple quadrupole analyzer. This instrument was used in the positive ion mode, with a cone voltage of 20 V in order to minimize in-source fragmentation. Desolvation and source block temperatures were set at 250 and 130°C, respectively. The scanning rate was 300 u/sec, and the scanning range, m/z 300 to 1500.

4.2.7 MALDI-TOF-MS and MALDI-QqTOF-MS

For comparison of relative ion abundances obtained for the PMP-labeled oligosaccharides, polyclonal human IgG glycans were investigated using five different instruments: a M@LDI-R and a M@LDI-L (Micromass, UK), a Voyager DE-PRO (Applied Biosystems, Foster City, CA), a BiFlex III (Bruker Daltonics, Billerica, MA), and a prototype MALDI-QqTOF built in-house in the Department of Physics and Astronomy, University of Manitoba [15]. In all cases, the matrix used was 2,5-dihydroxybenzoic acid (DHB), and sample deposition was performed using the dried-drop method. Accelerating voltages used were typical of each instrument used and were of the order of 10 kV.

4.2.8 MALDI-QqTOF-MS/MS

MS/MS spectra were acquired at 16 Hz repetition rate. Spectrum acquisition time was 20 s or more, depending on the abundance of precursor ions. The precursor ion window was set to 3 Da. Argon was used as cooling gas in q0 (preanalyzer quadrupole) and as collision gas in q2 (collision cell). The collision energy for each precursor was determined by applying a well-defined accelerating voltage at the entrance of the collision cell, and values were around 100 eV.

4.3 RESULTS

4.3.1 Suitability of MALDI-MS as a semi-quantitative technique

The *N*-linked glycans removed by PNGase F digestion from the human and bovine polyclonal IgGs, and each of the mAb preparations from the first set of cultures, were derivatized with PMP and analyzed by MALDI-QqTOF-MS. However, prior to this the standard glycan sets for MALDI-QqTOF-MS were examined.

Equimolar proportions were calculated volumetrically, and solutions were prepared based on the quantities specified by the manufacturer. DHB was used as the matrix for these studies. Figure 4.1 shows MALDI signals observed for an equimolar mixture of asialyl and sialylated standards, on the prototype MALDI-QqTOF-MS instrument. The circled numbers near each peak represents the peak height sum, in arbitrary units, of $[M+H]^+$, $[M+Na]^+$, and $[M-H+2Na]^+$ ion peaks. From sample to sample, ion abundances were reproducible within 10% of the values indicated on the spectrum shown. Asialyl standards produced mainly $[M+H]^+$ ions when analyzed without sialyl compounds (Figure 4.3), and $[M+Na]^+$ ions when mixed with the sialylated standards, which are supplied as sodium salts.

4.3.2 Comparative MALDI study using different instrument

In order to assess the possibility of preserving the quantitative aspect from one type of mass spectrometer to another, MALDI-TOF spectra of PMP-labelled polyclonal human and bovine IgG glycans were acquired on five different instruments. Samples were prepared in similar conditions using DHB as the matrix. It has been shown that shot to shot variation in signal strength varies widely. However, by averaging spectra from a sufficiently large number of shots taken from different areas of the target, uniform

average signal can be obtained. Figure 4.4 shows spectra obtained with the prototype MALDI-QqTOF instrument, and Table 4.1 lists the measured peak heights for the three predominant human IgG sugar compositions detected, versus abundances obtained from HPAEC-PAD measurements of Kunkel *et al.* [11,20], and those obtained by Raju *et al.* [10] using MALDI-TOF-MS and CE-LIF.

4.3.3 Qualitative characterization

MALDI-TOFMS and HPLC/ESI-MS were used for qualitative study of *N*-linked glycans released from human and bovine polyclonal IgG. RP- and NP-HPLC/ESI-MS were both performed to characterize the glycans. Table 4.2 lists all carbohydrate compositions identified in polyclonal human and bovine IgG. Figure 4.6 shows the SICs obtained for glycans of polyclonal human IgG by HPLC/ESI-MS, detected as various forms of parent ions. It is possible that a certain extent of in-source dissociation occurred resulting in lower mass ions smaller than the precursor. This was observed for standards run under similar conditions (Figure 4.7) and could possibly be due to using a high desolvation temperature (250 °C). Lower temperatures resulted in loss of signal. RP-HPLC/ESI-MS has able to detect the presence of disialylated oligosaccharides. Both modes were able to detect ions with *m/z* values indicating the presence of a high-mannose structure (M_4N_2). This composition was detected as a minor component.

Human and bovine IgG oligosacchaides were characterized by MALDI-QqTOF-MS. These experiments produced $[M+Na]^+$ ions. The molecular weights of the glycans were measured within 5 ppm of their calculated monoisotopic values. Most ions were of sufficient abundance to pursue CID-MS/MS and/or PSD experiments. MALDI-

CID-MS/MS data were acquired for all general sugar compositions shown in italics in Table 4.2, and supported the proposed structures.

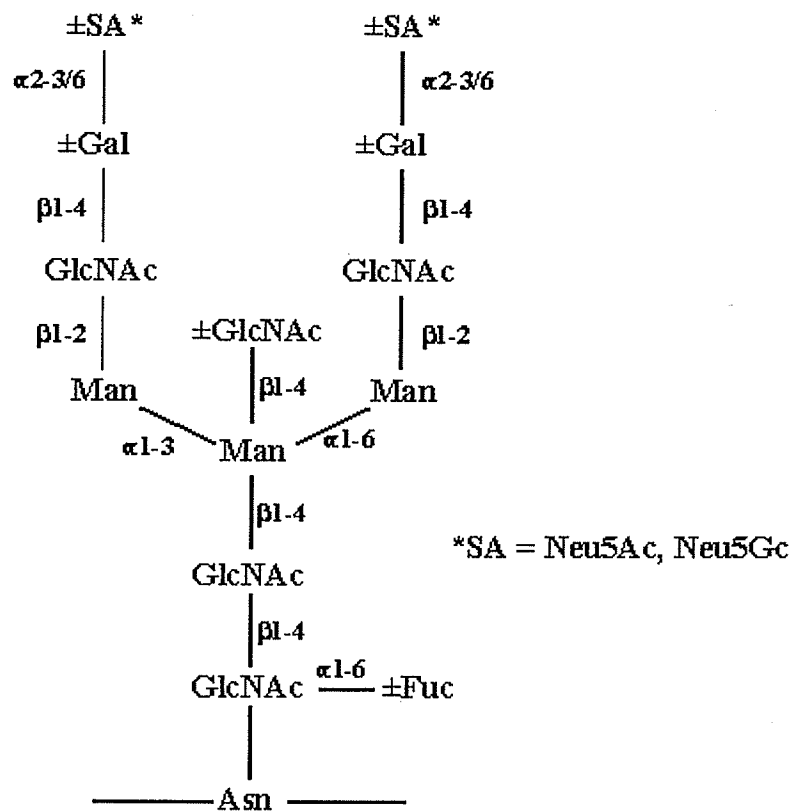
4.3.4 Monoclonal murine IgG₁ glycans

MALDI-QqTOF-MS spectra were acquired on glycans obtained using DO concentrations of 10, 50 and 100%. HPLC/ESI-MS was also used for qualitative characterization. Table 4.3 summarizes these results qualitatively. Under MALDI conditions, PMP-derivatized oligosaccharides were consistently ionized as $[M+Na]^+$ ions except M_3N_4 (always detected as $[M+H]^+$). MALDI-QqTOF-MS measurements were consistently within 5 ppm of the predicted monoisotopic m/z values. There were two peaks detected that could only be interpreted as hybrid structures (see bottom of Table 4.3). These ions will be discussed further in Chapter 5. Not included in Table 4.3 are ions observed at m/z 1709 in every spectrum (see Figures 4.4, and 4.10c, for example), and MS/MS analysis (not shown) indicated that they originated from non-carbohydrate impurities. HPLC/ESI-MS were able to detect minor amounts of high-mannose (M_4N_2) glycans.

Figure 4.10 compares the results obtained by MALDI-QqTOF-MS for the murine species at DO concentration of 10, 50 and 100% with those obtained by Kunkel *et al.* [11] by HPAEC-PAD and FACE. Quantitative figures are given in Table 4.4 for the three most abundant glycan compositions, which are the same as those compared in Table 4.1. MALDI peak heights were calculated by adding values for both $[M+Na]^+$ and $[M+H]^+$ peaks of each sugar ($[M+Na]^+$ were the predominant ions). While HPAEC-PAD and FACE results correlate quite well, MALDI data showed semi-quantitativeness due to possible in-source fragmentation.

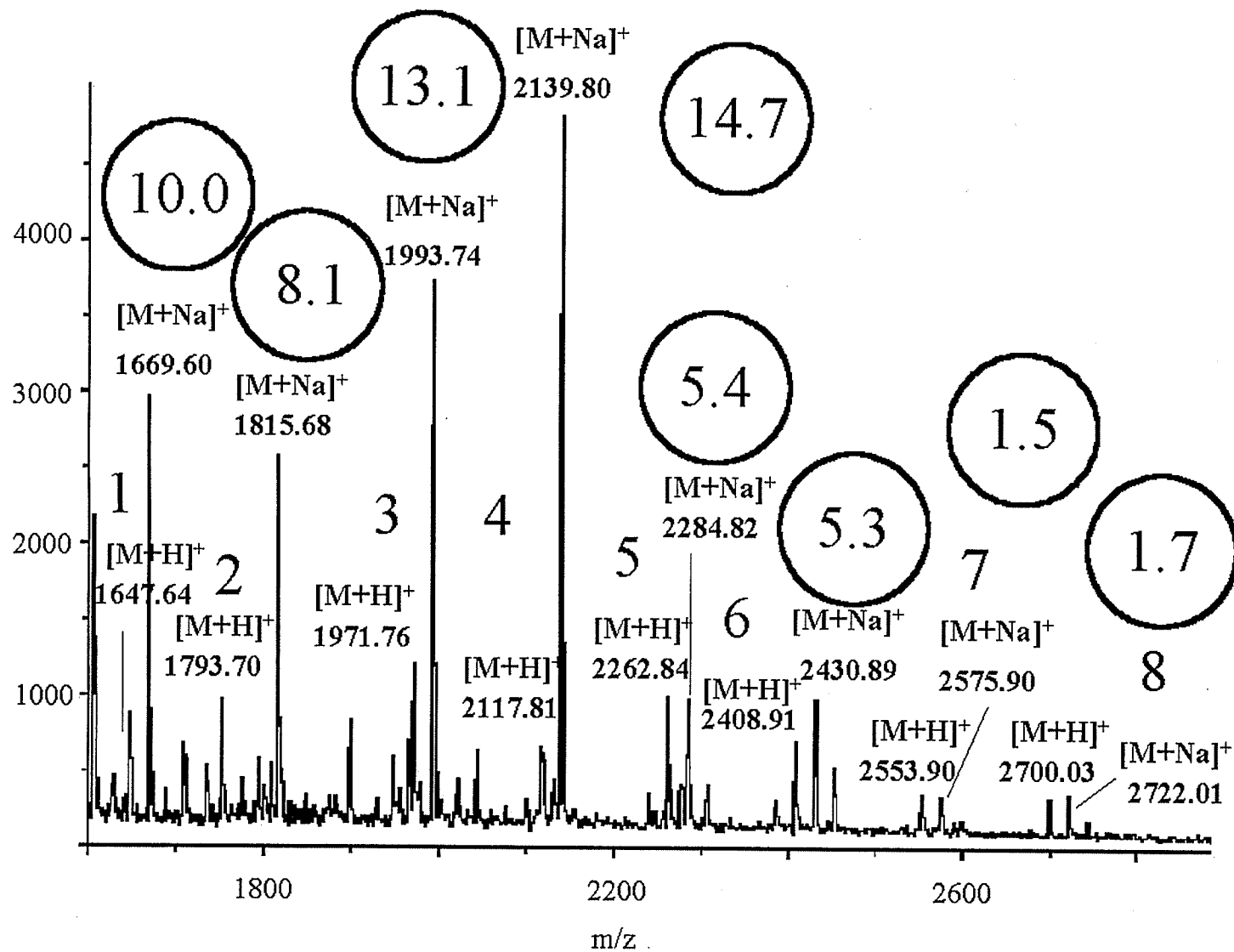
4.3.5 MALDI-MS/MS on prominent glycan compositions in IgG₁

The MS/MS spectra in Figures 4.7, 4.8, and 4.9 show the fragmentation patterns of $[M+Na]^+$ ions of the most abundant carbohydrate species in the murine mAb pool, identified as M₃N₄F, GM₃N₄F, and G₂M₃N₄F, respectively, in HPAEC-PAD and FACE analyses. MS/MS measurements were performed on as many MALDI-QqTOF-MS peaks as possible (see *italic characters* in Table 4.2), on ions with sufficient abundance.



Scheme 4.1 General biantennary structure for IgG glycans.

Figure 4.1 MALDI-QqTOF mass spectrum of an equimolar mixture of PMP-derivatized asialyl and sialylated *N*-linked oligosaccharides. Structures are indicated in Figure 4.2.



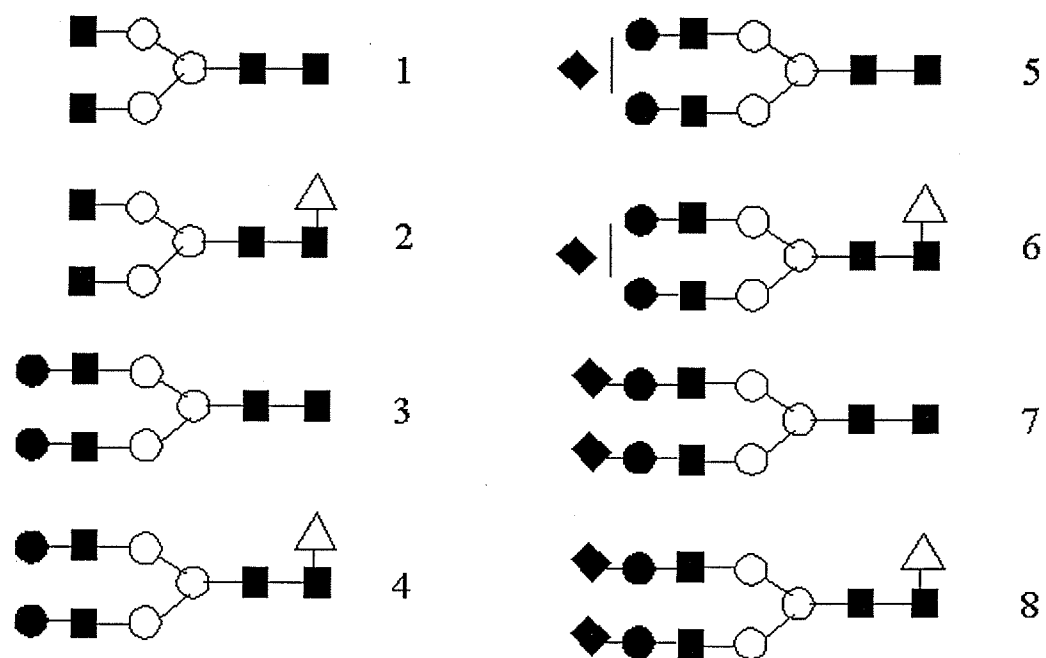
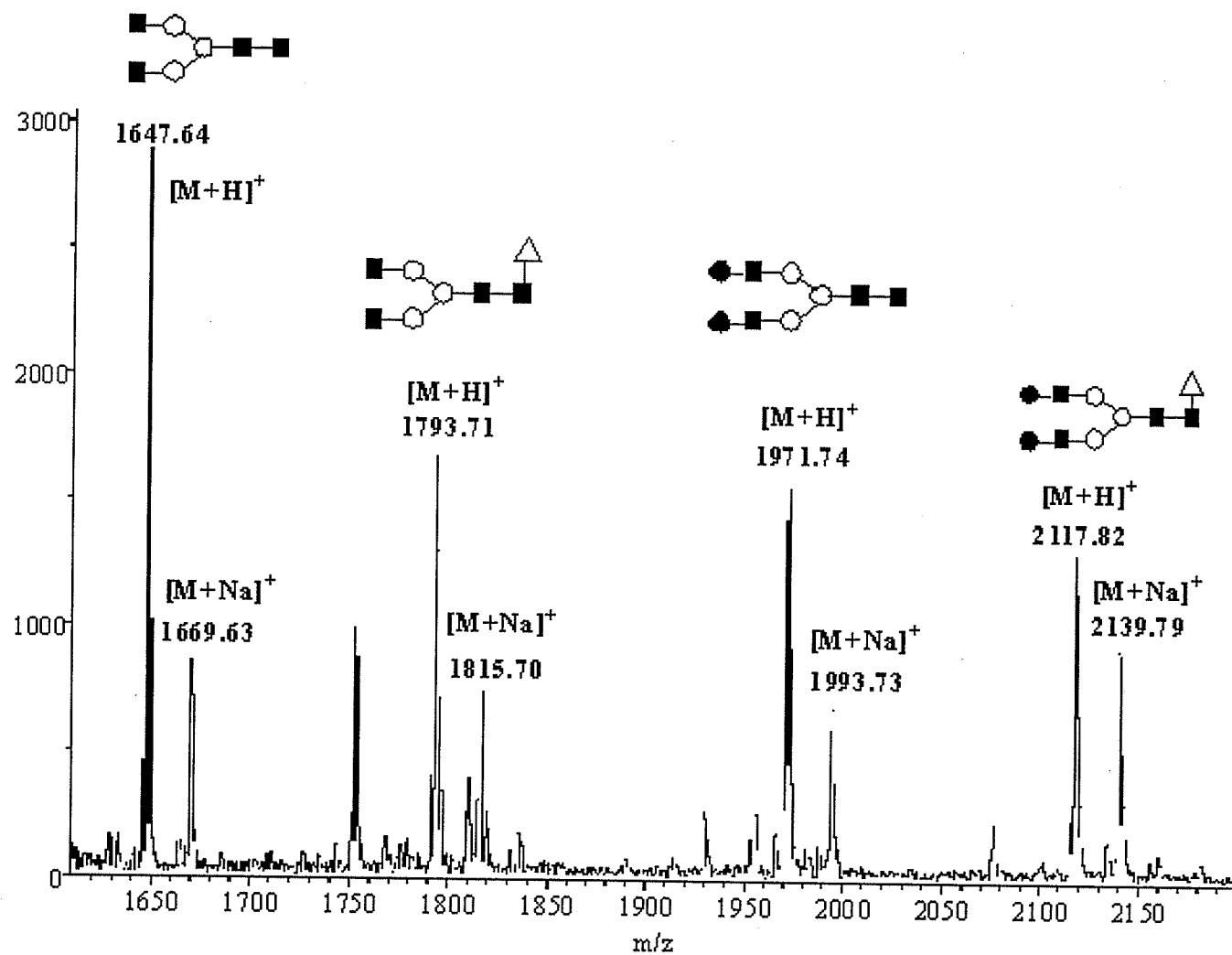


Figure 4.2 Asialyl and sialylated *N*-linked oligosaccharides standards.

Figure 4.3 MALDI-QqTOF mass spectrum of an equimolar mixture of PMP-derivatized asialyl *N*-linked oligosaccharides. Structures are indicated on the spectrum.



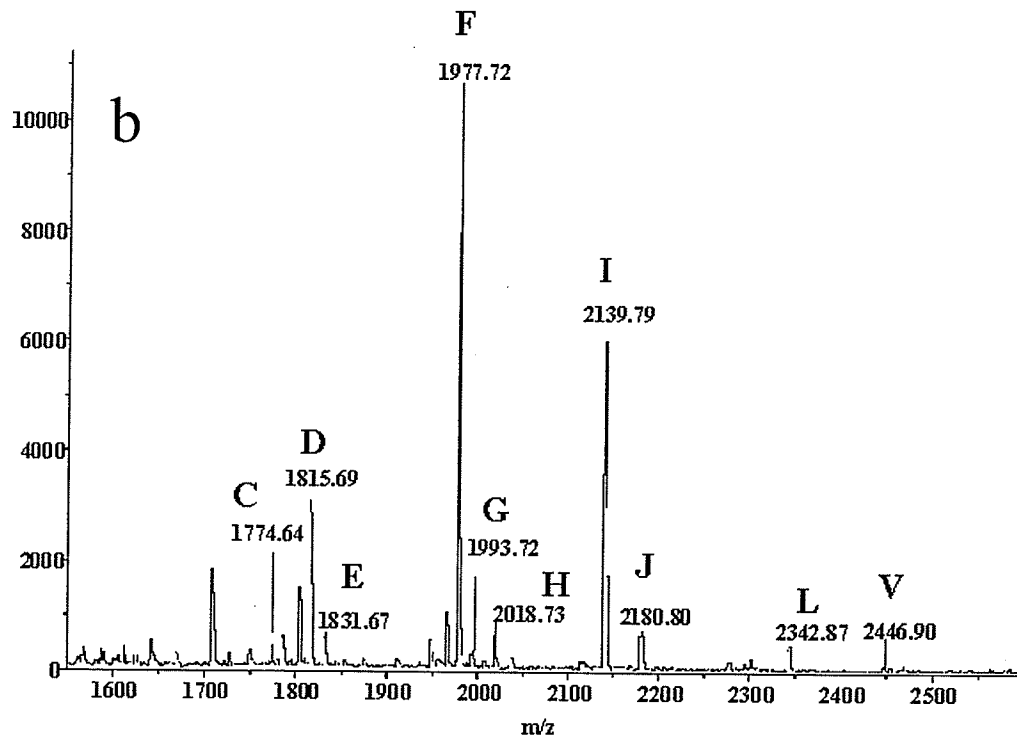
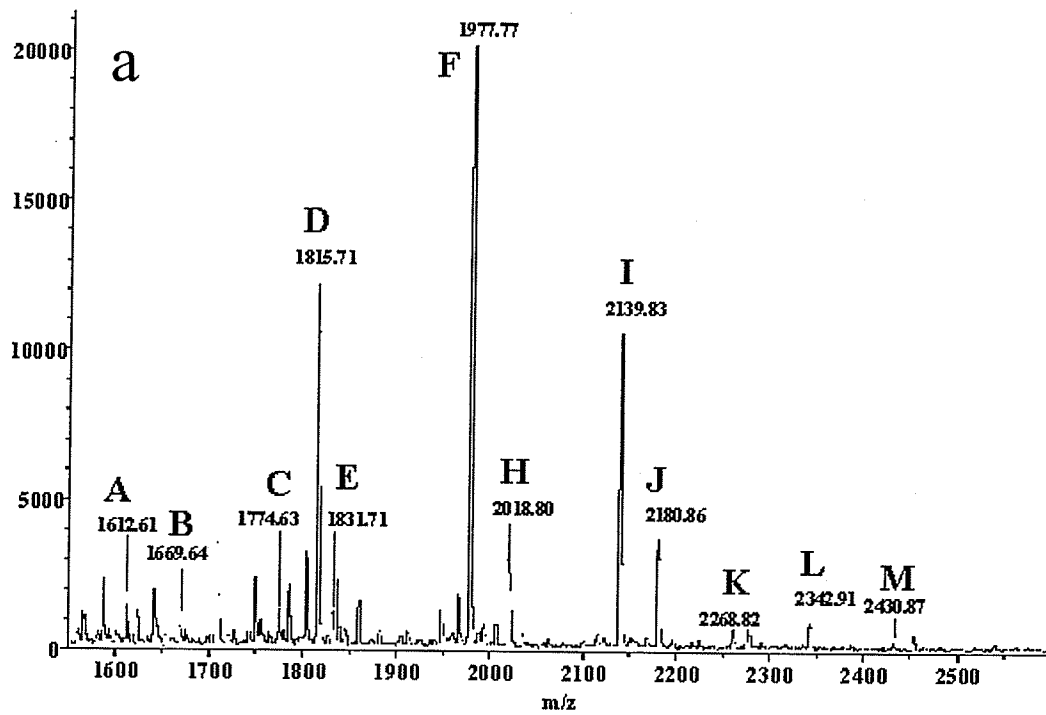


Figure 4.4 MALDI-QqTOF mass spectra obtained for PMP-derivatized polyclonal IgG glycans: (a) human and (b) bovine. Suggested structures are shown in Figure 4.5

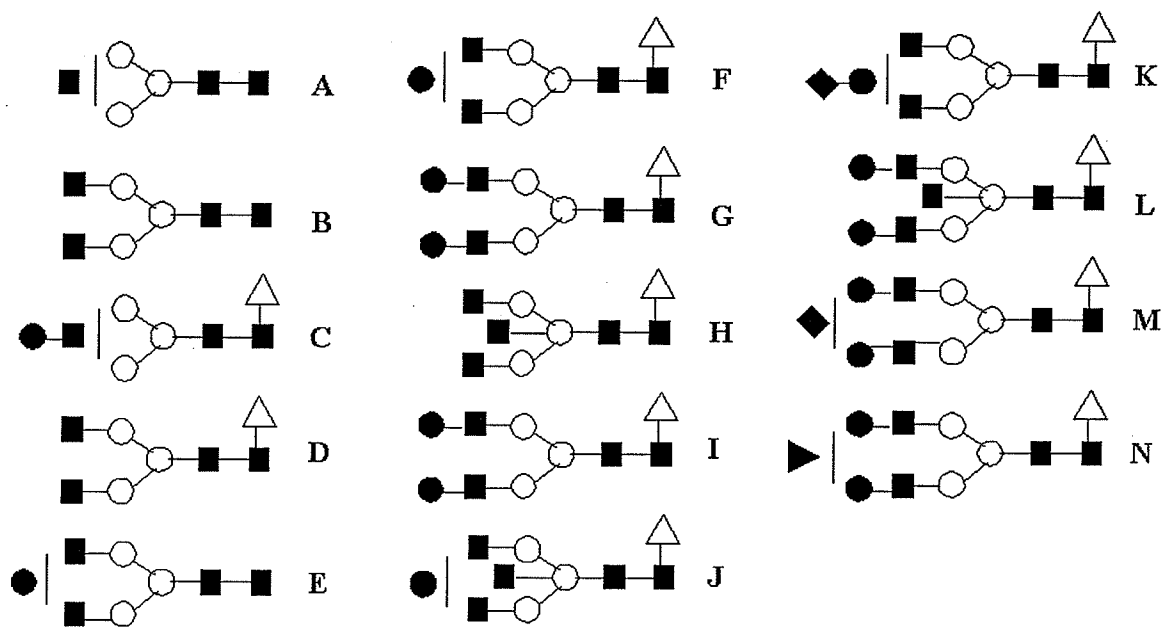


Figure 4.5 Suggested structures for bovine and human polyclonal IgG.

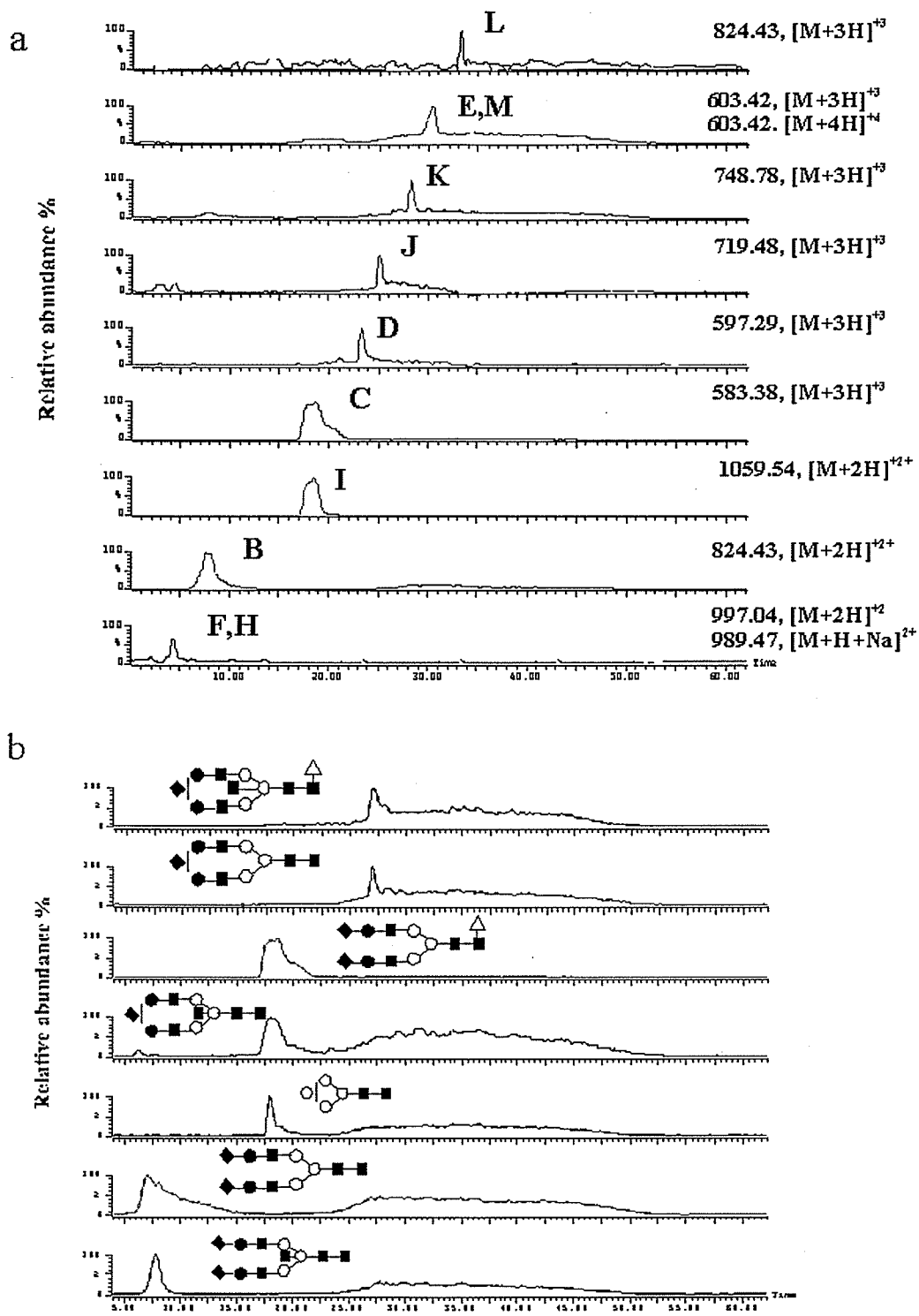


Figure 4.6 Reversed-phase HPLC/ESI-MS selected ion chromatograms of PMP-derivatized glycans from polyclonal human IgG: (a) observed by MALDI-MS and (b) not observed by MALDI-MS. Capital letters assigned to chromatograms correspond to structures suggested in Figure 4.5.

Figure 4.7 MALDI-QqTOF-MS/MS spectrum of PMP-derivatized core-fucosyl asialyl digalactosyl biantennary glycan from murine monoclonal IgG glycan pool at *m/z* 1815, obtained with 50% DO.

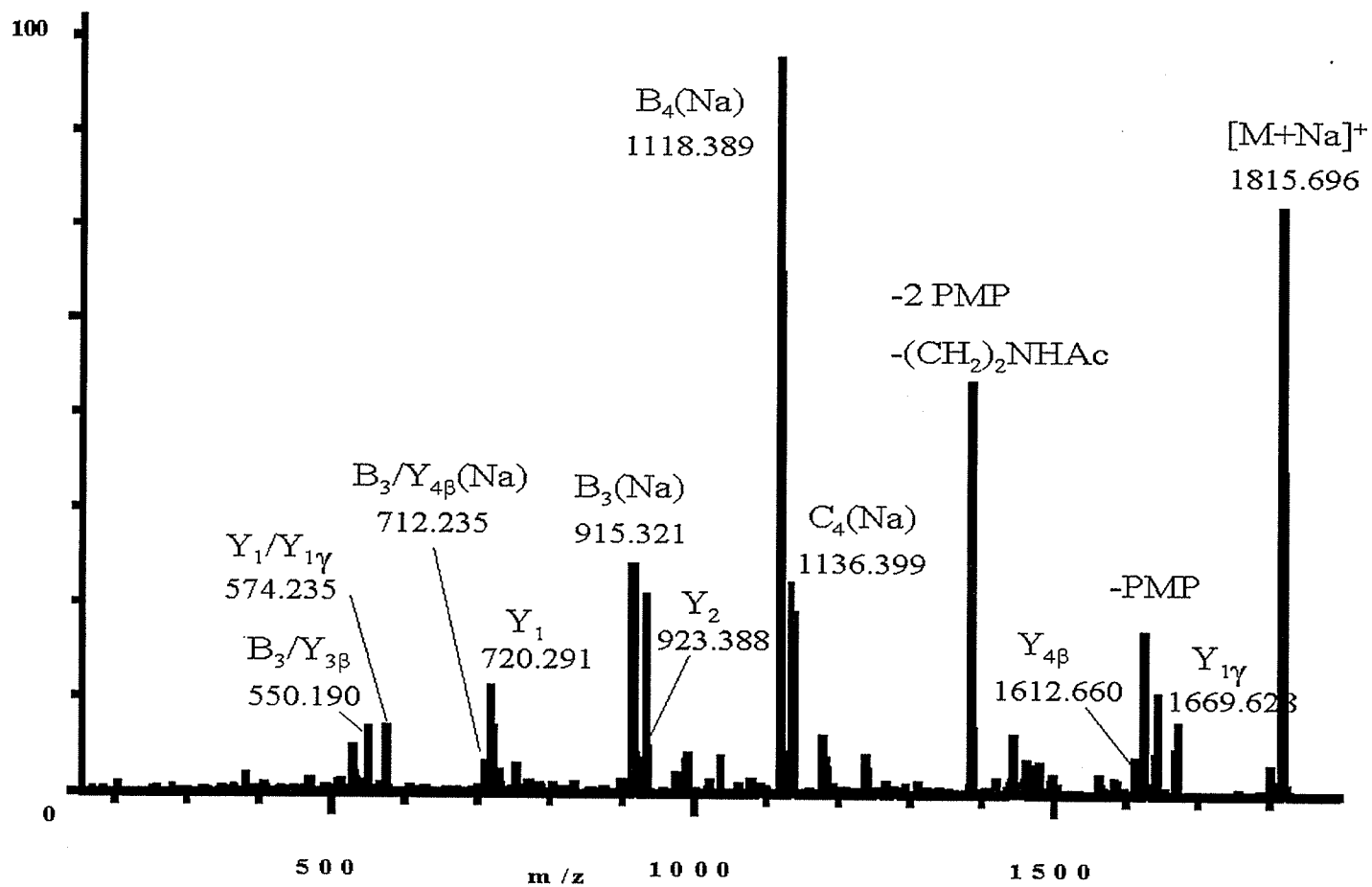


Figure 4.8 MALDI-QqTOF-MS/MS spectrum of PMP-derivatized core-fucosyl asialyl agalactosyl biantennary glycan from murine monoclonal IgG glycan pool, obtained with 50% DO.

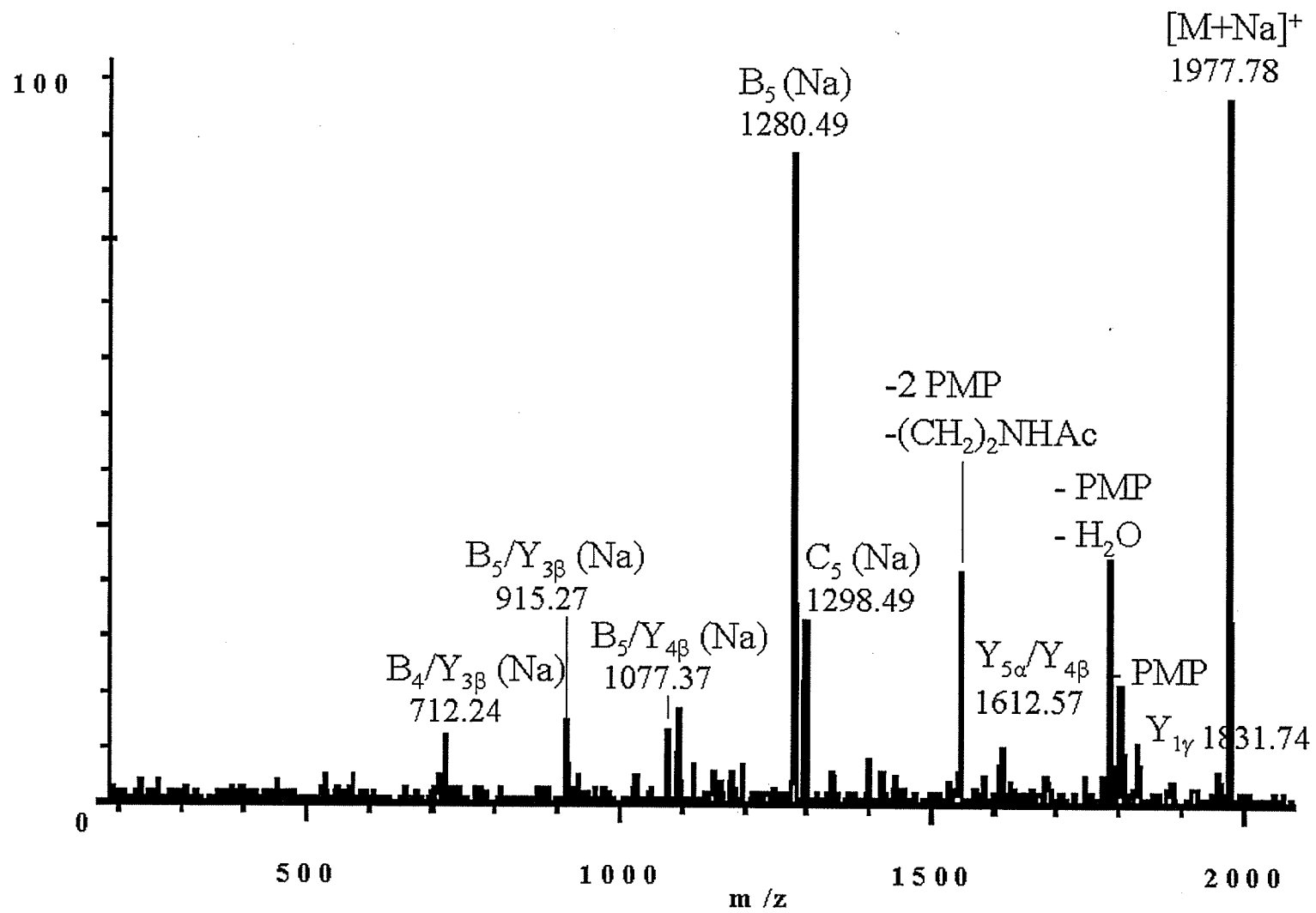
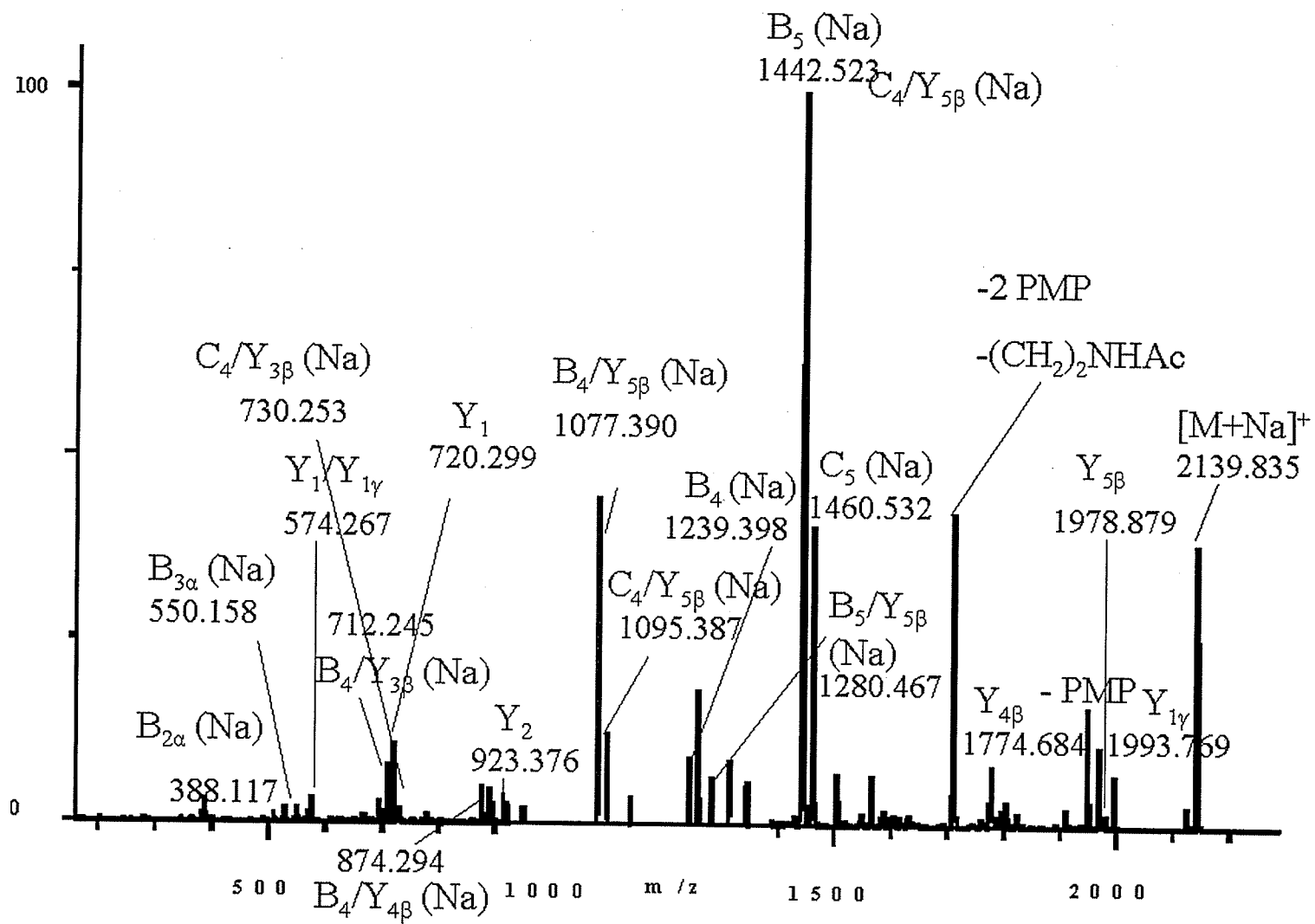


Figure 4.9 MALDI-QqTOF-MS/MS spectrum of PMP-derivatized core-fucosyl asialyl digalactosyl biantennary glycan from murine monoclonal IgG glycan pool, obtained with 50% DO.



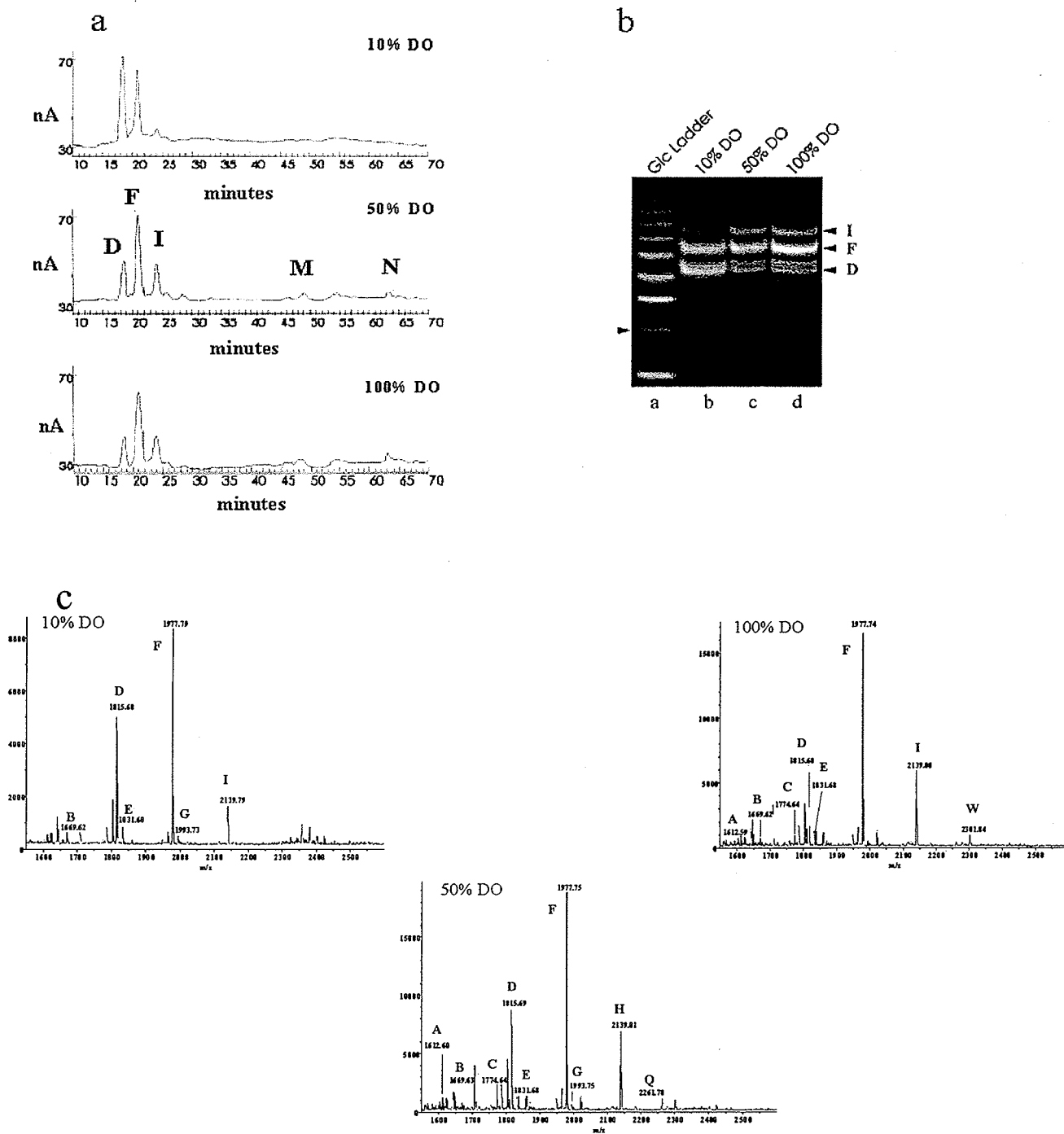


Figure 4.10 Comparison between (a) HPAEC-PAD, (b) FACE, and (c) MALDI-QqTOF-MS for the analysis of murine monoclonal IgG₁ glycans. The glycans were derivatized with PMP for MALDI. See Table 4.3 for quantitation. (a and b) Taken from Ref. 10. Capital letters assigned to peaks or bands correspond to structures suggested in Figure 4.4. See Table 2 for assignment of compositions to mass spectral peaks.

Table 4.1 Comparison of MALDI signal intensities measured on five instruments, versus results from HPAEC-PAD analyses [11].

Relative peak heights or *areas, normalized to the most abundant species (+8)

Instrument	MALDI QqTOF	M@LDI L	M@LDI R	BiFlex III	DePro	HPAEC PAD* [11] (+2)	HPAEC PAD* [20]	MALDI TOFMS [10]	CE-LIF* [10]
Glycan Composition									
M ₃ N ₄ F	60	66	47	61	95	49	53	59	71
GM ₃ N ₄ F	100	100	100	100	100	100	100	100	100
G ₂ M ₃ N ₄ F	53	58	58	49	36	89	81	57	43

Note. Data obtained on oligosaccharides released from polyclonal human IgG. Comparison with results found in the literature [10, 20]. M, mannose; N, *N*-acetylglucosamine; G, galactose; F, fucose.

Table 4.2 Suggested compositions of oligosaccharides released from human and bovine polyclonal IgG, as detected by MALDI-MS and HPLC/ESI-MS.

IgG Type/method: Glycan Composition	Human RP and NP HPLC/ESI-MS	Human MALDI-MS	Bovine RP and NP HPLC/ESI-MS	Bovine MALDI-MS
M ₃ N ₃ (A)	X	X		
M ₃ N ₄ (B)	X	X		
<i>M₃N₄F</i> (D)	X	X	X	X
<i>M₃N₅F</i> (H)	X	X	X	X
GM ₃ N ₃ F (C)	X	X	X	X
GM ₃ N ₄ (E)	X	X	X	X
GM₃N₄F (F)	X	X	X	X
GM ₃ N ₄ FSA (K)	X	X		
GM ₃ N ₅ F (J)	X	X	X	X
G ₂ M ₃ N ₄ (G)		X		X
G₂M₃N₄F (I)	X	X	X	X
G ₂ M ₃ N ₄ SA	X		X	
G ₂ M ₃ N ₄ FGA (N)			X	X
G ₂ M ₃ N ₄ FSA (M)	X	X	X	
G ₂ M ₃ N ₄ SA ₂	X			
G ₂ M ₃ N ₄ FSA ₂	X	X	X	
<i>G₂M₃N₅F</i> (L)	X	X	X	X
G ₂ M ₃ N ₅ GA			X	X
G ₂ M ₃ N ₅ FGA			X	X
G ₂ M ₃ N ₅ SA	X		X	
G ₂ M ₃ N ₅ FSA	X		X	
G ₂ M ₃ N ₅ SA ₂	X		X	
M ₄ N ₂ (hm)	X		X	

Note. Capital letters in parentheses refer to structures shown in Figure 4.5. M, mannose; N, *N*-acetylglucosamine; G, galactose; F, fucose; SA, *N*-acetylneuraminic acid; GA, *N*-glycolylneuraminic acid. Bold characters, three most abundant glycans detected. Italic characters, compositions for which MS/MS data were acquired.

Table 4.3 Suggested compositions of oligosaccharides released from murine monoclonal IgG₁, as detected by MALDI-MS and HPLC/ESI-MS.

IgG Type/method: Glycan Composition	HPLC/ESI-MS (all of 10, 50, 100% DO)	10% DO MALDI-MS	50% DO MALDI-MS	100% DO MALDI-MS
M ₃ N ₃		X	X	X
GM ₃ N ₃	X			
M ₃ N ₄		X	X	X
<i>M₃N₄F</i>	X	X	X	X
GM ₃ N ₄	X			
GM₃N₄F	X	X	X	X
<i>M₃N₅F</i>		X	X	X
GM ₃ N ₅	X			
G ₂ M ₃ N ₄		X	X	X
G₂M₃N₄F	X	X	X	X
GM ₃ N ₅ F	X			
GM ₃ N ₅ FSA		X	X	X
G ₂ M ₃ N ₄ FSA	X			
G ₂ M ₃ N ₅ FSA				
G ₂ M ₃ N ₅ FSA ₂	X			
M ₆ N ₄ F (hyb)			X	X
M ₇ N ₄ F (hyb)			X	X
M ₄ N ₂ (hyb)	X			

Note. M, mannose; N, *N*-acetylglucosamine; G, galactose; F, fucose; SA, *N*-acetylneuraminic acid. Bold characters, most abundant glycans detected. Italic characters, glycan compositions for which MS/MS data were obtained.

Table 4.4 Comparison of relative abundances of oligosaccharides released from monoclonal murine IgG1 as measured by MALDI-QqTOF-MS, FACE, and HPAEC-PAD, for varying DO concentrations during cell growth

Relative peak heights or areas, or band densities, normalized to the most abundant species

Method used Glycan Composition	10% DO			50% DO			100% DO		
	MALDI QqTOF (±8)	FACE (21) (±2)	HPAEC PAD (8) (±2)	MALDI QqTOF (±8)	FACE (21) (±2)	HPAEC PAD (8) (±2)	MALDI QqTOF (±8)	FACE (21) (±2)	HPAEC PAD (8) (±2)
M ₃ N ₄ F	64	97	98	54	45	39	44	42	33
GM ₃ N ₄ F	100	100	100	100	100	100	100	100	100
G ₂ M ₃ N ₄ F	17	18	19	34	47	46	33	52	57

Note. M, mannose; N, *N*-acetylglucosamine; G, galactose; F, fucose.

4.4 DISCUSSION

4.4.1 Suitability of MALDI-MS as a semi-quantitative technique

All of the standard sugars contain four GlcNAc residues and the same number of mannose residues. Since GlcNAc has the highest pK_a , it favours the production of positive ions. Ionization efficiency is affected by the addition of fucose and galactose but as seen for the four sugars at lower m/z values, not in a consistent manner. Presence of sialic acids greatly reduced the signal intensity in the positive mode. Addition of one sialic acid reduced the signal intensity by a factor of at least 2, and a second sialic acid lowered the signal to 1/5 or less of those observed for asialyl sugars.

4.4.2 Comparative MALDI study using different instruments

The HPAEC-PAD studies by Kunkel *et al.* shows a higher proportion of $G_2M_3N_4F$ (compared to GM_3N_4F and M_3N_4F) and a lower proportion of M_3N_4F (compared to $G_2M_3N_4F$ and GM_3N_4F) (M, mannose; G, galactose; F, fucose; N, *N*-acetylglucosamine) compared to all the MALDI instruments (with the exception of M@LDI-L, which measured a low abundance of M_3N_4F , as would be expected, since fragmentation in the linear mode subsequent to acceleration does not affect flight time).

The ionization process in MALDI has been shown to cause in-source fragmentation as well as dissociation during the flight time in the mass analyzer drift tube [21]. The glycans $G_2M_3N_4F$ and GM_3N_4F are the mono and digalactosylated versions of the glycan M_3N_4F . Because of possible in source fragmentation, $G_2M_3N_4F$ and GM_3N_4F may have undergone degalactosylation in the ion source upon laser irradiation, to produce their subspecies, M_3N_4F and GM_3N_4F , respectively. It is also possible that $G_2M_3N_4F$ and GM_3N_4F may have lost galactosyl residues along the flight path before

reaching the ion reflector. This would explain the presence of a smaller proportion of these compounds than in reality in the mixture. This is mainly noticeable in the data obtained with the DE-Pro instrument, which shows the lowest proportion of $G_2M_3N_4F$ and the highest of M_3N_4F . The DE-Pro is equipped with delayed extraction. In traditional MALDI instruments the ions are accelerated out of the ionization source as soon as they are formed; however, instruments fitted with time-lag focusing (delayed extraction (DE)), the ions are allowed to “cool” for ~150 ns before being accelerated to the analyzer. This cooling period generates a set of ions with a much lower kinetic energy distribution, ultimately reducing the temporal spread of ions once they enter the TOF analyzer. Overall, this results in increased resolution and accuracy, which would help explain the high proportion of M_3N_4F and support our theory of in-source collision. With other instruments, these losses seem to occur to different extents. Loss of galactose residues would occur as in formation of Y-type ions, i.e., would be characterized by a loss of 162 u [22].

Townsend *et al.* [23] have shown that relative peak areas will reflect relative quantities for glycans of similar size and compositions in HPAEC-PAD. Furthermore, Kunkel *et al.* [11,20] have achieved remarkable agreement in quantitation for two studies of human IgG derived from different batches of pooled sera from different years. Based on these results, it has been previously concluded that the *N*-linked glycan profile of IgG does not vary much in the general human population, making polyclonal human serum IgG an excellent standard glycoprotein for quantitative studies [10]. This reinforces HPAEC-PAD as a precise analytical method. The polyclonal human IgG analyzed by Raju *et al.* [20] was obtained from the same supplier and should reasonably

be expected to conform to the above conclusions. Therefore, it is difficult to consider MALDI as a quantitative technique for mixture analysis considering that FACE [19] and HPAEC-PAD have shown different proportions.

For the purposes of this study, MALDI will therefore be considered as a semi-quantitative technique, with enhanced capability for qualitative identification of the compounds.

4.4.3 Qualitative characterization

RP- and NP-HPLC/ESI-MS were both performed to characterize the glycans. The three structures highlighted in bold characters (Table 4.2) are the most abundant ones, as detected by Kunkel *et al.* [11]. RP-HPLC/ESI-MS has able to detect the presence of disialylated oligosaccharides, which were not detected by HPAEC-PAD [11]. Both modes were able to detect ions with m/z values indicating the presence of a high-mannose structure (M_4N_2). This composition was detected as a minor component. Such species had not been detected by Raju *et al.* [10], for either human or bovine IgG glycans. These authors observed high-mannose glycans only in polyclonal sheep and chicken IgG among all 13 animal species studied [10]. Because no ESI-MS/MS experiments were performed, it could not be ascertained whether the high-mannose and the disialylated glycan were correctly characterized. For the purposes of this particular study, MALDI-MS was in general considered more reliable than HPLC-MS for preliminary identification of major glycan compositions, although HPLC/MS was able to detect other minor components.

4.4.4 Monoclonal murine IgG₁ glycans

There were two peaks detected that could only be interpreted as hybrid structures, both species were not detected by Kunkel *et al.* [11] using FACE or HPAEC-PAD. Since the focus of the study by Kunkel *et al.* was to examine the degree of galactosylation, the presence of the hybrid structures might have been overlooked by the limitation of the objective of the experiment. Chapter 5 has a detailed explanation for the observation of the two observed hybrid structures.

4.4.5 MALDI-MS/MS on prominent glycan compositions in IgG₁

The MALDI-QqTOF-MS/MS spectrum, obtained by CID with argon, shows only ions which do not contain the reducing end, including two major peaks corresponding to losses of PMP and adjacent moieties

4.5 GLOBAL

Our results show that different cell culture conditions can affect the glycosylation of an IgG mAb, as has been shown for other mAbs and recombinant proteins [24]. This has important implications for the development and production of glycoproteins for diagnostic and therapeutic use [25]. The murine hybridoma, CC9C10, used in this study has been grown routinely with a relatively high mAb productivity in a serum-free formulation developed previously [26]. Work with steady-state continuous cultures of this hybridoma showed that cell viability, cell growth rate, and specific rate of mAb production do not change at DO concentrations of 10, 50, and 100% [27]. The vast majority of *N*-linked glycosylation occurred on the heavy chain, mostly on the Fc portion at the conserved Asn-297 site in the C_H2 domain. The only indication of *N*-linked glycosylation of the light chain is the observation of disialyl glycans by MS in this report,

which are unlikely to be found in the C_{H2} domain in appreciable quantity [11]. The absence of galactosyl residues in the Fc glycans is known to abolish specific associations between the C_{H2} domains. Galactosyl-linked glycans act as tether, and their absence leads to increased oligosaccharide mobility and to conformational changes in the C_{H2}/hinge region—and therefore to the observed biological and clinical effects attributed to agalactosyl IgG [28]. A marked decrease in galactosylation was observed at 10% DO versus 50 and 100% DO, and thus DO is not only an important factor for energy metabolism of the CC9C10 cell line [27], but it is also critical in determining the final structures of the *N*-linked oligosaccharide chains of the mAb produced by these cells. The mechanism which causes the extent of galactosylation of the mAb as a result of low DO is unclear. Speculative mechanisms have been discussed in more detail [11,19].

4.6 CONCLUSIONS

Mass spectrometry has been tested for its potential quantitative and qualitative capability for glycan structural analysis of polyclonal and monoclonal IgG glycans. The results here show that MALDI-MS can be used semi-quantitatively, partly because it involves competition between species for ionization, which was obvious from the positive-mode spectrum of an equimolar mixture of sialyl and asialyl glycans, where signal intensities decreased with the number of sialic acid residues. HPLC/ESI-MS was used on a qualitative basis in this study. The results obtained by MALDI-MS and HPLC/ESI-MS were in good agreement with the results obtained with HPAEC-PAD and FACE [11]. Both MALDI-MS and HPLC/ESI-MS allowed for detection of three major species (M₃N₄F, GM₃N₄F, and G₂M₃N₄F) which had previously been characterized by FACE and HPAEC-PAD [11], as well as minor amounts of sialylated glycans. MALDI-

QqTOF-MS/MS experiments were performed to confirm proposed glycan structures. The fragmentation patterns obtained from $[M+H]^+$ and $[M+Na]^+$ ions were different and complementary in the information they provided. Most IgG sugars produced $[M+Na]^+$ ions, which in turn fragmented into charged B-type ions (containing the nonreducing end). In summary, the MS results agreed with previous measurements using other techniques and showed that most monoclonal and polyclonal glycans were core-fucosyl, asialyl biantennary chains with varying galactosylation and that there were also minor amounts of afucosyl, bisected, and monosialyl oligosaccharides. MALDI-MS studies confirmed that higher DO concentration in serum-free culture of CC9C10 cells leads to higher degree of galactosylation of the mAb product.

4.7 REFERENCES

1. Burton, D.R., Calabi, F., and Neuberger, M.S. *In: Molecular Genetics of Immunoglobulin*, Eds. Elsevier, 1987,50.
2. Putnam, F.W., *Immunoglobulins: structure function and genes. In: The Plasma Proteins, Vol. V, 3rd ed.*, Putnam, F.W., Ed.; Academic Process, 1987,49.
3. Mizuochi, T., Hamako, J., and Titani, K. *Arch. Biochem. Biophys.* **257**, 387 (1987).
4. Parekh, R. B., Dwek, R. A., Sutton, B. J., Fernandes, D. L., Leung, A., Stanworth, D., Rademacher, T. W., Mizuochi, T., Taniguchi, T., Matsuta, K., Takeuchi, F., Nagano, Y., Miyamoto, T., and Kobata, A. *Nature* **316**, 452 (1985).
5. Kunkel, J. P., Jan, D. C. H., Butler, M., and Jamieson, J. C. *Biotechnol. Prog.* **16**, 462 (2000).
6. Wormald, M. R., Rudd, P. M., Harvey, D. J., Chang, S. C., Scragg, I. G., and Dwek, R.A. *Biochemistry* **36**, 1370 (1997).
7. Bond, A., Jones, M. G., and Hay, F. C. *J. Immunol. Methods* **166**, 27 (1993).
8. Wright, A., and Morrison, S. L. *Springer Semin. Immunopathol.* **15**, 259 (1993).
9. Parekh, R. B., and Rademacher, T. W. *Br. J. Rheumatol.* **27**, 162 (1988).
10. Raju, T. S., Briggs, J. B., Borge, S. M., and Jones, A. J. S. *Glycobiology* **10**, 477 (2000).
11. Kunkel, J. P., Jan, D. C. H., Jamieson, J. C., and Butler, M. *J. Biotechnol.* **62**, 55 (1998).
12. Hardy, M. R. and Townsend, R. R. *Proc. Natl. Acad. Sci. USA* **85**, 3289 (1988).
13. Harvey, D. J. *Methods Mol. Biol.* **61**, 243 (1996).
14. Honda, S., Akao, E., Suzuki, S., Okuda, M., Kakehi, K., and Nakamura, J. *Anal. Biochem.* **180**, 351 (1989).
15. Loboda, A. V., Krutchinsky, A. N., Bromirski, M. P., Ens, W., and Standing, K. G. *Rapid Commun. Mass Spectrom.* **14**, 1047 (2000).
16. Schroer, J. A., Bender, T., Feldman, R. J., and Kim, K. J. *Eur. J. Immunol.* **13**, 693 (1983).
17. Barnabe', N., and Butler, M. *J. Biotechnol.* **60**, 67 (1998).

18. Jackson, P. *Methods Enzymol.* **230**, 250 (1994).
19. Kunkel, J. P. (2001) The Effect of Dissolved Oxygen Concentration on Monoclonal Antibody Glycosylation in Serum-Free Continuous Culture, Ph.D. Thesis, University of Manitoba, Winnipeg, Manitoba, Canada.
20. Weitzhandler, M., Hardy, M., Co, M. S., and Avdalovic, N. *J. Pharm. Sci.* **83**, 1670 (1994).
21. Burlingame, A. L., Boyd, R. K., and Gaskell, S. *J. Anal. Chem.* **70**, 647R (1998).
22. Domon, B., and Costello, C. E. *Glycoconjugate J.* **5**, 397 (1988).
23. Townsend, R. R., Hardy, M. R., Hingsdaul, O., and Lee, Y. C. *Anal. Biochem.* **174**, 459 (1988).
24. Goochee, C. F., and Monica, T. *Bio/Technology* **8**, 421 (1990).
25. Goochee, C. F., Gramer, M. J., Andersen, M. J., Bahr, J. B., and Rasmussen, J. R. *Bio/Technology* **9**, 1347 (1991).
26. Barnabe', N., and Butler, M. *Biotechnol. Bioeng.* **44**, 1235 (1994).
27. Jan, D. C. H., Petch, D. A., Huzel, N., and Butler, M. *Biotechnol. Bioeng.* **54**, 153 (1997).
28. Axford, J. S., MacKenzie, L., Lydyard, P. M., Hay, F. C., Isenberg, D. A., and Roitt, I. M. *Lancet* **ii**, 1486 (1987).

5 MALDI-MS/MS AND POST SOURCE DECAY STUDIES OF IgG GLYCANS

5.1 INTRODUCTION

Mass determination through MALDI-MS can often lead to compositional data, additional information must be secured through other methodologies.

Monosaccharide sequences, branching, and, in some cases, linkages can be determined through fragmentation that a glycan may experience in either a PSD or a CID experiment. Fragmentation in MALDI-MS can result from (a) the PSD, which designates the fragments formed after ion extraction from the ion source and (b) CID, which designates the fragments formed in a collision cell filled with a gas. PSD spectra of sodiated ions from neutral carbohydrates tend to be dominated by glycosidic and internal cleavages with very weak cross-ring ions [1]. Major ions are the result of B and Y cleavages, and the information is related to sequence and branching.

While this approach is often structurally informative, a remaining challenge for carbohydrate analyses using mass spectrometry is the differentiation of isomeric *N*-glycan structures. Tandem mass spectrometry in combination with FAB has been demonstrated by others for structurally distinguishing branching and linkage isomers of small oligosaccharides [2-11]. ESI-MS/MS has been used to structurally characterize glycoprotein-released carbohydrate isomers [12].

With most non-mass spectrometry methods such as HPLC [13-15], HPAEC-PAD [16,17] and CE [18], identification of glycan isomers is possible only if the proper (isomeric) standards are available to establish their elution position [13]. And even if this is the case the peaks in question must represent single structures.

Strategies have also been devised to characterize unknown isomeric *N*-linked glycan structures that were referred to as “knowledge-based” [19]. This involves comparing specific fragment ion types and their distributions in the unknown PSD spectrum to those in the PSD spectra of standards possessing similar structural features.

In this chapter we explored the use of MALDI-MS/MS as a quick and efficient method for comparing known and unknown structures with the same composition. Spectra acquired on a quadrupole/time-of-flight mass spectrometer fitted with the MALDI ionization source are much simpler than PSD spectra due to the absence of ions resulting from metastable fragmentations occurring in the flight tube [20]. Furthermore, PSD experiments require more sample and expertise than CID-MS/MS data acquisition, which for one spectrum takes on average less than 1 min. MALDI-MS/MS spectra were acquired for standards. Characterization of unknown *N*-glycan isomeric structures involved comparing the peak ratios of specific fragment ion types in the unknown MS/MS spectrum to those of the *N*-glycan standard. These ratio comparisons are possible because the extent and distribution of fragmentation are highly reproducible in MALDI-QqTOF-MS/MS. In the second part of the chapter, we describe the use of the “knowledge-based” strategy to characterize the favoured position for galactosylation of GM₃N₄F biantennary isoforms. Even though Raju *et al.* [18] have used CE-LIF for quantitation of GM₃N₄F isoforms of human, bovine and mouse, ratios for α 1-6 to α 1-3 monogalactosylation being: human 59.9:40.1; cow 23.9:76.1; mouse 75.4:24.6. MS/MS methods will provide quicker analysis time and minimum sample size.

5.2 EXPERIMENTAL

5.2.1 Preparation of IgG samples

Bovine and human polyclonal IgG were obtained from Sigma (St. Louis, MO). The murine B-lymphocyte hybridoma cell line, CC9C10, was obtained from the American Type Culture Collection (ATCC HB-123). These cells, derived from Sp2/0 myeloma, secrete a IgG_{1k} mAb against insulins and proinsulins [21]. They were grown as chemostat cultures in DO concentrations of 10, 50, and 100%, as previously described [22]. Monoclonal antibody was purified from these cells also as described [22]. *N*-linked oligosaccharide standards as models of IgG glycans (e.g., core-fucosyl asialyl digalactosyl biantennary) were obtained from Oxford GlycoSciences (Oxford, UK).

5.2.2 *N*-deglycosylation

Samples of mAb and polyclonal IgG (1 mg) were subjected to PNGase F digestion using recombinant PNGase F (Glyko, Novato, CA) and accompanying protocol as described [23]. No detergent was used for this deglycosylation process.

5.2.3 Derivatization

The oligosaccharide pools obtained from monoclonal and polyclonal IgG samples were derivatized with PMP for MS [24].

5.2.4 MALDI-Post source decay (PSD) and MALDI-MS/MS

PSD studies were performed on a BiFlex III mass spectrometer (Bruker Daltonics, Billerica, MA). For MS/MS studies, a prototype MALDI-QqTOF built in-house in the Department of Physics and Astronomy, University of Manitoba [25] was used. MS/MS spectra were acquired at 16 Hz repetition rate. Spectrum acquisition time was 20 s or more, depending on the abundance of precursor ions. The precursor ion

window was set to 3 Da. Argon was used as cooling gas in q0 (preanalyzer quadrupole) and as collision gas in q2 (collision cell). The collision energy for each precursor was determined by applying a well-defined accelerating voltage at the entrance of the collision cell, and values were around 100 eV. In all cases, the matrix used was DHB, and sample deposition was performed using the dried-drop method. Accelerating voltages used were typical of each instrument used and were of the order of 10 kV.

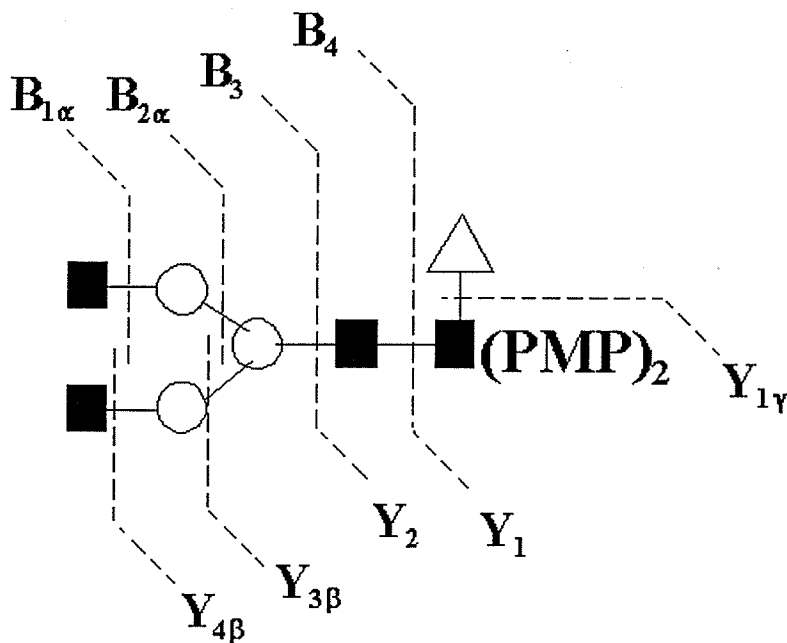
5.3 RESULTS

Characterization of unknown *N*-glycan isomeric structures involved comparing the peak ratios of specific fragment ion types in the unknown MS/MS spectrum to those of the *N*-glycan standard. Mass spectrum was acquired for the standard oligosaccharide, core-fucosyl asialyl agalactosyl biantennary (Scheme 5.1). The MALDI-QqTOF spectrum acquired for a standard oligosaccharide (core-fucosyl asialyl agalactosyl biantennary) produced both $[M+H]^+$ and $[M+Na]^+$ allowing MS/MS to be performed on each precursor, $[M+H]^+$ (Figure 5.1) and $[M+Na]^+$ (Figure 5.2) ions. For sugars with the same composition (M_3N_4F) in the murine monoclonal IgG glycan pool (obtained using 50% DO), MS/MS (Figure 5.3), spectrum was obtained for the $[M+Na]^+$ ion. PSD spectra were also obtained for the standard (Figure 5.4) and the mAb derived glycan (Figure 5.5). Because it was not possible to produce protonated parent ions with the mAb derived glycans, MS/MS and PSD were performed on the sodiated molecular ions.

Similar comparisons were done for standard and mAb-derived core-fucosyl asialyl digalactosyl biantennary glycans (Scheme 5.2). MALDI-QqTOF spectrum acquired for a standard oligosaccharide (core-fucosyl asialyl digalactosyl biantennary)

produced both $[M+H]^+$ and $[M+Na]^+$ allowing MS/MS to be performed on each precursor, $[M+H]^+$ (Figure 5.6) and $[M+Na]^+$ (Figure 5.7). For sugars with the same composition ($G_2M_3N_4F$) in the murine monoclonal IgG glycan pool (obtained using 50% DO), MS/MS (Figure 5.8) spectrum was obtained for the $[M+Na]^+$ ion. PSD spectra were also obtained for the standard (Figure 5.9) and the mAb derived glycan (Figure 5.10).

More comparative MS/MS experiments were performed on ions at m/z 1978. MS/MS spectra were obtained to attempt further characterization of the position of the terminal galactosyl residue, which can be located on either antenna. MS/MS spectra were acquired for core-fucosyl asialyl monogalactosyl biantennary glycan at m/z 1978 for the mAb glycans grown at 10%, 50% and 100% DO (Figure 5.13). MS/MS were also performed on m/z 1978 ion for human and bovine IgG glycans (Figure 5.13). The MS/MS spectra obtained were all nearly identical suggesting both possible isomeric forms produce nearly identical daughter spectra.



Scheme 5.1 Scheme showing the nomenclature for describing the major fragment ions from core-fucosylated asialyl agalactosyl biantennary glycan.

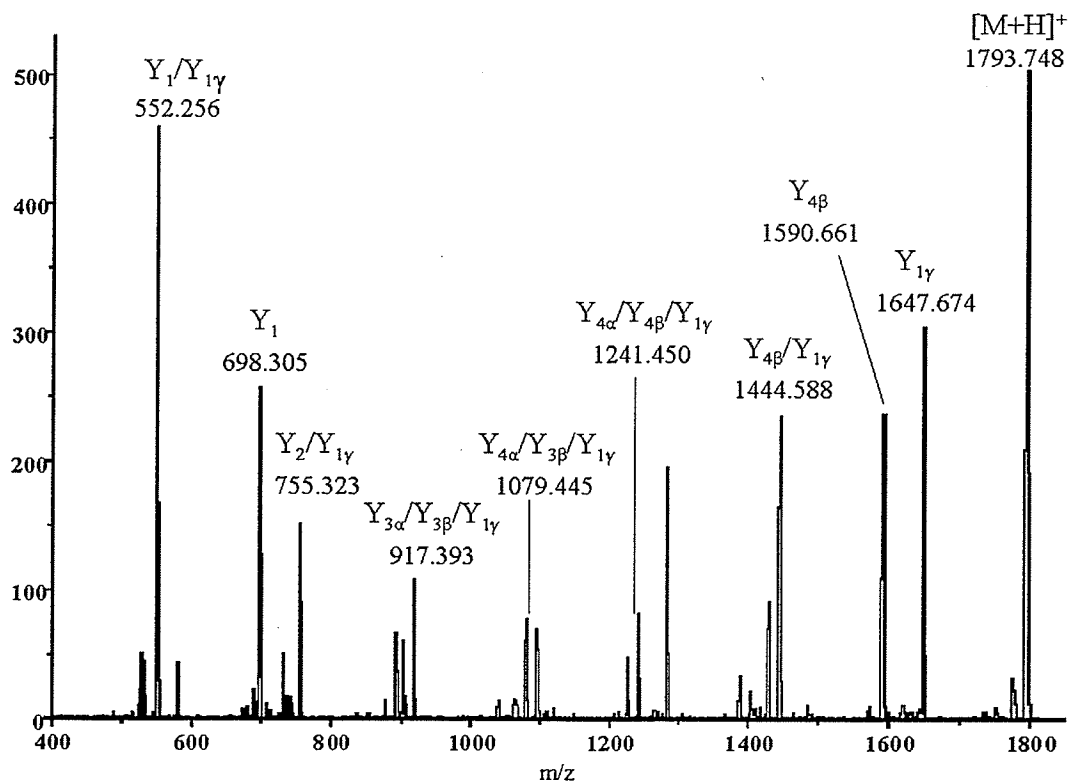


Figure 5.1 MALDI-QqTOF-MS/MS spectrum of PMP-derivatized core-fucosylated asialyl agalactosyl biantennary glycan: $[M+H]^+$ ions of standard at m/z 1794.

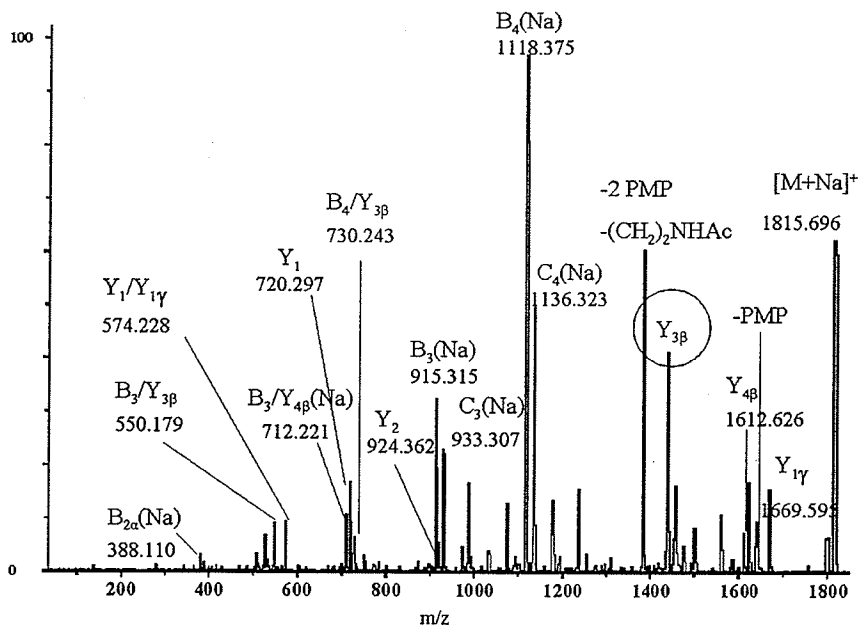


Figure 5.2 MALDI-QqTOF-MS/MS spectrum of PMP-derivatized core-fucosylated asialyl agalactosyl biantennary glycans: $[M+\text{Na}]^+$ ions of standard at m/z 1816.

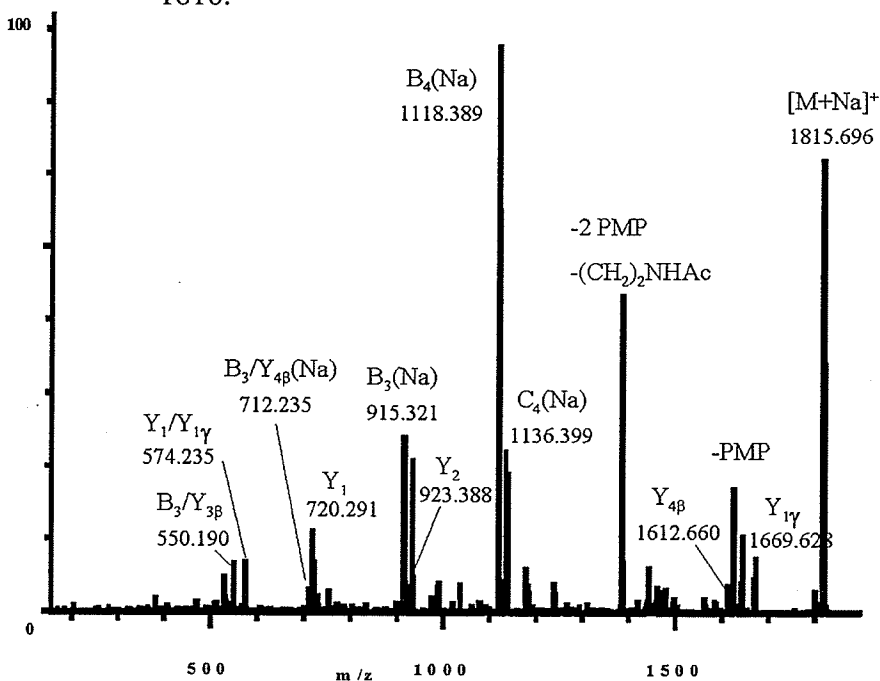


Figure 5.3 MALDI-QqTOF-MS/MS spectrum of PMP-derivatized core-fucosylated asialyl agalactosyl biantennary glycans: $[M+\text{Na}]^+$ ions at m/z 1816, from murine monoclonal IgG glycan pool, obtained with 50% DO.

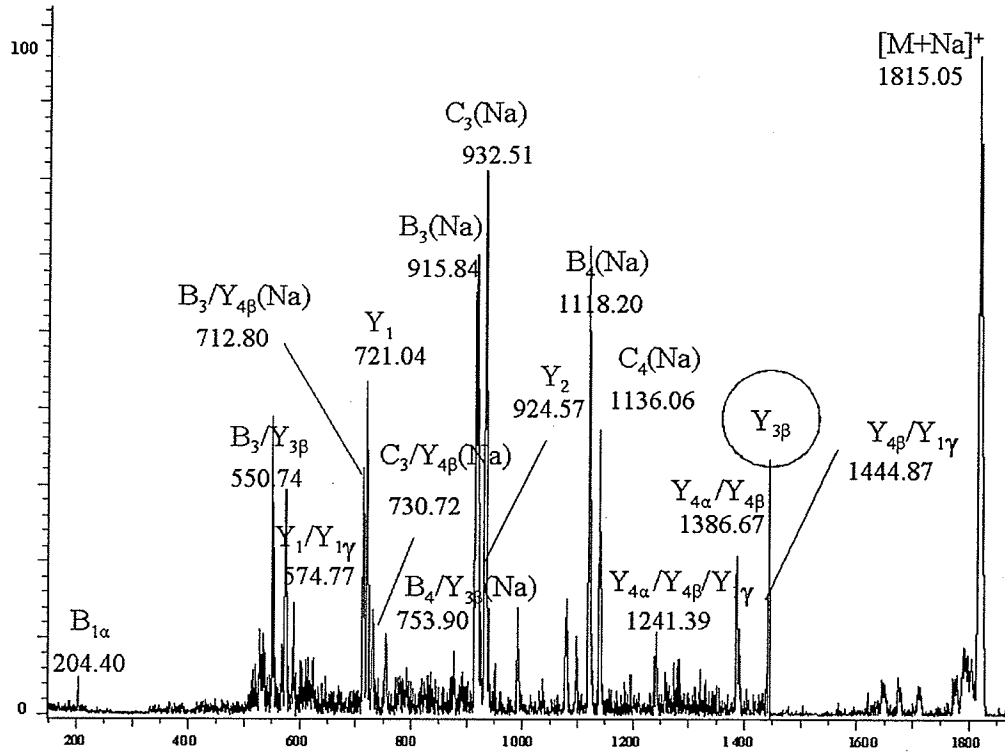


Figure 5.4 MALDI-TOF-PSD spectrum of PMP-derivatized core-fucosylated asialyl agalactosyl biantennary glycans: $[M+Na]^+$ ions of standard at m/z 1816.

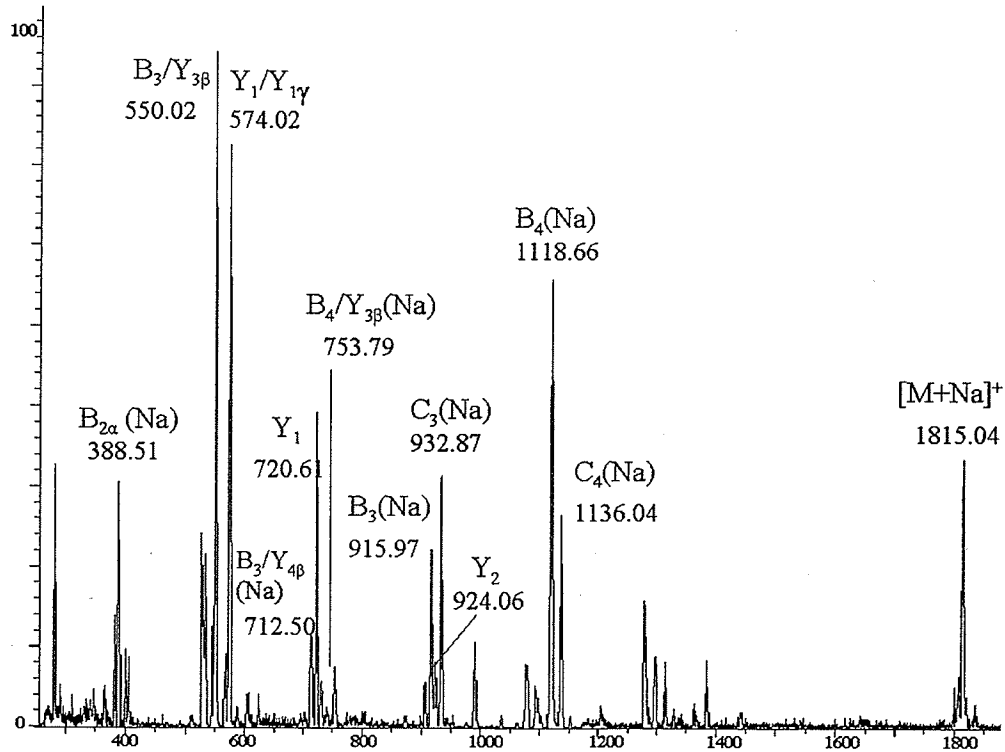
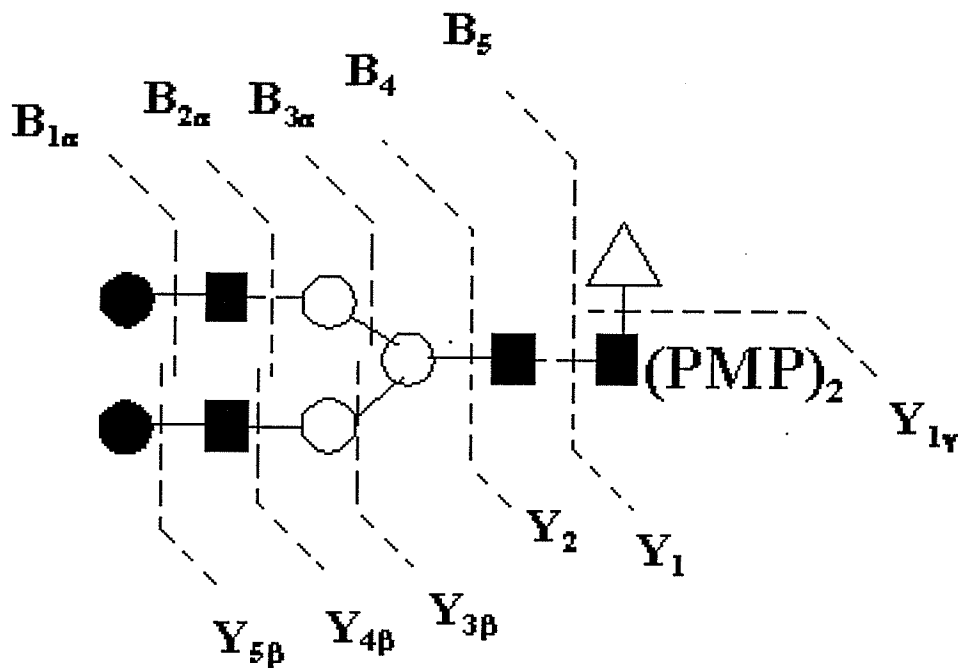


Figure 5.5 MALDI-TOF-PSD spectrum of PMP-derivatized core-fucosylated asialyl agalactosyl biantennary glycans: $[M+Na]^+$ ions at m/z 1816, from murine monoclonal IgG glycan pool, obtained with 50% DO.



Scheme 5.2 Scheme showing the nomenclature for describing the major fragment ions from core-fucosylated asialyl digalactosyl biantennary glycan.

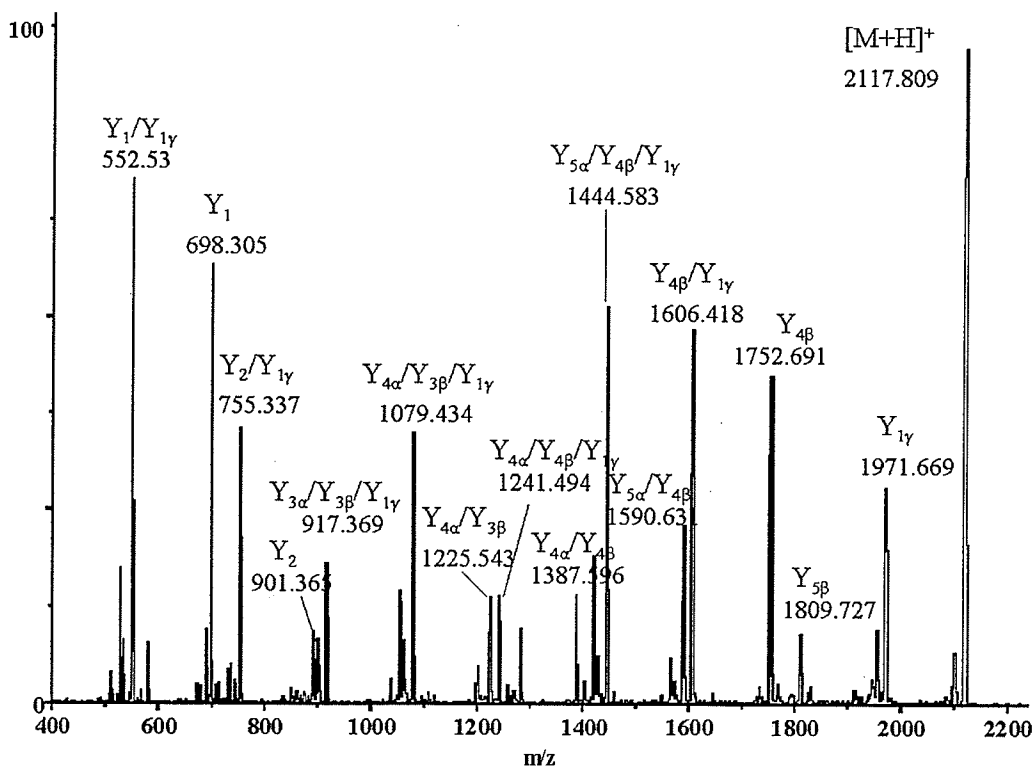


Figure 5.6 MALDI-QqTOF-MS/MS spectrum of PMP-derivatized core-fucosyl asialyl digalactosyl biantennary glycans: $[M+H]^+$ ions of standard at m/z 2118.

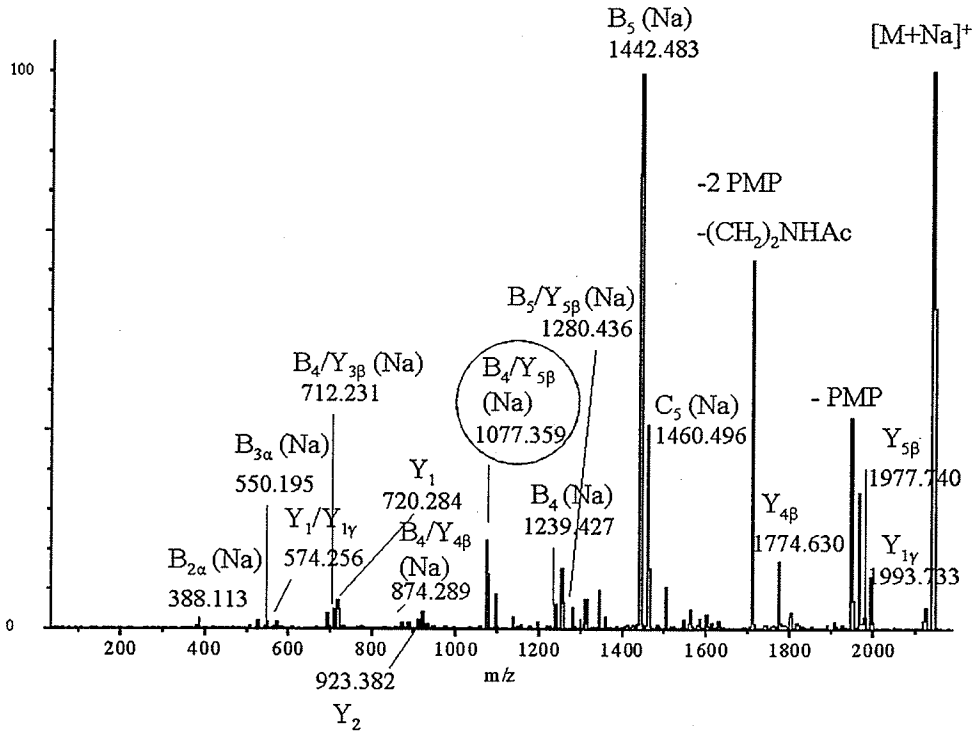


Figure 5.7 MALDI-QqTOF-MS/MS spectrum of PMP-derivatized core-fucosyl asialyl digalactosyl biantennary glycan: $[M+Na]^+$ ions of standard at m/z 2140.

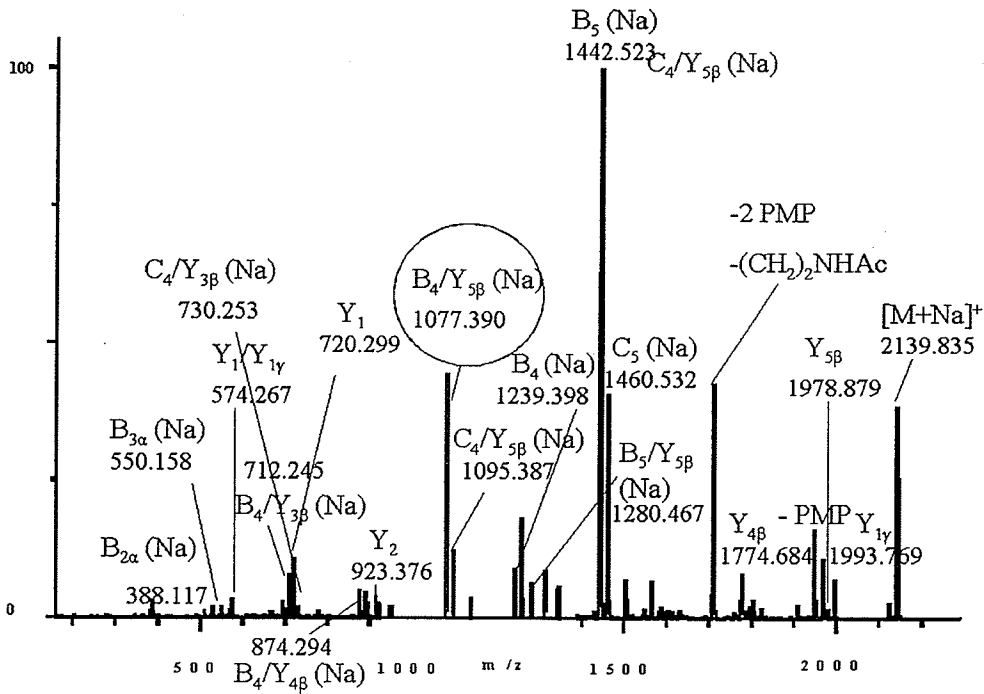


Figure 5.8 MALDI-QqTOF-MS/MS spectrum of PMP-derivatized core-fucosyl asialyl digalactosyl biantennary glycan: $[M+Na]^+$ ions at m/z 2140, from murine monoclonal IgG glycan pool, obtained with 50% DO.

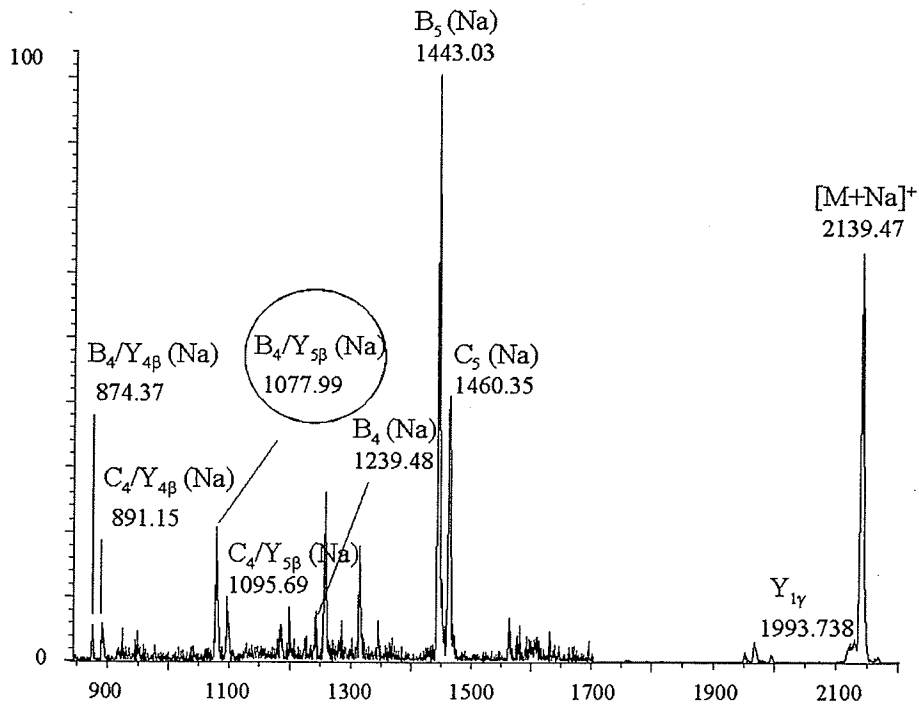


Figure 5.9 MALDI-TOF-PSD spectrum of PMP-derivatized core-fucosyl asialyl digalactosyl biantennary glycans: $[M+Na]^+$ ions of standard at m/z 2140.

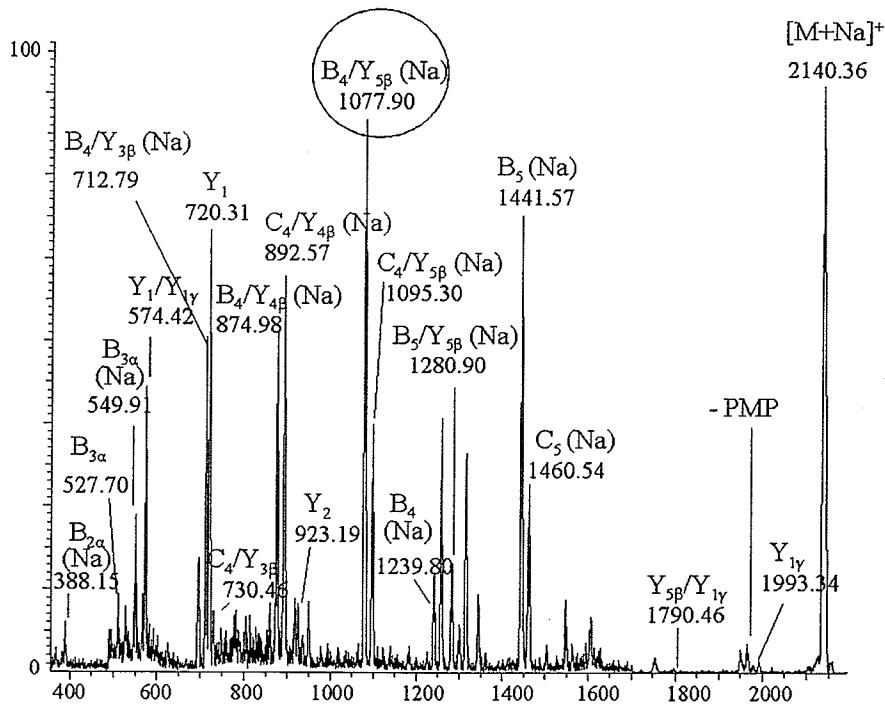


Figure 5.10 MALDI-TOF-PSD spectrum of PMP-derivatized core-fucosyl asialyl digalactosyl biantennary glycans: $[M+Na]^+$ ions at m/z 2140, from murine monoclonal IgG glycan pool, obtained with 50% DO.

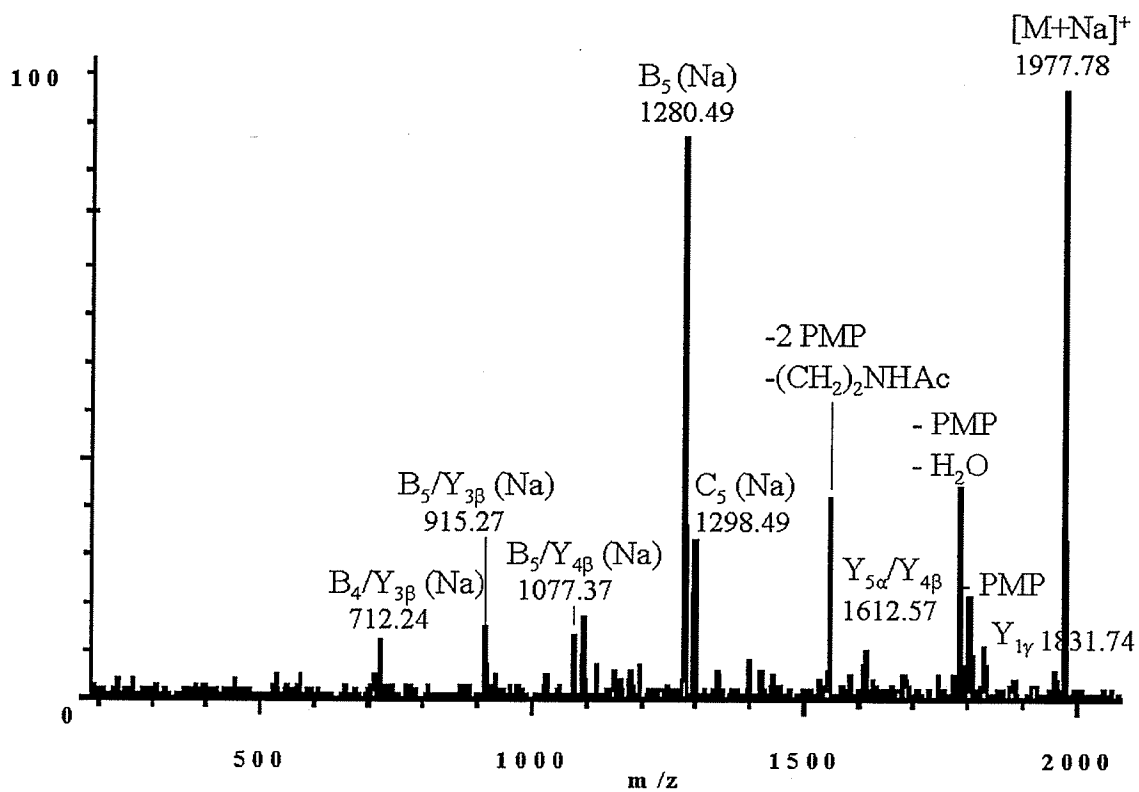


Figure 5.11 MALDI-QqTOF-MS/MS spectrum of m/z 1978 ions, $[M+Na]^+$ corresponding to PMP-derivatized core-fucosyl asialyl monogalactosyl biantennary structures.

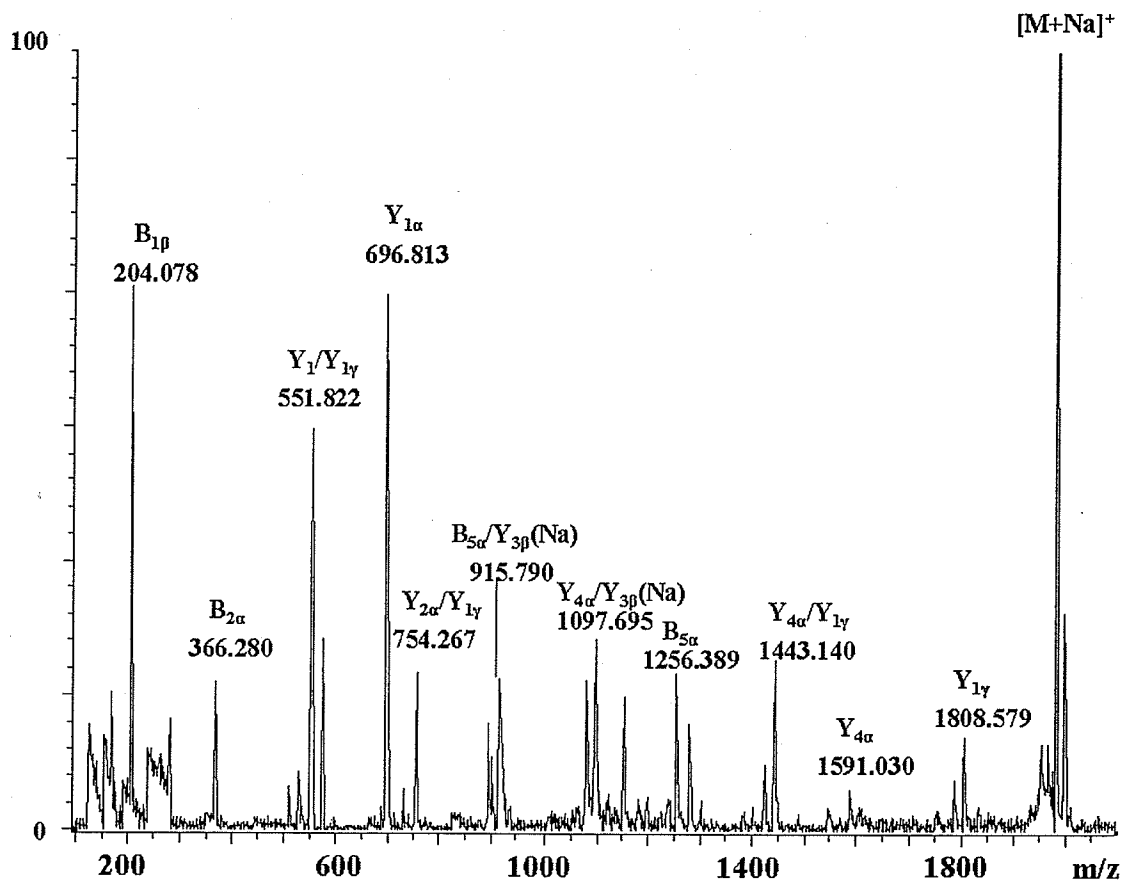


Figure 5.12 MALDI-PSD spectrum of m/z 1978 ions, $[M+Na]^+$ corresponding to PMP-derivatized core-fucosyl asialyl monogalactosyl biantennary structures.

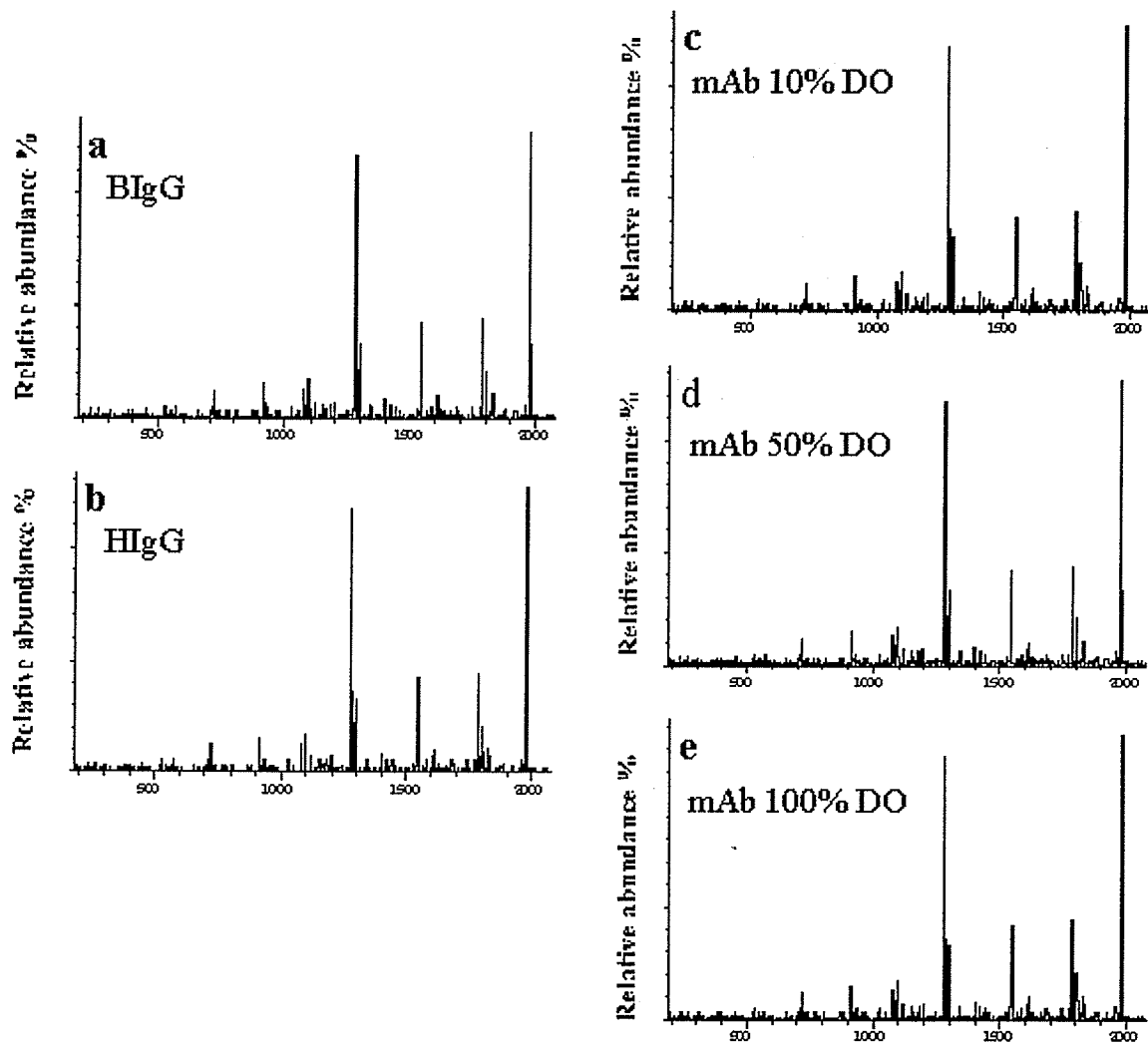


Figure 5.13 MALDI-QqTOF-MS/MS spectra of m/z 1978 $[M+Na]^+$ ions of PMP-derivatized oligosaccharides released from different IgG species. (a and b) Polyclonal; (c–e) monoclonal.

5.4 DISCUSSION

5.4.1 Comparison of MALDI-MS/MS data between standards and IgG₁ glycans.

The spectrum acquired for a standard oligosaccharide (core-fucosyl asialyl agalactosyl biantennary) produced both $[M+H]^+$ and $[M+Na]^+$ allowing MS/MS to be performed on each precursor, $[M+H]^+$ (Figure 5.1) and $[M+Na]^+$ (Figure 5.2). For sugars with the same composition (M_3N_4F) in the murine monoclonal IgG glycan pool (obtained using 50% DO), MS/MS (Figure 5.3) and PSD (Figure 5.5) spectra were obtained for the $[M+Na]^+$ ions. Comparison of the $[M+Na]^+$ MS/MS and PSD spectra between the standard and the murine monoclonal IgG glycan pool showed few differences between relative abundances of some product ions, suggesting possible isomeric parent structures. The main difference between the spectra are the presence of abundant $Y_{3\beta}$ (and/or $Y_{3\alpha}$) ions in the standard (Figure 5.2 and 5.4), almost absent in the monoclonal IgG glycan pool (Figure 5.3 and 5.5). This could indicate the presence of more than one branching pattern because identical glycans produce similar fragmentation patterns with similar peak ratios. Possible alternative structures for m/z 1816 ions are given Scheme 5.3a. It is possible to obtain these structures biosynthetically in a hybrid glycan (GlcNAc on the $\alpha 1,3$ antenna only [26]) or from the fragmentation of a complex glycan during the MALDI process (GlcNAc on either antenna). Therefore the weak signal of $Y_{3\beta}$ or $Y_{3\alpha}$ ions in Figure 5.3 and 5.5 could be attributed to a smaller probability of types of ions with structures, such as these in Scheme 5.3a occurring, with possibility of cleavage of only one branch. For the standard compound, isobaric $Y_{3\beta}$ and $Y_{3\alpha}$ ions can be produced by cleavage of either branch (see Scheme 5.1). MALDI-QqTOF-MS/MS on $[M+H]^+$ produce mainly PMP-containing fragment ions, and the positive charge seems localized

on the labeled portion of the molecule. In comparison, $[M+Na]^+$ precursors tend to fragment from both ends of the molecule, making structural interpretation rather difficult. Abundant fragment ions are consistently produced from the loss of 2 PMP units and of a portion of the GlcNAc ring (see Scheme 5.4). Unfortunately, the amount of Na^+ in IgG glycan samples could not be reduced enough to produce predominant $[M+H]^+$ ions even after sample cleanup using cation-exchange beads prior to application of the sample on the MALDI target.

Similar comparisons were undertaken with standard and mAb-derived core-fucosyl asialyl digalactosyl biantennary glycans (Scheme 5.2). In a fashion similar to results observed in the previous study, $[M+H]^+$ and $[M+Na]^+$ tended to produce very different fragmentation patterns under MS/MS conditions. The spectrum was easier to interpret for $[M+H]^+$ due to uniform observation of Y-related ions containing the label. Comparison of the $[M+Na]^+$ spectra for standard against the mAb-derived glycan showed similar fragmentation patterns, with the main difference being the fragments at m/z 1077.4 being more abundant in the mAb spectra (Figures 5.8 and 5.10) than in those of the standard (Figures 5.7 and 5.9). These ions are interpretable as $B_4/Y_{5\beta}$ or $B_5/Y_{4\beta}$ in Figures 5.7 and 5.9, according to the structure of the standard (Scheme 5.2). It is difficult to speculate on isobaric structures different from the one proposed in Scheme 5.2, unless a hybrid structure is also present (Scheme 5.3b). If the ions at m/z 1077.4 in Figures 5.8 and 5.10 are in part due to the proposed hybrid structure, they would be interpreted as $B_5/Y_{5\beta}$ fragments, which have a different conformation relative to the $B_4/Y_{5\beta}$ or $B_5/Y_{4\beta}$ ions mentioned above. In Scheme 5.3, the structure in Scheme 5.3b could be a precursor to the structure in Scheme 5.3a, but this could only occur by fragmentation within the

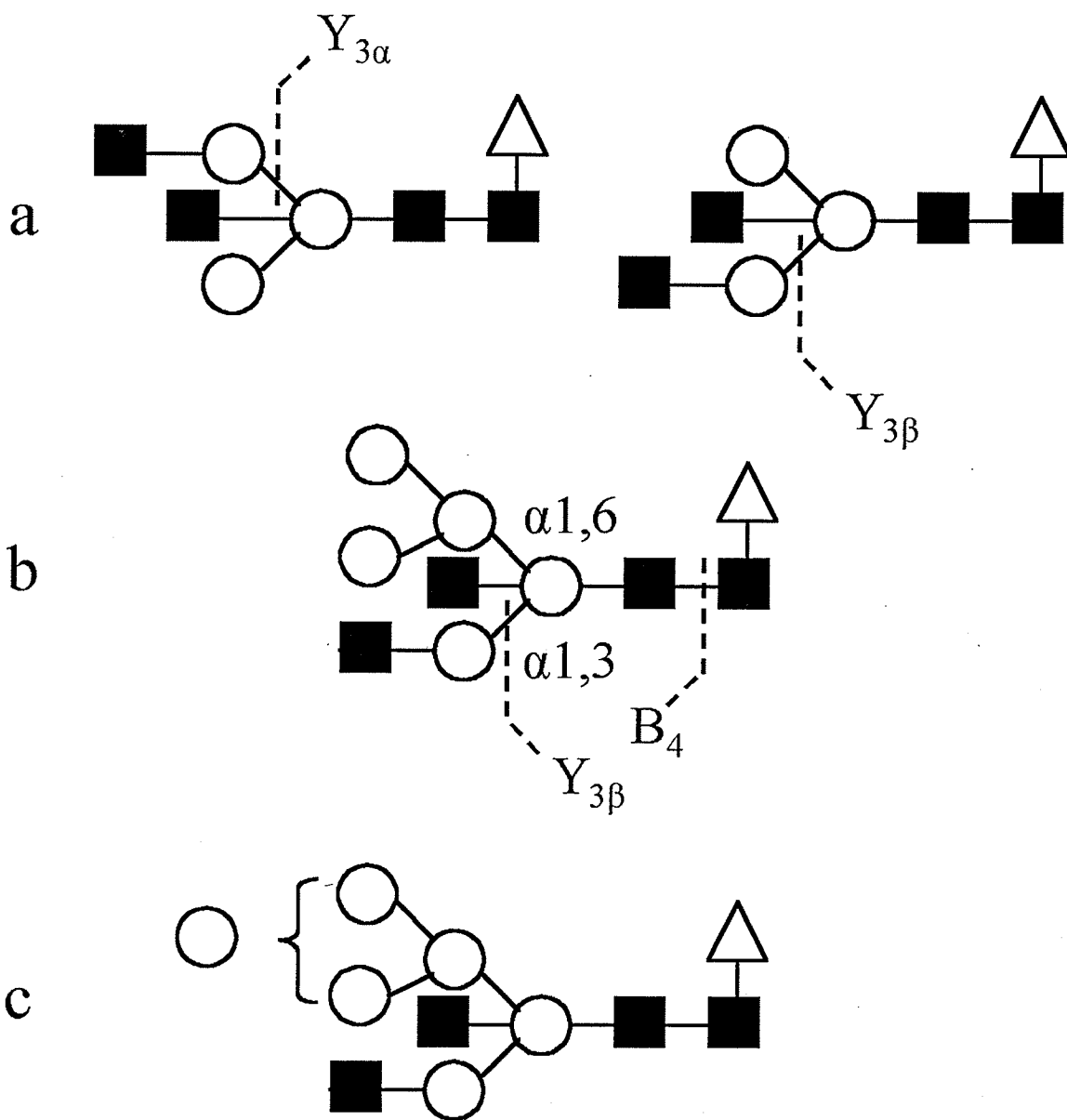
mass spectrometer, because biosynthetically this process is not possible. The bisecting GlcNAc (by the action of *N*-acetylglucosamine transferase III) blocks the action α -mannosidase-II. This would help to explain the observation of ions at m/z 2302 (Figure 4.10c), which can only correspond to the hybrid structure M_6N_4F (Scheme 5.3c), a possible biosynthetic precursor to the structure of Scheme 5.3b [26]. Qualitative comparison of MS/MS spectra of isobaric precursor ions potentially allows differentiation of structures; however, this remains speculative at this time.

5.4.2 Comparison of MALDI-PSD and MALDI-MS/MS data

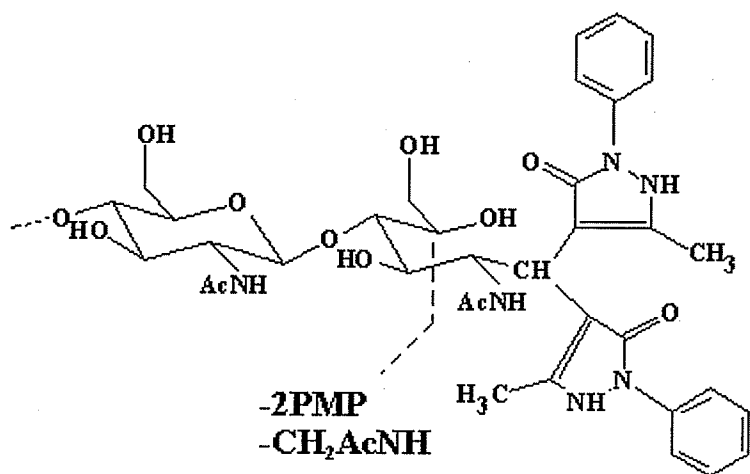
MALDI-PSD and MALDI-QqTOF-MS/MS spectra were acquired for m/z 1978 ions, $[M+Na]^+$ (Figure 5.11 and 5.12), corresponding to core-fucosyl asialyl monogalactosyl biantennary structures. The MALDI-QqTOF-MS/MS spectrum (Figure 5.11) produced similar fragmentation as those observed in Figures 5.3 and 5.8. The PSD spectrum (Figure 5.12) for m/z 1978 shows unimolecular fragmentation, resulting in easier interpretation than for the MS/MS spectrum, because most ions contain the reducing end (PMP group), and the only B-related ions ($B_{1\beta}$, $B_{2\alpha}$, and $B_{5\alpha}$) arise from cleavages directly adjacent to a GlcNAc group. The MALDI-QqTOF-MS/MS spectrum, obtained by CID with argon, shows only ions from the non-reducing end, including two major peaks corresponding to losses of the PMP label and adjacent moieties (m/z 1786 and 1547). The MALDI-PSD spectrum is similar to the CID-MS/MS of the $[M+H]^+$ ions and more useful than the $[M+Na]^+$ ions. However, PSD experiments require more sample and expertise than CID-MS/MS data acquisition, which for one spectrum takes on average less than 1 min.

5.4.3 Comparison of MS/MS data on m/z 1978 ions from IgG₁

Studies have shown that terminal galactosylation is branch specific for different species [18]. With increasing DO concentration in the cell culture, we attempted to characterize the favored position for terminal galactosylation using MS/MS of the m/z 1978 ions, expecting different fragmentation patterns for GM₃N₄F biantennary isoforms. Unfortunately, the spectra were identical, suggesting both possible isoforms produce identical daughter ion spectra (Figure 5.13). Assignments of fragment ions are as in Figure 5.11. Because the isobaric complex sugars that are known to be α 1-6 or α 1-3 monogalactosylated in varying ratios all produce identical fragmentation pattern as in Figure 5.13, then the noticeable differences observed in MS/MS spectra from the isobaric species previously discussed indicate the presence of alternate structures and support our hypothesis of the presence of the hybrid structures.



Scheme 5.3 Possible alternative structures for (a) M_3N_4F and (b) $G_2M_3N_4F$ from IgG. In (c), possible hybrid structure, with formula M_6N_4F .



Scheme 5.4 Formation of abundant fragment ions in the MS/MS spectra of $[M+Na]^+$ ions of PMP-derivatized IgG glycans.

5.5 CONCLUSIONS

MALDI-QqTOF-MS/MS experiments were performed to confirm proposed glycan structures. The fragmentation patterns obtained from $[M+H]^+$ and $[M+Na]^+$ ions were different and complementary in the information they provided. Most IgG sugars produced $[M+Na]^+$ ions, which in turn fragmented into charged B-type ions (containing the nonreducing end). We could not prove a systematic dependence of the relative abundances of fragment ions on sugar structure; more specifically we could not differentiate GM_3N_4F isomers using MS/MS of their $[M+Na]^+$ ions.

5.6 REFERENCES

1. Spengler, B., Kirsch, D., Kaufmann, R. and Lemoine, J. *J. Mass Spectrom.* **30**, 782 (1995).
2. Laine, R. A., Pamidimukkala, K. M., French, A. D., Hall, R. W., Abbas, S. A., Jain, R. K. and Matta, K. L. *J. Am. Chem. Soc.* **110**, 6931 (1988).
3. Garozzo, D., Giuffrida, M., Impallomeni, G., Ballistreri, A. and Montaudo, G. *Anal. Chem.* **62**, 279 (1990).
4. Orlando, R., Bush, C. A. and Fenselau, C. *Biomed. Environ. Mass Spectrom.* **19**, 747 (1990).
5. Hofmeister, G. E., Zhou, Z. and Leary, J. A. *J. Am. Chem. Soc.* **113**, 5964 (1991).
6. Dongre, A. R. and Wysocki, V. H. *Org. Mass Spectrom.* **29**, 700 (1994).
7. Johnson, R. S., Costello, C. E. and Reinhold, V. N. Proceedings of the 37th ASMS Conference on Mass Spectrometry and Allied Topics, p. 1192, Miami Beach, FL.
8. Domon, B., Müller, D. R. and Richter, W. J. *Biomed. Environ. Mass Spectrom.* **19**, 390 (1990).
9. Domon, B., Müller, D. R. and Richter, W. J. *Int. J. Mass Spectrom. Ion Processes* **100**, 301 (1990).
10. Gillece-Castro, B. L. and Burlingame, A. L. (1990) in *Mass Spectrometry* (McCloskey, J. A., Ed.), Methods in Enzymology, Vol. 193, Chap. 37, Academic Press, San Diego, CA.
11. Domon, B., Müller, D. R. and Richter, W. J. *Org. Mass Spectrom.* **29**, 713 (1994).
12. Reinhold, V. N., Reinhold, B. B. and Costello, C. E. *Anal. Chem.* **67**, 1772 (1995).
13. Hardy, M. R. and Townsend, R. R. *Proc. Natl. Acad. Sci. USA* **85**, 3289 (1988).
14. Davis, M.J., Smith, Harbin, A.M. and Hounsell E.F. *J. Chromatogr.* **609**, 125 (1992).
15. Lipniunas, P.H., Neville, D.C. A., Trimble, R.B. and Townsend, R.R. *Anal. Biochem.* **243**, 203 (1996).
16. Lee, Y.C. *J. Chromatogr. A* **720**, 137 (1996).
17. Townsend, R.R., Hardy, M.R., Cumming, D.A., Carver, J.P. and Bendiak, B. *Anal. Biochem.* **182**, 1 (1989).

18. Raju, T.S., Briggs, J.B., Borge, S.M. and Jones, A.J.S. *Glycobiology* **10**, 477 (2000).
19. Rouse, J.C., Strang, A., Yu, W. and Vath, J.E. *Anal. Biochem.* **256**, 33 (1996).
20. Harvey, D. J., Bateman, R. H., Bordoli, R. S. and Tyldesley, R. *Rapid Commun. Mass Spectrom.* **14**, 2135 (2000).
21. Schroer, J. A., Bender, T., Feldman, R. J., and Kim, K. J. *Eur. J. Immunol.* **13**, 693 (1983).
22. Kunkel, J. P., Jan, D. C. H., Jamieson, J. C., and Butler, M. *J. Biotechnol.* **62**, 55 (1998).
23. Kunkel, J. P., Jan, D. C. H., Butler, M., and Jamieson, J. C. *Biotechnol. Prog.* **16**, 462 (2000).
24. Honda, S., Akao, E., Suzuki, S., Okuda, M., Kakehi, K., and Nakamura, J. *Anal. Biochem.* **180**, 351 (1989).
25. Loboda, A. V., Krutchinsky, A. N., Bromirski, M. P., Ens, W., and Standing, K. G. *Rapid Commun. Mass Spectrom.* **14**, 1047 (2000).
26. Varki, A., Cummings, R., Esko, J., Freeze, H., Hart, G., and Marth, J. (Eds.) (1999) *Essentials of Glycobiology*, Cold Spring Harbor Laboratory Press, Cold Spring Harbor, NY.

6 SEQUENCING THE PRIMARY STRUCTURE OF ANIONIC POTATO PEROXIDASE

6.1 INTRODUCTION

In every day life plant cells are exposed to environmental stresses such as injuries, pathogens and desiccating environment. Over the course of evolution, plant cells have developed effective ways of dealing with these environmental challenges. The defense mechanisms tend to be site specific, affected cells are isolated from the healthy ones and healed. In the case of wounding, high quantity of toxic chemicals are produced by the affected cell to kill the pathogens. This is followed by the formation of polymeric barrier next to the infected site (suberized layer).

The term suberin is applied to specific cell wall modification deposited in periderm, wound periderm, and endo- and exodermal cells that involves the biosynthesis of a poly(phenolic) domain (SPPD) within the cell wall as well as a poly(aliphatic) domain (SPAD) between the plasma membrane and the cell wall [1]. The polymerization of phenolics into the SPPD of potato has been hypothesized to occur via a peroxidase/H₂O₂ mediated free radical coupling process [2] and a specific anionic potato peroxidase is involved in the step [3-5]. Recently, Razem *et al.* [6] have shown that H₂O₂ is required for the polymerization of the SPPD of potato but suberin-specific role for the anionic peroxidase of potato remains tenuous, and more definitive evidence is required to unambiguously assign this specific function to it.

Anionic potato peroxidase has not been fully characterized biochemically, however, it has been cloned and its molecular biology has been studied [7,8].

Furthermore, studies have focused on the role H₂O₂ plays and the role anionic peroxidase

plays has not received much attention. Also, the structural features of the peroxidase has not been characterized. Thus, structural characterization of the anionic potato peroxidase was undertaken to aid in understanding the role it plays in suberization.

In an earlier study by Bernards *et al.* [9] the purified anionic potato peroxidase had a measured molecular weight (MW) of 45.8 kDa by SDS-PAGE and 44.9 kDa by calibrated molecular-sieving chromatography. Deglycosylation with trifluoromethane sulfonic acid (TFMS) yielded a 35.3 kDa protein. There is also a published sequence available for the protein which lists the MW around 37.3 kDa [10]. Hopefully, mass spectrometry methods will aid in solving some of these discrepancies.

In the present chapter, a combination of derivatization, isotopic labelling and MALDI-MS has been used for structural characterization of the peroxidase. Traditionally, isotopic labelling has been used for the identification of C-terminal peptide in a protein and in simplifying the interpretation of tandem mass spectra [11-17]. Incorporation of an isotopic label on the C-terminus of a peptide allows for easier identification of the C-terminal or Yⁿ ions [17] by their characteristic isotopic pattern. For the work described in this chapter ¹⁸O isotopic label was employed. Specifically, protein digestion by trypsin in the presence of ¹⁸O water incorporates the ¹⁸O atom selectively into the C-terminal carboxyl groups of the peptides. Subsequent fragmentation by MS/MS reveals the Yⁿ ions by a characteristic 2 mass unit shift or split which facilitates 'read-out' of the sequence.

Additionally, glycans released from the anionic potato peroxidase were characterized, which involved derivatization with PMP and the use of a prototype double

quadrupole/time-of-flight (QqTOF) mass spectrometer. PMP was chosen as the label due to its sensitivity enhancement for MS detection of carbohydrates by MALDI [18].

6.2 EXPERIMENTAL

6.2.1 Plant material

The anionic potato peroxidase was provided by M. Bernards, Department of Plant Sciences, University of Western Ontario, London, Ontario, Canada.

6.2.2 Removal of heme groups

Potato Peroxidase is overall anionic (pI approx. 3.5). It is a hollow enzyme containing a heme group. The heme groups were removed prior to any experiment. The glycoprotein was dissolved in 100 μ L of water and made up to 1mL with 0.5% HCl/acetone. The glycoprotein was precipitated out in an ice bath. The heme group remain in the HCl/acetone mixture.

6.2.3 N-deglycosylation

Anionic potato peroxidase (100 μ g) were subjected to PNGase A digestion using recombinant PNGase A (Seikagaku Corporation, Tokyo, Japan) and accompanying protocol as described [19]. No detergent was used for this deglycosylation process.

6.2.4 Derivatization

The oligosaccharide pools obtained from anionic potato peroxidase were derivatized with PMP for MS [20,21].

6.2.5 Tryptic digestion

Peroxidase protein (10 μ g) was dissolved in 1 μ L of 100 mM ammonium bicarbonate. Trypsin (1 μ g) (Sigma-Aldrich, St. Louis, MO, USA) was added and the

sample was incubated for 4 hours at 37 °C. Digestion was stopped by adding 1 μ L of a 1% solution of acetic acid.

6.2.6 Glu-C digestion

Peroxidase protein (10 μ g) was dissolved in 1 μ L of 100 mM ammonium bicarbonate. Glu-C (1 μ g) (Roche Diagnostics Co., Indianapolis, IN, USA) was added and the sample was incubated for 16 hours at 37 °C.

6.2.7 ^{18}O isotopic labelling

To perform ^{18}O isotopic labelling, proteins were digested using the same method except that the digestion buffer contained 50% v/v of H_2^{18}O (^{18}O , enrichment greater than 98%).

6.2.8 Peptide fractionation

Digested peptides were bound to ZipTip_{C18} pipette tips (Millipore, Billerica, MA). The tips were washed with 10 μ L of 5% methanol in 0.1% TFA/water to improve desalting efficiency. Peptides were fractionated with increasing ACN concentration (10 to 40%).

6.2.9 MALDI and MALDI-MS/MS

MS studies were performed on a BiFlex III mass spectrometer (Bruker Daltonics, Billerica, MA). For MS/MS studies, a prototype MALDI-QqTOF built in-house in the Department of Physics and Astronomy, University of Manitoba [22] was used. MS/MS spectra were acquired at 16 Hz repetition rate. Spectrum acquisition time was 20 s or more, depending on the abundance of precursor ions. The precursor ion window was set to 3 Da. Argon was used as cooling gas in q0 (preanalyzer quadrupole) and as collision gas in q2 (collision cell). The collision energy for each precursor was

determined by applying a well-defined accelerating voltage at the entrance of the collision cell, and values were around 100 eV. In all cases, the matrix used was DHB, and sample deposition was performed using the dried-drop method. Accelerating voltages used were typical of each instrument used and were of the order of 10 kV.

6.3 RESULTS

6.3.1 MW measurement

The MW measurement of the fully glycosylated apoprotein by MALDI-TOF-MS is 37.6 kDa (Figure 6.1a). The MW of the deglycosylated protein is 36.2 kDa (Figure 6.1b).

6.3.2 Glycan characterization

Glycans released from the anionic potato peroxidase were derivatized with PMP and examined by MALDI-MS with 2,5-DHB as the matrix. The resulting profile is shown in Figure 6.2 with proposed structures shown in Figure 6.3. All ions are sodium cationized. Sixteen glycans were detached using PNGase A. Some ions were of sufficient abundance to allow CID-MS/MS experiments to be performed (Figure 6.4). MALDI-CID-MS/MS data were acquired for all general sugar compositions shown in italics in Table 6.1. Two types of glycans were observed, high mannose and complex type. The complex type contained xylose within the core structure. Denaturation of the protein by boiling the sample in a hot water bath was required for complete removal of the glycans.

6.3.3 Protein Sequencing

De novo peptide sequencing was undertaken to characterize the protein. Because of its high resolution without loss of sensitivity, the QqTOF [22] was ideal for the application of labelling the C-terminal ions with the ^{18}O isotope. The protein was

digested by trypsin or Glu-C in a buffer containing 50% v/v of ^{18}O water. The MALDI-QqTOF mass spectrum resulting from the digestion is shown in Figure 6.5 and 6.6. In the peptide map, labelled peptides could be determined by their characteristic 2 mass unit isotopic spacing.

In order to determine the amino acid sequence of the peptide fragments, each clearly observed peptide ion was selected in turn as a parent by the mass-selecting quadrupole of the QqTOF instrument, and subjected to CID. For example, the resulting daughter ion spectrum from the m/z parent ion 842.5 is shown in Figure 6.7. Figure 6.7 shows how ^{18}O labelling, in conjunction with the high resolution provided by the QqTOF makes sequence readout very straightforward. The Y'' ion series could be extended all the way to the N-terminus of the peptide allowing unambiguous determination of the sequence. The spectrum also evidently shows the advantage of the $^{16}\text{O}/^{18}\text{O}$ addition for distinguishing the C- and N-terminal ions. The Y'' ions, which contain the C-terminus, all show the doublet structure superimposed on the usual isotopic pattern, whereas the b ions, containing the N-terminus, have a normal pattern.

In this manner, after tryptic digest, 13 peptides were sequenced, covering 161 amino acid residues and 27 peptides were sequenced covering 224 amino acid residues for Glu-C digest (Tables 6.2 and 6.3).

Ionization of peptides can be quenched by competing ions, resulting in either low signal intensity or the absence of ions. In order to maximize ionization efficiency potential, the pool of peptides (after Glu-C and tryptic digest) were fractionated. Peptides were loaded onto C-18 ZipTips and eluted with increasing aqueous ACN concentration (10-40 %) into four different fractions (Figures 6.8 and 6.9). Figure

6.10 (a) shows a spectrum acquired after Glu-C digestion. Figure 6.10 (b) shows a spectrum of a fraction collected with 30 % ACN. Comparison of the spectra in Figures 6.10 (a) and (b) reveals a number of differences. The spectra of fractions are simpler to interpret because the ionization of peptides is more efficient and there are fewer peaks. For example consider the peak at m/z 1836.3 (G19). The ion is more abundant in the spectrum of the fraction than in that of the whole digest. Fractionation allows for MS/MS to be performed on this ion. Fractionation has also allowed for ions that might have been quenched due to competition to be detected (e.g. m/z 2018.3 (G33-34)). Fractionation was performed on both Glu-C and tryptic digests.

6.3.4 Glycosylation sites

According to the published sequence [10], anionic potato peroxidase contains 7 possible sites of glycosylation (Asn-24, Asn-114, Asn-149, Asn-187, Asn-201, Asn-213 and Asn-251) with the motif Asn-Xaa-Thr/Ser, where Xaa can be any amino acid residue except for proline. Four of these sites were sequenced during peptide map coverage of the protein (Asn-114, Asn-149, Asn-213 and Asn-251). The Glu-C peptide G14-15 contained potential glycosylation site Asn-114. Glu-C peptide G16-17 and tryptic peptide T11 both contained potential glycosylation site Asn-149. The Glu-C peptide G22 and tryptic peptide T17 both contained potential glycosylation site Asn-213, and the tryptic peptide T19 contained potential glycosylation site Asn-251. All four of these sites were sequenced without finding any glycans attached.

Figures 6.11a and 6.11b show the MALDI-MS spectra obtained for tryptic digests of glycosylated and deglycosylated anionic potato peroxidase. Comparison of the two figures shows very similar spectra except for the peak at m/z 2273.7, which is present

in the glycosylated peroxidase digest spectrum (Figure 6.11a) but absent in the deglycosylated peroxidase digest spectrum (Figure 6.11b). The absence of this ion in the spectra of deglycosylated peroxidase fractions confirmed that the ion might be due to a post-translational modification, more specifically glycosylation. MALDI-QqTOF-MS/MS data were acquired for the ions at m/z 2273.7 (Figure 6.12). There is an initial loss of fucose, followed by losses of amino acids from the N-terminus leading up to glycosylated Asn-24. Also observed is the peak due to the glycan moiety itself.

6.3.5 Peptide mapping

The approach used here for sequencing this protein was to treat it as a novel protein. The task of fitting together the peptides was undertaken next. Based on the MS/MS data, a peptide map was constructed on the sequence of the protein (Figure 6.13). A comparison of the results with the predicted sequence is shown in Figure 6.14. The mass spectral data cover more than 79.2% of the predicted sequence. It was possible to see the C-terminal peptide during tryptic digest, but the signal was weak in order for MS/MS studies to be performed. Overall this method enabled to achieve 80.6 % coverage. It was still not possible to determine the signal peptide. It is believed that the glycosylated peptide IIMNN is located at the N-terminus of the protein, i.e. it could “start” the sequence rather than the predicted signaling peptide (see Figure 6.14).

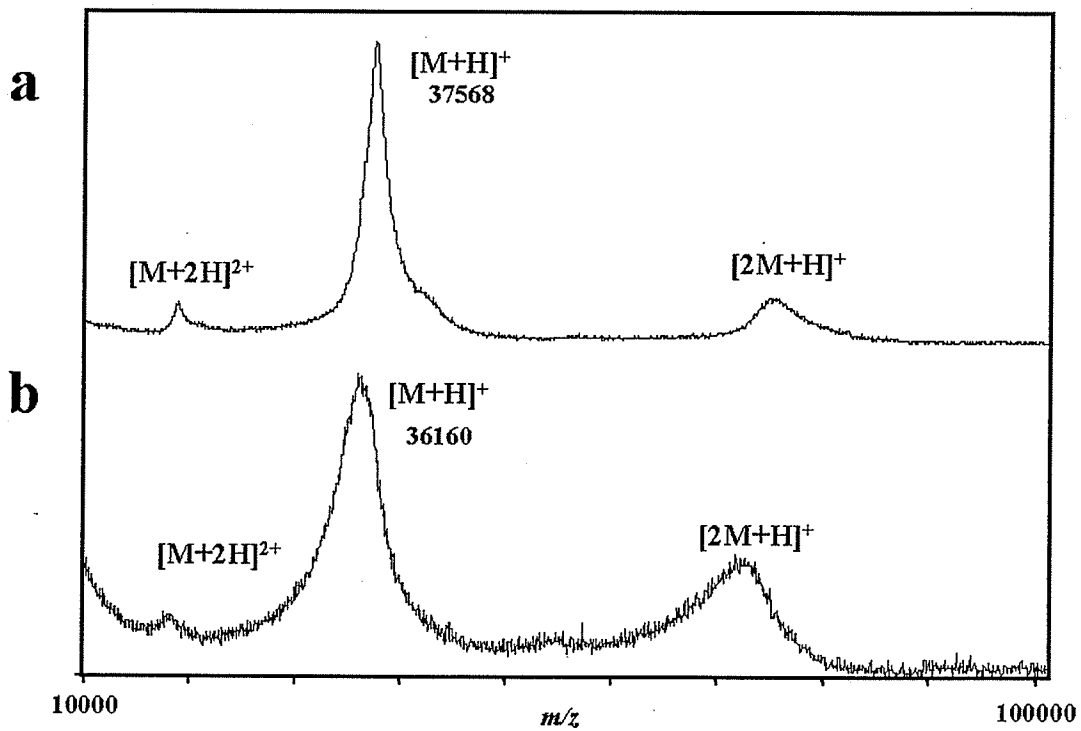


Figure 6.1 MALDI linear-TOF spectra of (a) glycosylated anionic potato peroxidase (b) deglycosylated anionic potato peroxidase.

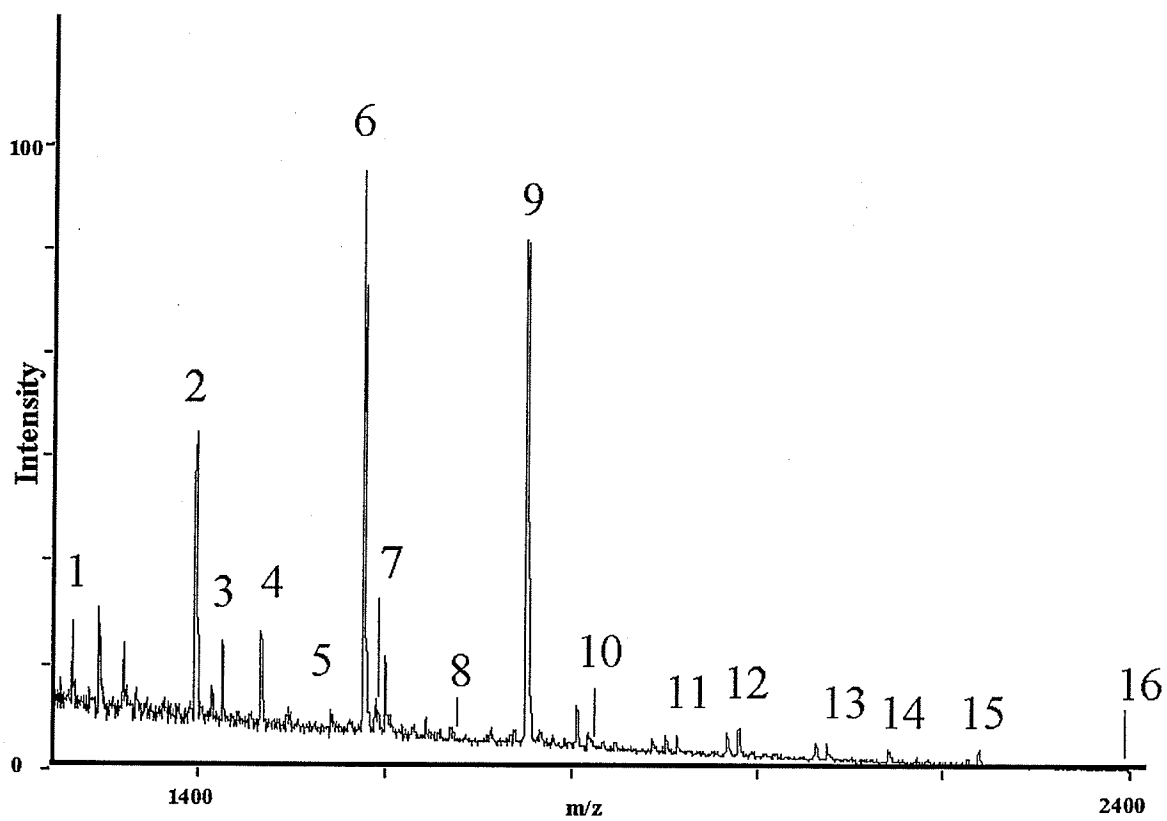


Figure 6.2 MALDI-QqTOF mass spectrum obtained for PMP-derivatized anionic potato peroxidase glycans.

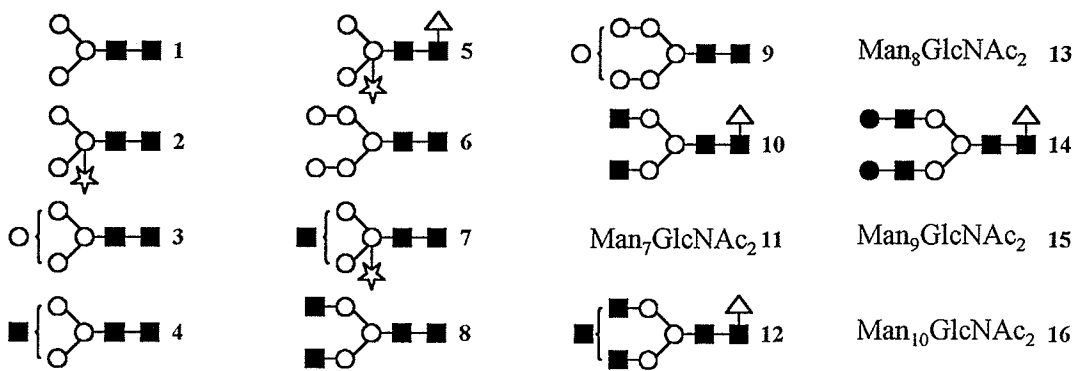


Figure 6.3 Suggested structures.

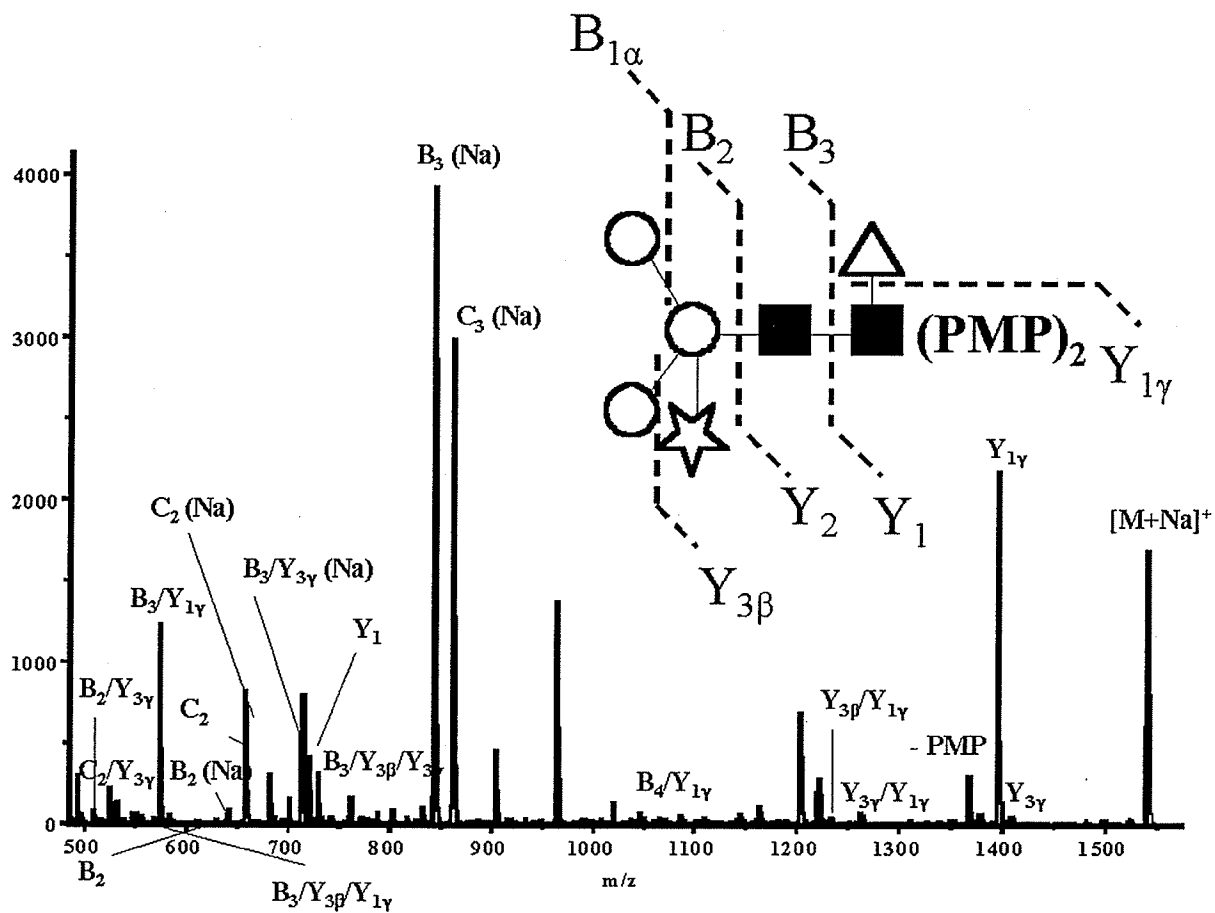


Figure 6.4 MALDI-QqTOF-MS/MS spectrum of PMP-derivatized glycan at m/z 1541.

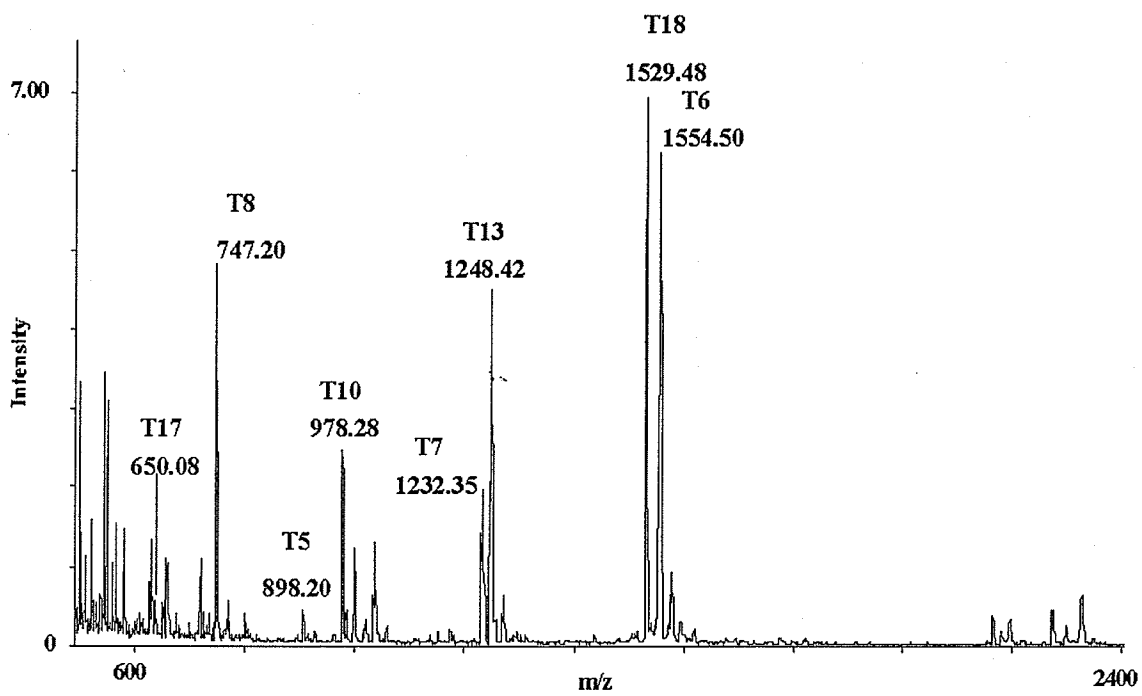


Figure 6.5 Mass spectrum for the tryptic digest of anionic potato peroxidase.

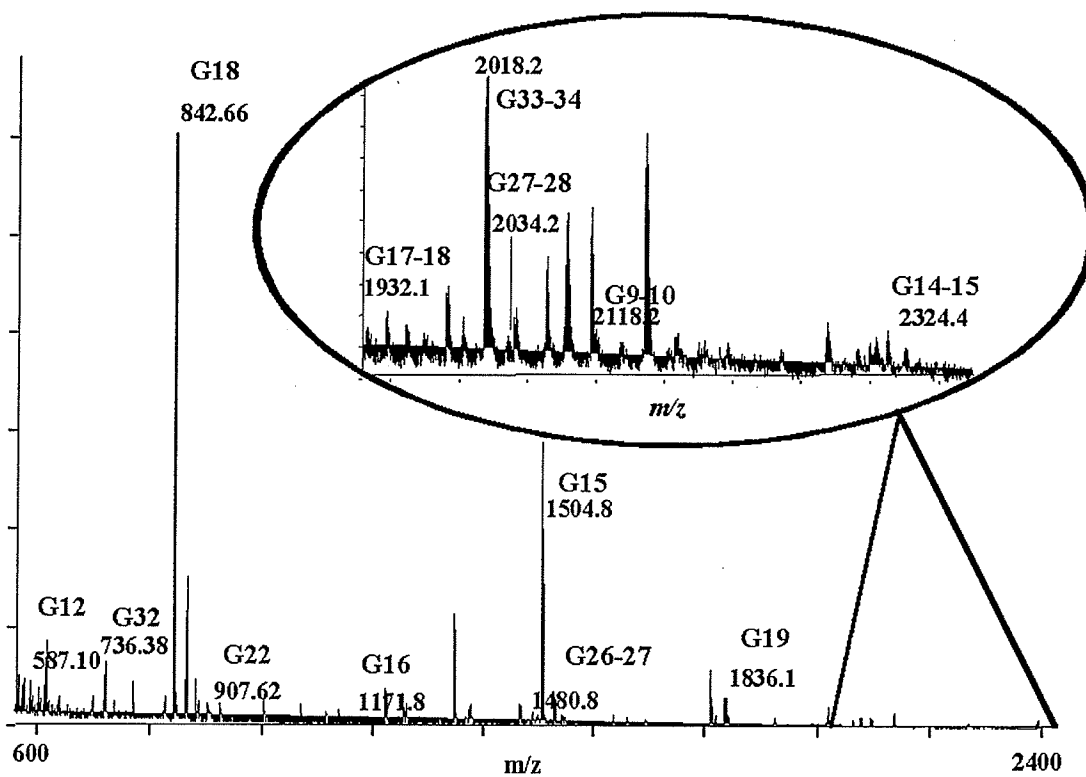


Figure 6.6 Mass spectrum of the Glu-C digest of anionic potato peroxidase.

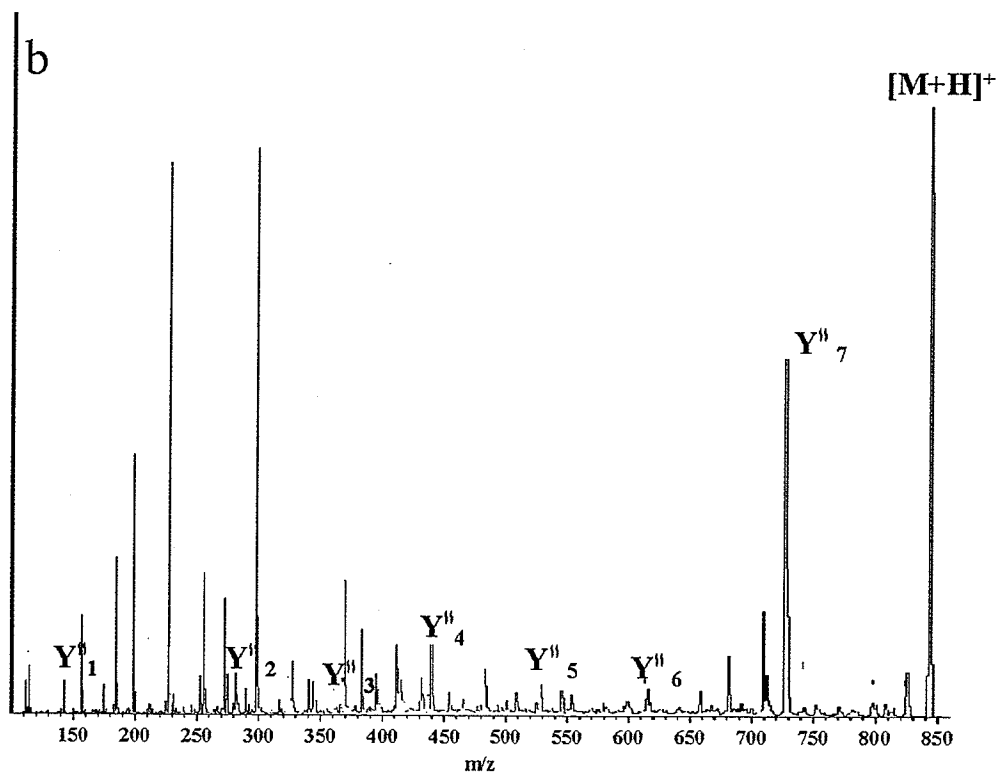
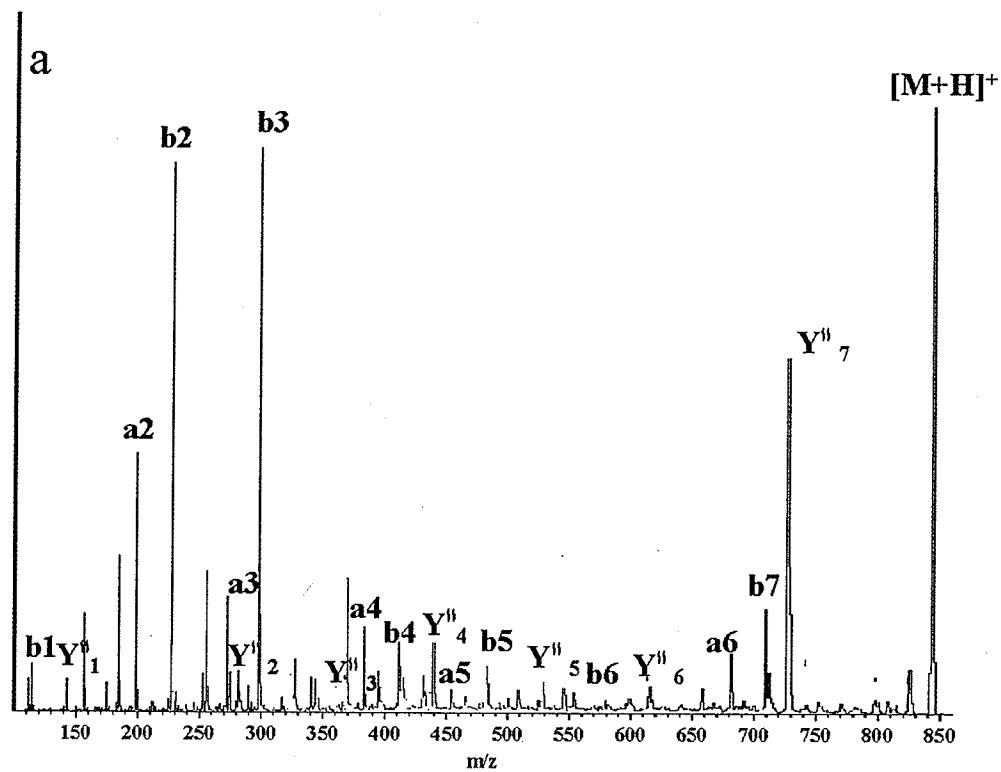


Figure 6.7 MALDI-QqTOF-MS/MS spectrum of a peptide at m/z 842.7. (a) shows a, b and Y'' ions labelled. (b) shows Y'' ions labelled (c) shows the amino acid composition of the peptide.

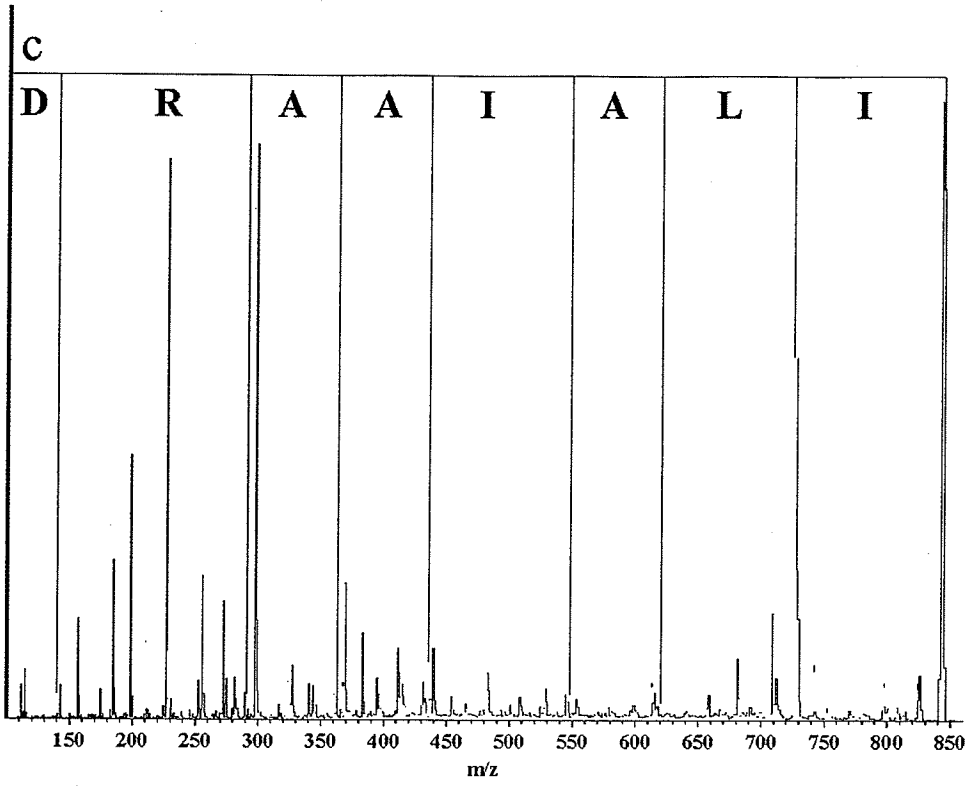


Figure 6.7 (cont'd)

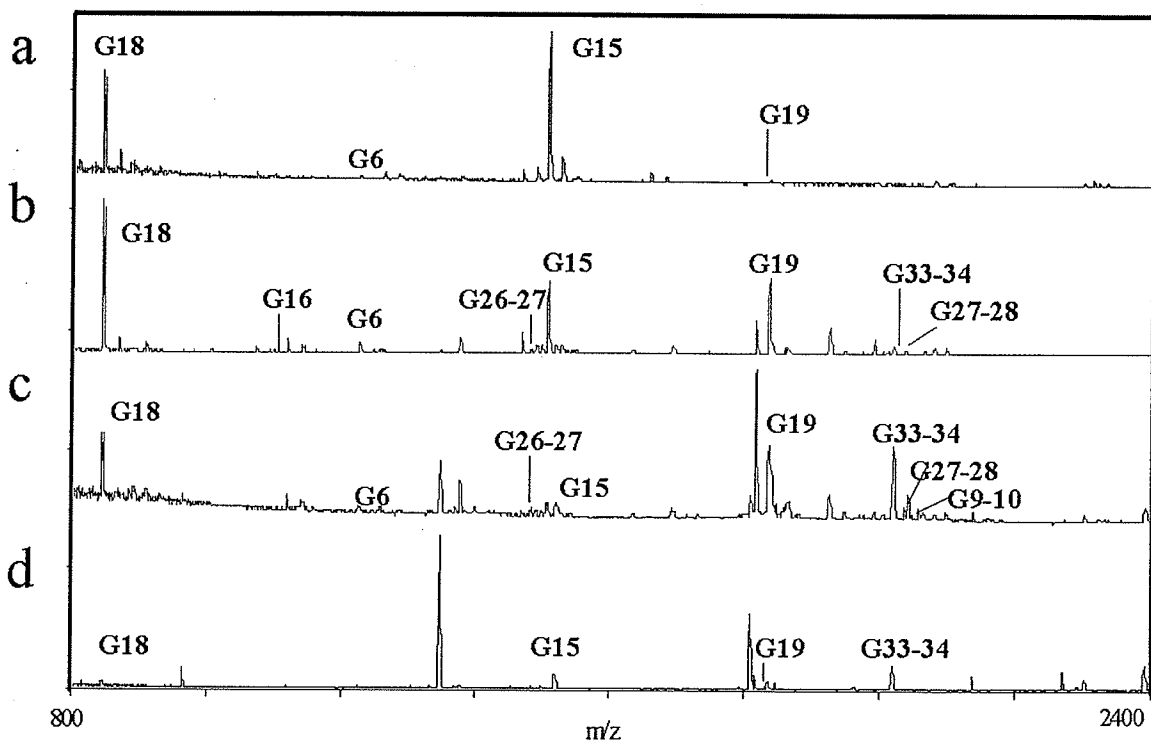


Figure 6.8 Spectra of fractionated Glu-C digest of anionic potato peroxidase (a) at 10% ACN (b) at 20% ACN (c) at 30% ACN and (d) at 40% ACN.

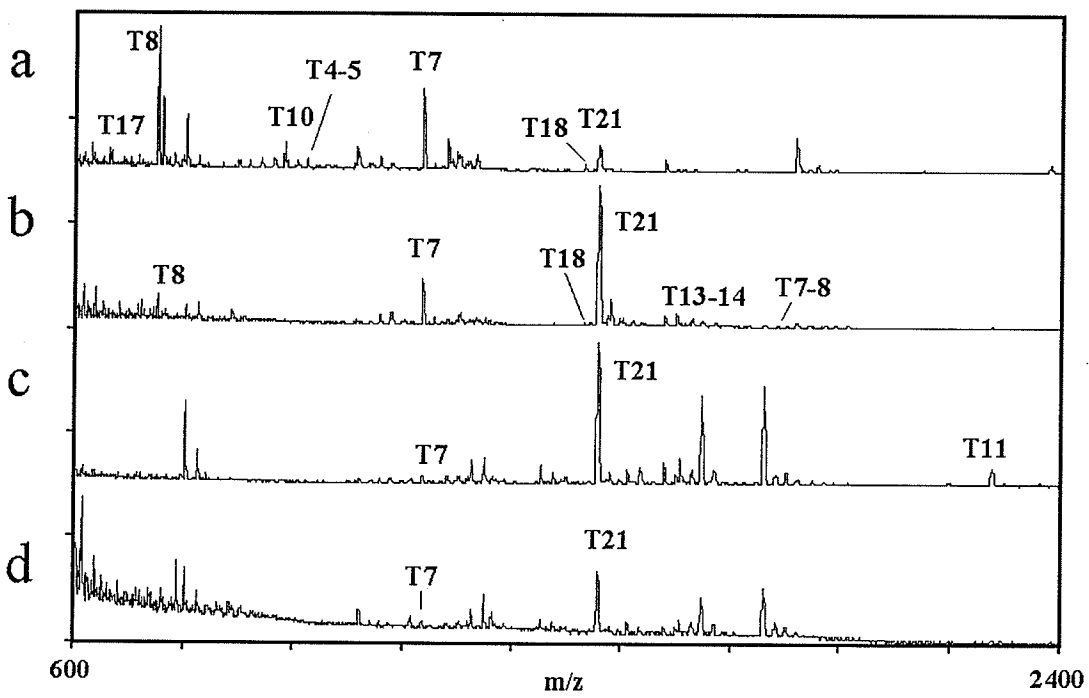


Figure 6.9 Spectra of fractionated tryptic digest of anionic potato peroxidase (a) at 10% ACN (b) at 20% ACN (c) at 30% ACN and (d) at 40% ACN.

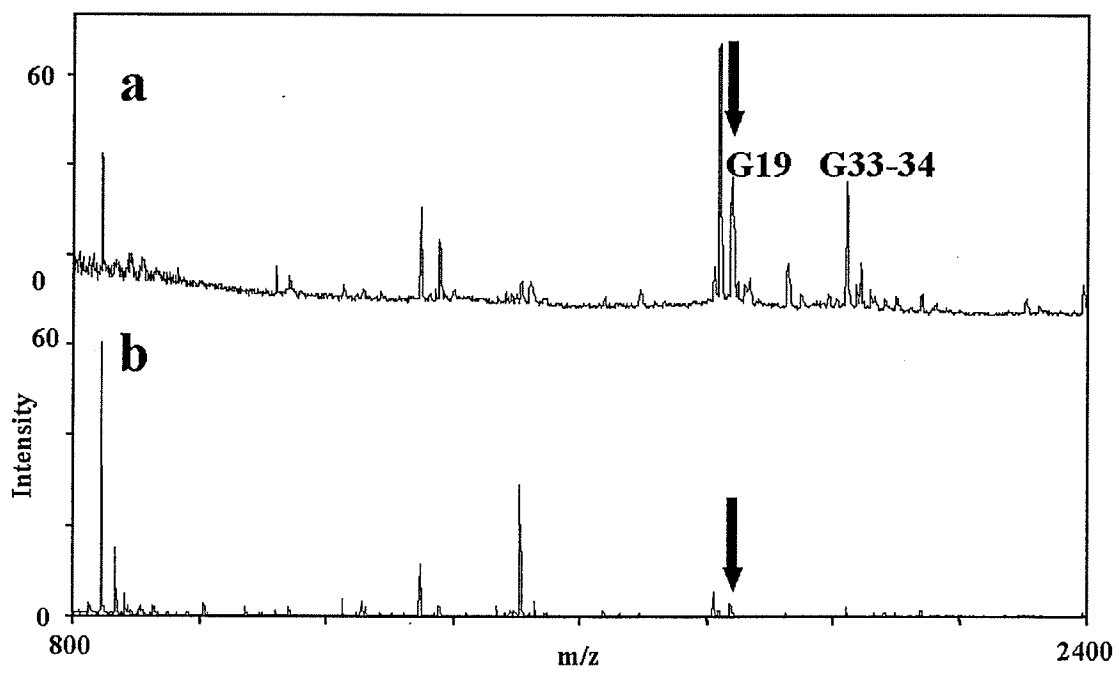


Figure 6.10 Mass spectrum of (a) C18 separated fraction at 30% ACN (b) Glu-C digest mixture.

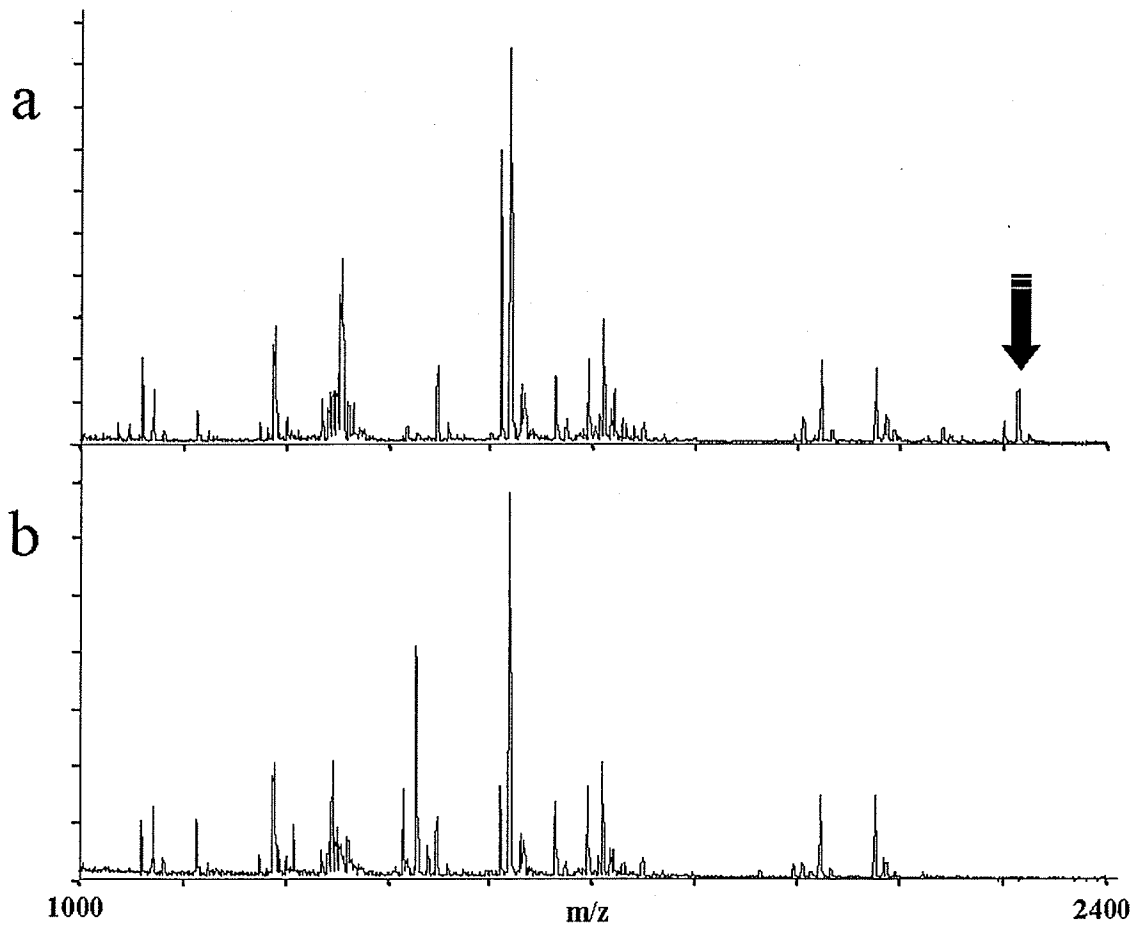


Figure 6.11 MALDI mass spectrum of tryptic digests of (a) glycosylated anionic potato peroxidase (b) deglycosylated anionic potato peroxidase.

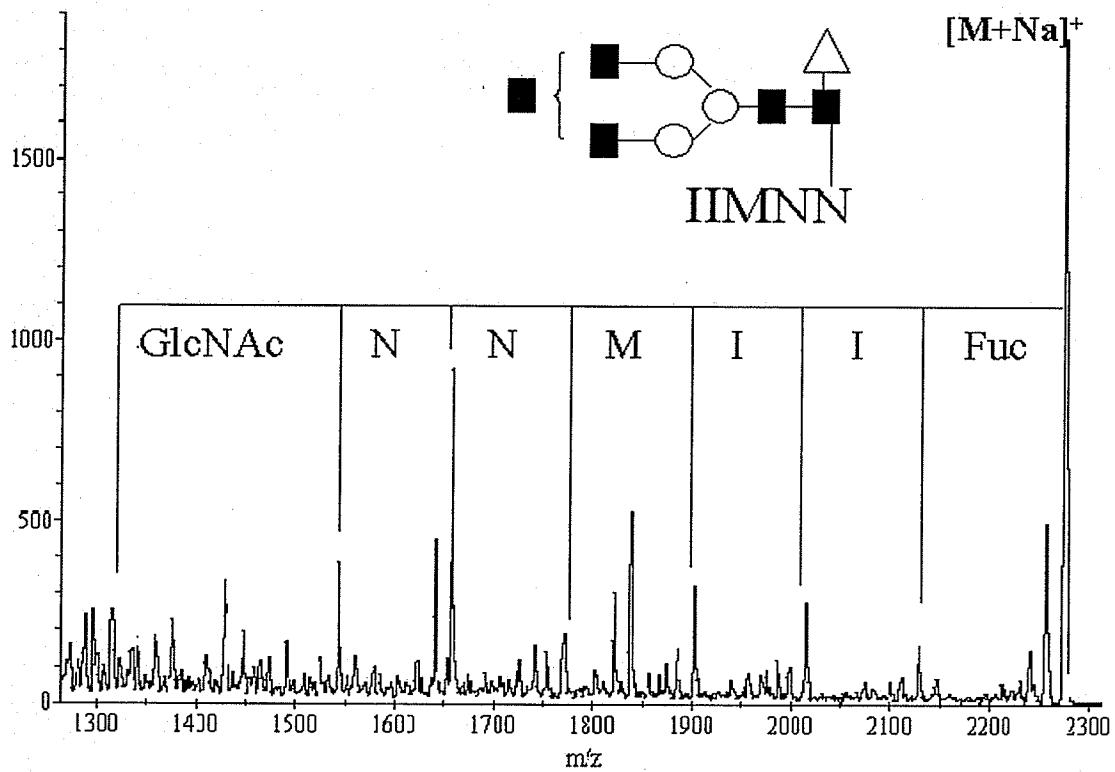


Figure 6.12 MALDI-QqTOF-MS/MS spectrum of non-specific tryptic glycosylated peptide.

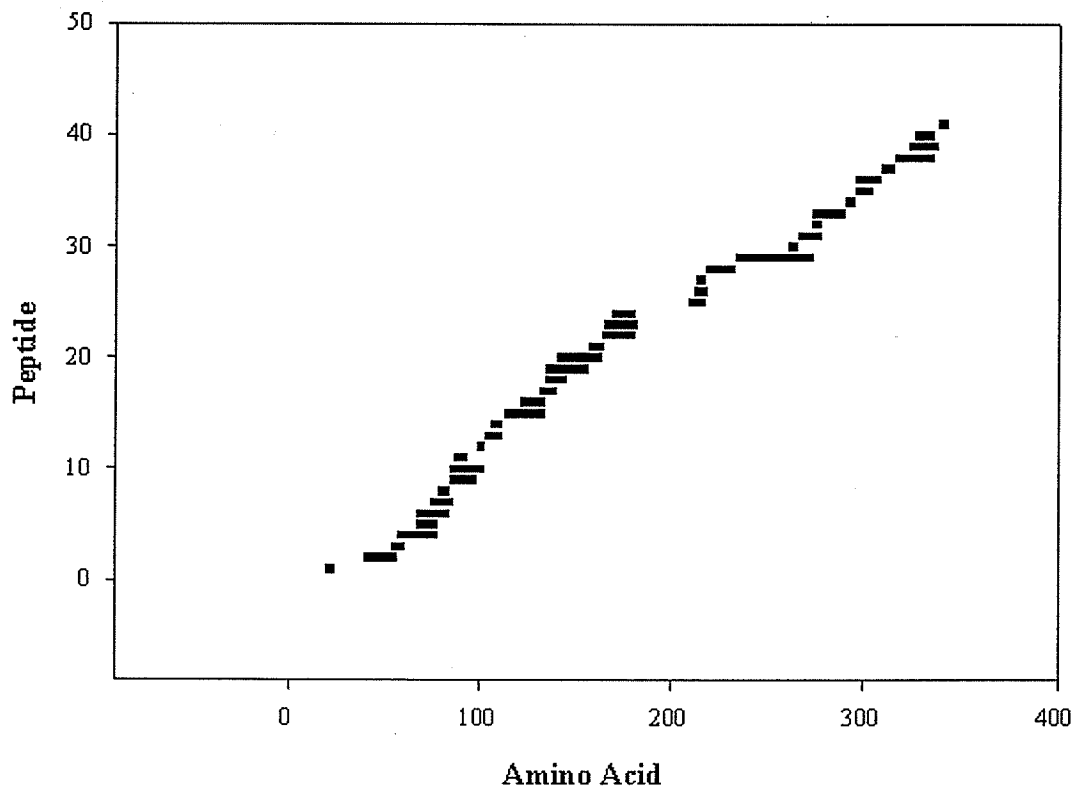


Figure 6.13 Experimental peptide map of anionic potato peroxidase.

SFVALALAGVAIYRNTYEAIIMNNGSLQNASPHFDSLESGVASILTL
IIMNN ESGVASILTL

NNKKRNSDMYLRQQLTPEACVFSAVRQVVD SAID AETRMGASLRL
NNKKRNSDMYLRQQLTPEACVFSAVRQVVD SAID AETRMGASLRL

HFHDCFVDGCDGGILLDDINGTFTGEQNSPPNANSARGYEVIAQAKQ
HFHDCFVDGCDGGILLDDINGTFTGEQNSPPNANSARGYEVIAQAKQ

SVIDTCPNISVSCADILAI AARDSVAKLGGQTYNVALGRSDARTANF
SVIDTCPNISVSCADILAI AARDSVAKLGGQTYNVALGRSD

TGALTQLPAPFDNLT VQIQKFNDKNFTLREMVALAGAHTVGFARCS
FNDKNFTLREMVALAGAHTVGFARCS

TVCTSGNVNPA AQLQCNC SATLTDSDLQQLDTPPTMFDKVYYDNL
TVCTSGNVNPA AQLQCNC SATLTDSDLQQLDTPPTMFDKVYYDNL

NNNQGIMFSDQVLTGDATTAGFVTDYSNDVSVFLGDFAAAMIKMG
NNNQGIMFSDQVLTGDATTAGFVTDYSNDVSVFLGDFAAAMIKMG

DLPPSAGA QLEIRDVCSR VNPTSVASM
DLPPSAGA QLEIRDVCSR

Figure 6.14 Comparison of the published sequence of anionic potato peroxidase with experimental peptide coverage.

Table 6.1 Suggested compositions of oligosaccharides released from anionic potato peroxidase, as detected by MALDI-MS.

Glycan composition	Experimental molecular weight [M+Na]⁺ (Monoisotopic)	Theoretical molecular weight [M+Na]⁺ (Monoisotopic)
<i>Man₃GlcNac₂</i>	1263.58	1263.46
<i>Man₃GlcNac₂Xyl</i>	1395.57	1395.51
<i>Man₄GlcNac₂</i>	1425.50	1425.51
<i>Man₃GlcNac₃</i>	1466.54	1466.54
<i>Man₃GlcNac₂XylFuc</i>	1541.55	1541.56
<i>Man₅GlcNac₂</i>	1587.59	1587.57
<i>Man₃GlcNac₃Xyl</i>	1598.53	1598.59
<i>Man₃GlcNac₄</i>	1669.61	1669.62
<i>Man₆GlcNac₂</i>	1749.58	1749.62
<i>Man₃GlcNac₄Fuc</i>	1815.62	1815.68
<i>Man₇GlcNac₂</i>	1911.70	1911.68
<i>GalMan₃GlcNac₄Fuc</i>	1977.74	1977.73
<i>Man₈GlcNac₂</i>	2073.80	2073.73
<i>Gal₂Man₃GlcNac₄Fuc</i>	2139.67	2139.78
<i>Man₉GlcNac₂</i>	2235.67	2235.78
<i>Man₁₀GlcNac₂</i>	2397.70	2397.83

Table 6.2 Glu-C digest of anionic potato peroxidase.

Fragment number	Residue number	Sequence	Measured [M+H] ⁺ (Monoisotopic)	Theoretical [M+H] ⁺ (Monoisotopic)
G10	99-102	(D) CFVD (G)	483.37	483.19
G12	106-111	(D) GGILLD (D)	587.36	587.34
G7-8	79-84	(D) SAIDAE (T)	605.29	605.28
G25	261-265	(D) LQQLD (T)	616.31	616.33
G29	290-295	(D) QVLTGD (A)	632.31	632.33
G27	273-277	(D) KVYYD (N)	687.32	687.34
G32	309-315	(D) VSVFLGD (F)	736.38	736.39
G18	157-164	(D) ILAIAARD (S)	842.51	842.51
G11-12	103-111	(D) GCDGGILLD (D)	862.42	862.40
G30	296-304	(D) ATTAGFVTD (Y)	882.44	882.42
G22	212-218	(D) KNFTLRE (M)	907.48	907.50
G34	326-335	(D) LPPSAGAQL (I)	982.50	982.52
G16	135-145	(E) VIAQAKQSVID (T)	1171.80	1171.67
G6	67-78	(E) ACVFSAVRGVVD (S)	1222.63	1222.63
G30-31	296-308	(D) ATTAGFVTDYSND (V)	1361.34	1361.59
G26-27	266-277	(D) TTPTMFDKVYYD (N)	1480.69	1480.67
G15	121-134	(E) QNSPPNANSARGYE (V)	1504.68	1504.68
G9	85-98	(E) TRMGASLIRLHFHD (C)	1653.87	1653.86
G6-8	67-84	(E) ACVFSAVRGVVDSIDA (T)	1808.55	1808.89
G4	40-56	(E) SGVASILTLNNKRN (M)	1817.58	1817.00
G19	165-182	(D) SVAKLGGQTYNVALGRSD (A)	1835.96	1835.96
G33-34	316-335	(D) FAAAMIKMGDLPPSAGAQL (I)	2018.01	2018.01
G27-28	273-289	(D) KVYYDNLNNNQGIMFSD (Q)	2034.07	2034.92
G9-10	85-102	(E) TRMGASLIRLHFHDCFVD (G)	2118.25	2118.04
G16-17	135-156	(E) VIAQAKQSVIDTCPNISVSCAD (I)	2262.09	2262.11
G14-15	113-134	(D) INGTFTGEQNSPPNANSARGYE (V)	2324.26	2324.05
G5-6	57-78	(D) MYLRQQLTPEACVFSAVRGVVD (S)	2482.03	2482.26

Table 6.3 Tryptic digest of anionic potato peroxidase.

Fragment number	Residue number	Sequence	Measured [M+H] ⁺ (Monoisotopic)	Theoretical [M+H] ⁺ (Monoisotopic)
T22	338-342	(R) DVCSR (V)	579.25	579.26
T17	213-217	(K) NFTLR (E)	650.29	650.36
T8	87-93	(R) MGASLIR (L)	747.42	747.42
T5	54-60	(R) NSDMYLR (Q)	898.43	898.41
T10	132-140	(R) GYEVIAQAK (Q)	978.52	978.53
T4-5	53-60	(K) RNSDMYLR (Q)	1054.48	1054.51
T16-17	209-217	(K) FNDKNFTLR (E)	1154.55	1154.60
T7	75-86	(R) GVVDSAIDAETR (M)	1232.60	1232.61
T13	169-180	(K) LGGQTYNVALGR (S)	1248.53	1248.67
T18	218-232	(R) EMVALAGAHTVGFAR (C)	1529.53	1529.79
T21	323-337	(K) MGDLPSPSAGALEIR (D)	1554.80	1554.80
T12-13	164-180	(R) DSVAKLGGQTYNVALGR (S)	1748.80	1748.93
T11	141-163	(K) QSVIDTCPNISVSCADILIAAR (D)	2360.00	2360.20
T19	233-273	(R) CSTVCTSGNVNPAALQCN CSATLTDSLQQLDTPMFDK (V)	4321.81	4321.90

6.4 DISCUSSION

Traditionally, complete structural analysis of glycoproteins is a tedious task involving cleavage of glycans from the polypeptide backbone in solution, separation, purification steps and finally, spectroscopic determination of the individual glycans. Besides the obvious complexity of the procedures, sample losses necessarily occur during the multiple manipulations. But the advent of MALDI-MS and its ancillary techniques represents a major step forward in terms of sensitive detection and structural analysis.

Amino acid sequence information can be obtained by one of several methods using MALDI-MS. The first is called protein mass mapping which consists of the site-specific enzymatic or chemical degradation of a protein followed by mass spectrometric analysis of the released peptides. Owing to the complexity of mixtures generated during proteolysis, MALDI-TOF-MS is most ideally suited for such analyses. The traditional analytical methods used to characterize the released peptides consist of HPLC or gel electrophoresis followed by N-terminal (Edman) sequencing and/or amino acid analysis. However, such methods are considerably more time-consuming and in some cases are not capable of separating individual peptides because of their low resolution. Consequently, high-resolution MALDI-TOF analysis can provide for a more rapid, accurate, and highly sensitive analysis of these complex peptide mixtures.

The MW measurement of the fully glycosylated apoprotein by SDS-PAGE is 45.8 kDa and from GFC is 44.9 kDa [9]. MALDI-TOF-MS measured the protein at 37.6 kDa (Figure 6.1a). By SDS-PAGE the deglycosylated protein was measured to be 35.3 kDa [9]. MALDI-TOF-MS measured it to be 36.2 kDa (Figure 6.1b). The discrepancy between MALDI-TOF-MS and SDS-PAGE/GFC may come from the

fact that anionic potato peroxidase contains disulfide bridges and carbohydrates and does not readily unfold (protein retains its activity if electrophoresed without prior heating). Thus the glycoprotein was reduced and alkylated prior to MW measurement.

N-linked oligosaccharides from glycoproteins can be released by hydrazinolysis [23-25] or by the action of enzymes such as PNGase F [26]. PNGase F treatment is superior over hydrazinolysis because the glycans are generally cleaner and less extensively modified than those obtained from chemical release. Furthermore, the harsh conditions of the hydrazinolysis treatment destroy the polypeptide backbone and prevent further analysis of the protein moiety. PNGase F is used when dealing with mammalian glycoproteins, where the fucosylation of the core GlcNAc occurs by α 1-6 linkage [27]. Plant glycoproteins contain fucoses that are α 1-3 linked. For such proteins PNGase A is employed because they release all *N*-linked glycans. Although PNGase A will remove glycans from many glycoproteins in their native conformation, denaturation was performed to ensure complete hydrolysis of all susceptible bonds. In order for denaturation to be maintained, all cysteines were reduced and alkylated.

Initial efforts to identify the protein, (based on database search against the peptide fingerprint), yielded a single match. But according to the published sequence it has not been fully characterized biochemically, rather it has been cloned and its molecular biology studied. Thus, *de novo* peptide sequencing was undertaken in order to characterize it. The QqTOF [22] instrument provides high resolution without the loss of sensitivity, making it ideal for the application of ^{18}O isotope labelling method. The protein was digested by trypsin in a buffer containing 50% v/v of ^{18}O water. The MALDI-QqTOF mass spectrum resulting from the digestion is shown in Figure 6.5.

Because both ^{18}O or ^{16}O are added to the peptide during enzymatic cleavage, the spectra yields both species and thus distinguishes fragments containing the C-terminus from those containing the N-terminus by their distinctive isotopic pattern. In the peptide map, labelled peptides could be determined by their characteristic 2 mass unit isotopic spacing.

Identification of glycan site occupancy generally depends on enzymatic or chemical cleavage of the protein chain, separation of the resulting peptides and glycopeptides by RP-HPLC and detection by mass spectrometry. A variety of mass spectrometric techniques can be used, either off-line as in the case of MALDI or, more commonly, on-line as with electrospray [28-31]. Enzymatic removal of the sugars with endoglycosidases such as PNGase F or endo H and revaluation of the residual peptide mixture by LC/MS reveals the glycopeptides by their shift in the chromatogram [32].

Alternatively, glycosylation sites can be determined by performing CID on a glycosylated peptide ion and observing for characteristic glycan fragmentation, i.e. monosaccharide losses. Typical glycosylated peptides under CID conditions exhibit successive monosaccharide losses from the non-reducing end of the glycan leading up to the loss of the whole oligosaccharide moiety. The MALDI-QqTOF has produced similar characteristic fragmentation in the past [32]. Under CID conditions in the QqTOF, glycosylated peptides show the presence of three abundant distinctive ions. These peaks are due to (i) the peptide, (ii) the peptide with a GlcNAc attached, and (iii) a cross-ring cleavage of the GlcNAc attached to the peptide. The MS/MS fragmentation for m/z 2273.7 do not follow similar fragmentation pathways. There is an initial loss of fucose, followed by losses of amino acids from the N-terminus leading up to glycosylated Asn-24. Also observed is the peak due to the glycan moiety itself. The type of fragmentation

pathway observed might be due to the fact that the ions observed result from a non-specific tryptic peptide. Furthermore, glycosylation is on the terminal amino acid rather than in the middle of the peptide. This might make the amino acids more susceptible for fragmentation than monosaccharides. In general the MS/MS studies on the *m/z* 2273.7 confirms the presence of glycans on Asn-24.

6.5 CONCLUSION

The combination of derivatization, ¹⁸O labelling and MALDI-QqTOF were used to sequence the glycoprotein anionic potato peroxidase. Even though total sequence coverage was not possible in our study, it was still possible to determine 80.6% peptide coverage and identify at least one site of glycosylation (Asn-24).

MALDI-QqTOF-MS allowed the detection of two types of glycans, high mannose and complex types. MALDI-QqTOF-MS/MS experiments were performed to confirm the proposed glycan structures.

6.6 REFERENCES

1. Bernards, M.A. and Lewis, N.G. *Phytochem.* **47**, 915 (1998).
2. Kolattukudy, P.E. *Science* **208**, 990 (1980).
3. Borchert, R. and Decedue, C.J. *Plant Physiol.* **62**, 794 (1978).
4. Espelie, K.E. and Kolattukudy, P.E. *Arch. Biochem. Biophys.* **240**, 539 (1985).
5. Espelie, K.E., Franceschi V.R. and Kolattukudy P.E. *Plant Physiol.* **81**, 487 (1986).
6. Razem, F.A. and Bernards, M.A. *J. Agric. Food Chem.* **50**, 1009 (2002)
7. Roberts, E., Kutchan, T. and Kolattukudy P.E. *Plant Mol. Biol.* **11**, 15 (1988).
8. Roberts, E. and Kolattukudy, P.E. *Mol. Gen. Genet.* **217**, 223 (1989).
9. Bernards, M.A., Fleming, W.D., Llewellyn D.B., Priefer, R., Yang, X., Sabatino, A. and Plourde, G.L. *Plant Physiol.* **121**, 135 (1999).
10. <http://us.expasy.org/cgi-bin/niceprot.pl?P12437>
11. Desiderio, D. and Kai, M. *Biomed. Mass Spectrom.* **10**, 471 (1983).
12. Rose, K., Simona, M., Offord, R., Prior, C. and Thatcher, D. *Biochem. J.* **215**, 273 (1983).
13. Gaskell, S.J., Haroldsen, P.E. and Reilly, M.H. *Biomed. Environm. Mass Spectrom.* **16**, 31 (1988).
14. Rose, K., Savoy, L., Simona, M., Offord, R. and Wingfield, P. *Biochem. J.* **250**, 253 (1991).
15. Takao, T., Hori, H., Okamoto, K., Harada, A., Kamachi, M. and Shimonishi, Y. *Rapid Commun. Mass Spectrom.* **5**, 312 (1991).
16. Whaley, B. and Caprioli, R.M. *Biol. Mass Spectrom.* **20**, 210 (1991).
17. Schnolzer, M., Jedrzejewski, P. and Lehmann, W.D. *Electrophoresis* **17**, 945 (1996).
18. Pitt, J.J. and Gorman, J.J. *Anal Biochem.* **248**, 63 (1997).
19. O'Neill, R.A. *J. Chromatogr. A* **720**, 201 (1996).

20. Honda, S., Akao, E., Suzuki, S., Okuda, M., Kakehi, K. and Nakamura, J. *Anal Biochem.* **180**, 351 (1989).
21. Saba, J.A., Shen, X., Jamieson, J.C. and Perreault, H. *Rapid Commun. Mass Spectrom.* **13**, 704 (1999).
22. Loboda, A. V., Krutchinsky, A. N., Bromirski, M. P., Ens, W. and Standing, K. G. *Rapid Commun. Mass Spectrom.* **14**, 1047 (2000).
23. Takasaki, S., Misuochi, T. and Kobata, A. *Methods Enzymol.* **83**, 263 (1982).
24. Patel, T., Bruce, J., Merry, A., Bigge, C., Wormald, M., Jaques, A. and Parekh, R. *Biochemistry* **32**, 679 (1993).
25. Patel, T. P. and Parekh, R. B. *Methods Enzymol.* **230**, 57 (1994).
26. Tarentino, A. L., Gómez, C. M. and Plummer, T. H., Jr. *Biochemistry* **24**, 4665 (1985).
27. Tretter, V., Altmann, F. and März, L. *Eur. J. Biochem.* **199**, 647 (1991).
28. Carr, S.A., Barr, J.R., Roberts, G.D., Anumula, K.R. and Taylor, P.B. *Methods Enzymol.* **193**, 501 (1990).
29. Huddleston, M.J., Bean, M.F. and Carr, S.A. *Anal. Chem.* **65**, 877 (1993).
30. Carr, S.A., Huddleston, M.J. and Bean, M.F. *Protein Sci.* **2**, 183 (1993).
31. Hunter, A.P. and Games, D.E. *Rapid Commun. Mass Spectrom.* **9**, 42 (1995).
32. Liu, J.P., Volk, K.J., Kerns, E.H., Klohr, S.E., Lee, M.S. and Rosenberg, I.E. *J. Chromatogr.* **632**, 45 (1993).

7 CONCLUSIONS

7.1 CONCLUSIONS

At the present time the analysis of carbohydrates by MS has reached a high degree of development, however, its main shortcoming with respect to proteomics is sensitivity. MS itself is comparatively sensitive; the main problems lie in the area of sample preparation and transfer of the glycans into the mass spectrometer in a relatively pure form. This problem is heightened when dealing with small sample size. The most promising approaches for glycan appear to be those that involve the minimum sample manipulation. This being the case, it is fortunate that MALDI gives representative glycan profiles from underivatized glycans and from the glycans tagged at the reducing terminus without the need for further chemical treatment. The recent ability to obtain fragmentation spectra at high sensitivity, either by use of QqTOF instruments or with ion-traps, further enhances the utility of MS and it would be hoped that in the future, the assembly of suitable libraries of fragmentation spectra would enable on-line data-base searching to automate the identification of glycans attached to glycoproteins.

This research extends our laboratory's PMP-oligosaccharide studies to asialo and sialylated *N*-linked oligosaccharides. The latter have not been studied in great detail to date, and are important since numerous sialylated glycoproteins exist and need to be characterized. It is pointed out that native free *N*-linked carbohydrates have very low affinities for the C18 reversed phases commonly used in HPLC and sialylated glycans have low sensitivity for detection by ESI-MS. The PMP derivatization method is simple to use and prevents the loss of sialic acid moieties from carbohydrates. The PMP labelling of asialo and sialylated sugars yielded higher affinities for HPLC C18 columns

and, even at the early stages of method development, it was possible to separate three PMP-labeled standards to a useful extent. The methodology developed with standards was applied to glycans detached from ovalbumin and on-line RP- and NP- HPLC/ESI-MS separation was achieved.

In ESI-MS, PMP-asialo sugars did not yield a significant increase in sensitivity vs. the native species; however, fragmentation produced by in-source CID was more directed as all predominant fragment ions contained the bis-PMP label. This feature is particularly useful when structural determination of an unknown sugar is required. PMP-sialylated sugars gave rise to very clean and informative ESI mass spectra. The monosialo sugar yielded a 100-fold sensitivity improvement vs. its native analog and, in the case of the disialylated compound, a 100% improvement was obtained in the positive mode. Most fragment ions were informative and contained the reducing end on the molecules, thus facilitating spectral interpretation. The combination of PMP derivatization with on-line HPLC/ESI-MS is a promising method for the analysis of asialo and sialylated carbohydrate mixtures.

This research demonstrates the first use of ANTS derivatization as a suitable derivative for HPLC/ESI-MS analysis. Novelty aspects of this work include the use of ANTS derivatization of *N*-linked glycans and detection of ANTS-labelled standards by normal-phase HPLC/MS. Prior to this work all ANTS derivatization for mass spectrometry have involved CE.

We report on the use and comparison of derivatization, HPLC, FACE and ESI-MS to characterize the molecular masses of glycoforms and glycans of ovalbumin. ANTS derivatization was used for FACE analysis. We also tested the suitability of ANTS

derivatives for HPLC/ESI-MS, in an attempt to include only one step of derivatization (ANTS) while allowing two types of analysis (FACE and HPLC/ESI-MS). The results confirm those found in the literature, and emphasize the greater specificity of on-line HPLC/ESI-MS analysis than FACE analysis alone.

The first detailed MS characterization of anionic potato peroxidase was presented which confirmed earlier results in literature derived via more traditional methods. This work also first demonstrates the first example of the structural characterization of glycans detached from the anionic potato peroxidase, as well as determination of the glycosylation site.

7.2 FUTURE WORK

Glycosylation is an abundant posttranslational modification, which exhibits particular degree of sophistication in mammalian systems. It has been estimated that 60-90% of all mammalian proteins are glycosylated. The glycosylated structures play critical roles in numerous biological systems. The roles range from issues as important as developmental biology, immune response, pathogens homing on their host tissues, cell division processes, cancer cells camouflaging to escape detection by the immune system, injury and inflammation, and prion diseases. The relevant biochemical and biomedical literature of the past decade underscores the future importance of glycobiology research and its expected growth. However, given the structural variation of glycan structures and their frequently low abundance, glycobiology will continue demanding the best out of analytical tools and methodologies.

The currently available knowledge on the structure and function of glycoconjugates give credit to the analytical methodologies developed during the last 15

years. Some of the instrumental advances in the field of glycomics are being currently shared with the field of proteomics: the isolation and purification methodologies and MS in particular. It is thus likely that the current transition from the successful beginning of the glycobiology field toward one of the last great frontiers of biochemistry will require even greater gains in sensitivity and compound resolution than what is currently being practiced.

This research has been accepted well by the scientific community and has been referenced by number of groups in similar areas. The glycan structural characterization work done on the IgG is currently being used by other members of the laboratory. A new computer program for automated interpretation of tandem MS spectra of complex *N*-linked glycans is being developed based on the structural data gathered from the IgG experiments.

The peroxidase experiments involving glycan structural characterization and site of glycosylation is being used in the explanation of the suberin-specific role for the anionic peroxidase. Further experiments still need to be done for determination the signal peptide loss as well as potential of one more glycosylation site.

Refereed Journal Publications:

1. Saba, J.A., Ens, W., Standing, K.G., Bernards, M. and Perreault., Sequencing the Primary Structure of Anionic Potato Peroxidase, *in press*.
2. Ethier, M., Saba, J.A., Spearman, M., Krokhn, O., Ens, W., Standing, K.G., Butler, M. and Perreault, H., Application of the StrOligo algorithm for the automated structure assignment of complex N-linked Glycans from Glycoproteins Using Tandem Mass Spectrometry, *Rapid Commun. Mass Spectrom*, 2003, 17, 2713-2720.
3. Ethier, M., Saba, J.A., Ens, W., Standing, K.G. and Perreault, H., Automated Structural Assignment of Derivatized Complex N-linked Oligosaccharides from Tandem Mass Spectra, *Rapid Commun. Mass Spectrom*, 2002, 16, 1743-1754.
4. Saba, J.A., Kunkel, J.P., Jan, D.C.H., Ens, W.E., Standing, K.G., Butler, M., Jamieson, J.C. and Perreault, H., A Study of Immunoglobulin G Glycosylation in Monoclonal and Polyclonal Species by Electrospray and Matrix-Assisted Laser Desorption/Ionization Mass Spectrometry, *Anal. Biochem.* 2002, 305, 16-32.
5. Saba, J.A., Shen, X., Jamieson, J.C. and Perreault, H., Investigation of Different Combinations of Derivatization, Separation Methods and Electrospray Ionization Mass Spectrometry for Standard Oligosaccharides and Glycans from Ovalbumin, *J. Mass Spectrom.* 2001, 36, 563-574.
6. Saba, J.A., Shen, X., Jamieson, J.C. and Perreault, H., Effect of 1-Phenyl-3-methyl-5-pyrazolone Labeling on the Fragmentation Behavior of Asialo and Sialylated N-linked Glycans Under Electrospray Ionization Conditions, *Rapid Commun. Mass Spectrom*, 1999, 13, 704-711.

Conference Proceedings, Non-Refereed:

1. Perreault, H., Lattova, E., Snovida, S., Saba, J.A., Lee, C.H., Chen, V.C., and Ethier, M., 2004, Glycomics: Sampling Protocols, Mass Spectrometry and Automated Data Interpretations, 87th Chemical Society of Canada Conference and Exhibition, Toronto, Ontario, May 28 - June 1, 2004.
2. Perreault, H., Lattova, E., Saba, J.A. and Ethier, M., 2004, Nouvelles Approches Bioanalytiques et Bioinformatiques dans le Monde de la Glycomique, 72^e Congrès de l' Acfas, Quebec, , May 10 - 14, 2004.
3. Saba, J.A., Ens, W., Standing, K.G., Bernards, M. and Perreault, H., 2003, Sequencing the Primary Structure of Anionic Potato Peroxidase Using MALDI-MS, 51st ASMS Conference on Mass Spectrometry and Allied Topics, Montreal, Quebec, June 8 - 13, 2003.
4. Ethier, M., Saba, J.A., Spearman, M., Krokhn, O., Butler, M., Ens, W., Standing, K.G. and Perreault, H., 2003, Towards High-Throughput Glycomics: Development of the StrOligo Program for Automated Analysis of N-linked Glycans MS/MS Spectra for Structure Determination, 51st ASMS Conference on Mass Spectrometry and Allied Topics, Montreal, Quebec, June 8 - 13, 2003.
5. Saba, J.A., Kunkel, J.P., Ens, W., Standing, K.G., Jamieson, J.C. and Perreault, H., 2002, MALDI-MS/MS and PSD Studies of IgG Glycans, 50th ASMS

- Conference on Mass Spectrometry and Allied Topics, Orlando, Florida, June 8 - 13, 2002. # WPG 176.
6. Saba, J.A., Ens, W., Standing, K.G., Berenards, M. and Perreault, H., 2002, Study of the Primary Structure of Anionic Potato Peroxidase Using MALDI-MS, 50th ASMS Conference on Mass Spectrometry and Allied Topics, Orlando, Florida, June 8 - 13, 2002. # ThPF 120.
 7. Ethier, M., Saba, J.A., Kunkel, J.P., Ens, W., Standing, K.G. and Perreault, H., 2002, Automated Interpretation of N-linked Oligosaccharides Tandem Mass Spectra Obtained by Matrix-Assisted Laser Desorption Ionization Mass Spectrometry for Structure Determination, 50th ASMS Conference on Mass Spectrometry and Allied Topics, Orlando, Florida, June 8 - 13, 2002. # TPL 326.
 8. Saba, J.A., Bromirski, M.P., Ens, W., Standing, K.G., Bernards, M.A. and Perreault, H., Determination of Glycan Composition and Structure in Potato Peroxidase, 49th ASMS Conference on Mass Spectrometry and Allied Topics, Chicago, Illinois, May 27-31. # MPK 289.
 9. Kunkel, J.P., Saba, J.A., Ens, W., Standing, K.G., Jamieson, J.C. and Perreault, H., Comparative ESI, MALDI, HPAEC-PAD and FACE Studies of N-linked Oligosaccharides from a Monoclonal Antibody Produced in Continuous Culture: Effect of Dissolved Oxygen Concentration, 49th ASMS Conference on Mass Spectrometry and Allied Topics, Chicago, Illinois, May 27-31. # MPL 297.
 10. Saba, J.A., Kunkel, J.P., Bromirski, M.P., Ens, W., Standing, K.G., Jamieson, J.C. and Perreault, H., Development of ESI-MS and MALDI-QqTOF-MS Methods for the Analysis of PMP-Labelled N-Linked Oligosaccharides from Polyclonal IgG Standards: Comparison with HPAEC-PAD Analysis, 49th ASMS Conference on Mass Spectrometry and Allied Topics, Chicago, Illinois, May 27-31. # ThPG 167.
 11. Saba, J.A., Kunkel, J.P., Ens, W., Standing, K.G., Jamieson, J.C. and Perreault, H.P., A Study of IgG Glycosylation in Monoclonal Antibody by Electrospray and Matrix-Assisted Laser Desorption/Ionization Mass Spectrometry, 2001, Annual Conference of The Society for Glycobiology, San Francisco, California, November, 14 - 17, 2001.
 12. Perreault, H., Saba, J.S., Kunkel, J.P. and Jamieson, J.C., New Strategies Involving Mass Spectrometry for the Determination of Composition and Structure of Oligosaccharides Derived from Glycoproteins, 2001, 84th Chemical Society of Canada Conference and Exhibition, Montreal, Quebec, May 26 - May 30, 2001.
 13. Saba, J.A., Jamieson, J.C. and Perreault, H., Normal-Phase HPLC/ESI-MS Studies of Derivatized Glycans, 48th ASMS Conference on Mass Spectrometry and Allied Topics, Long Beach, California, June 11-15. # TPC 070.
 14. McComb, M.E., Lee, C.H., Saba, J.S., Williams, T.T. and Perreault, H., New LC/MS and CE/MS Approaches for the Analysis of Protein and Glycoprotein Components, 2000, 83rd Chemical Society of Canada Conference and Exhibition, Calgary, Alberta, May 27 - June 1, 2000.
 15. Saba, J.A., Shen, X., Jamieson, J.C. and Perreault, H., Glycan Characterization using Derivatization, HPLC/ESI-MS and FACE Methods, 47th ASMS Conference on Mass Spectrometry and Allied Topics, Dallas, Texas, June 13-18. # MPJ 283.

16. Saba, J.A., Jamieson, J.C. and Perreault, H., Glycan Characterization using Derivatization, HPLC/ESI-MS and FACE Methods, 1999, 82nd Chemical Society of Canada Conference and Exhibition, Toronto, Ontario, May 30 - June 2, 1999.